(NASA-CR-165590) DEVELOPMENT OF ELECTRICAL TEST PROCEDURES FOR QUALIFICATION OF SPACECRAFT AGAINST EID. VOLUME 2: REVIEW AND SPECIFICATION OF TEST PROCEDURES Progress Report, Mar. - Sep. (IRT Corp., San

N83-12137

Unclas

G3/18 01172

1. Report No.	2. Government Accession No.	3. Recipient's Catalog No.
NASA CR-165590		

4. Title and Subtitle	5. Report Date
Development of Electrical Test Procedures for Qualification of Spacecraft Against EID Volume II: Review and Specification of Test Procedures	April 1982 6. Performing Organization Code

7. Author(s)	8. Performing Organization Report No.
J.M. Wilkenfeld, B.L. Harlacher, and D. Mathews	8195-022-1 10. Work Unit No.

9. Performing Organization Name and Address	11. Contract or Grant No.
IRT Corporation P. O. Box 80817 San Diego, California 92138	NAS 3-21967 13. Type of Report and Period Covered

12. Sponsoring Agency Name and Address	14. Sponsoring Agency Code
National Aeronautics and Space Administration Lewis Research Center 21000 Brookpark Road, Cleveland, Ohio 44135	3/81 - 9/81 5532

15. Supplementary Notes

Project Manager, John V. Staskus
NASA - Lewis Research Center
Cleveland, Ohio 44135

16. Abstract

This two volume report describes a combined experimental and analytical program to develop system electrical test procedures for the qualification of spacecraft against damage produced by space-electron-induced discharges (EID) occurring on spacecraft dielectric outer surfaces to be incorporated into a proposed EID MIL-STD (or into a modified MIL-STD 1541).

Volume I presents the data on the response of a simple satellite model, called CAN, to electron-induced discharges. The experimental results were compared to predicted behavior and to the response of the CAN to electrical injection techniques simulating blowoff and arc discharges. Also included is a review of significant results from other ground tests and the P78-2 program to form a data base from which is specified those test procedures which optimally simulate the response of spacecraft to EID. The electrical and electron spraying test data were evaluated to provide a first-cut determination of the best methods for performance of electrical excitation qualification tests from the point of view of simulation fidelity.

Volume II presents a review and critical evaluation of possible approaches to qualify spacecraft against space electron-induced discharges (EID). A variety of possible schemes to simulate EID electromagnetic effects produced in spacecraft have been studied, and candiate electrical injection techniques for electrically exciting spacecraft have been developed. These techniques form the principal element of a provisional, recommended set of test procedures for the EID qualification spacecraft. The report also identifies significant gaps in our knowledge about EID which impact the final specification of an electrical test to qualify spacecraft against EID.

17. Key Words (Suggested by Author(s))	18. Distribution Statement
Spacecraft Charging, SCATHA, Electron-Induced Discharges, Electrical Testing, Qualification Testing, Spacecraft	Publicly Available

19. Security Classif. (of this report)	20. Security Classif. (of this page)	21. No. of Pages	22. Price*
UNCLASSIFIED	UNCLASSIFIED		

* For sale by the National Technical Information Service, Springfield, Virginia 22161

TABLE OF CONTENTS

TABLE OF CONTENTS (continued)

FIGURES

TABLES

1. OVERVIEW

1.1 INTRODUCTION

This report presents a review and critical evaluation of possible approaches to qualify spacecraft against space electron induced discharges (EID). A variety of possible schemes to simulate the electromagnetic effects produced in spacecraft have been studied, and candidate electrical injection techniques for electrically exciting spacecraft have been developed. These techniques form the principal element of a recommended set of test procedures for EID qualification of spacecraft described in this report.

This report represents the second of two major deliverables for the present program, entitled "SCATHA Model Tests" (Contract NAS3-21967) jointly sponsored by NASA-Lewis Research Center and the USAF-Space Division. This work is a continuation of a program begun under joint Space Division and Defense Nuclear Agency (DNA) sponsorhip entitled "Electrostatic Discharge Modeling, Testing, and Analysis for SCATHA," under Contract DNA001-77-C-0180.

The major objective of this combined experimental and analytical program has been the development of validated system electrical test procedures for the qualification of spacecraft against damage produced by space-electron-induced discharges occurring on spacecraft dielectric outer surfaces (EID) tc be incorporated into a proposed EID MIL-STD (or into a modified MIL-STD 1541).

The results of this program have been documented in two reports.

1. The first report presents the data on the response of a simple satellite model, called CAN, to electron-induced discharges. The experimental results were compared to predicted behavior and to the response of the CAN to electrical injection techniques simulating blowoff and arc discharges. Also reviewed and included are significant results from other ground tests and the P78-2 programs to form part of the data base for specifying those test procedures which optimally simulate the response of spacecraft to EID. The electrical

and electron spraying test data were evaluated to provide a first-cut determination of the best methods for performance of electrical excitation qualification tests from the point of view of simulation fidelity.

2. The major content of this report is the specification of a set of test procedures to qualify spacecraft for reliable performance when subjected to a charged particle environment conducive to producing discharges. These specifications have been prepared for incorporation into the proposed EID appendix to MIL-STD 1541 (USAF), Electromangetic Con atibility Requirements for Space Systems. This report includes a description of the tradeoff analyses by which they were selected, the recommended sources, method of injection, drive levels, measurement techniques, sensors, data to be recorded, test configuration and test conduct.

While this report provides a recommended set of test procedures, the information presented herein is meant to summarize what we presently (September 1981) know about EID electromagnetic effects in satellites. As the balance of this report makes clear, there is a lack of critical information about the nature of the discharge process, the relationship betwen ground test and on orbit discharge data, and internal EID coupling. Therefore, the test procedures specified are meant to be provisional, and reflect the state of our knowledge as described herein. However, we believe that the electrical injection tests for EID qualification proposed in Section 3 provide a much more valid simulation of the electromagnetic fields, currents, and charge distributions induced on the satellite surface and coupled into interior circuitry than the present MIL-STD 1541 arc injection test.

1.2 SUMMARY

The report is divided into two major sections. In Section 2, the various possible approaches to spacecraft EID qualification have been reviewed and evaluated. The approaches considered were:

1. Flying a qualification spacecraft in the real environment adequately instrumented to observe its EID susceptibility.

2. Testing the qualification spacecraft in a charged particle and photon environment which simulates the important aspects of that found on orbit.

3. Testing the qualification spacecraft by global external electrical excitation in a manner which simulates the distribution of levels and pulse widths of the the external tangential magnetic fields (surface currents) and/or the normal displacement fields (surface charge) produced on the spacecraft surface by EID.

4. Electrical injection of cable bundles connecting subsystem components or directly into pins of individual boxes at levels and pulse shapes which simulate those produced by EID coupling into the spacecraft.

The approaches were evaluated in terms of ease of implementation, technical maturity of the approach, technical risk in relying on a particular method, cost, schedule impact and confidence in the test results. The conclusions drawn from this assessment include:

1. The first two qualification tests are the most realistic, and would yield the greatest confidence in the results obtained. However, the technical benefits are outweighed by the probable cost, schedule impact and technical risk. For Procedure 1, it might involve loss of a spacecraft. For Procedure 2, there is fairly high technical risk and cost because a fully instrumented facility to perform such tests does not exist. However, the necessary instrumentation and sources are available.

2. Subsystem and box electrical testing is a relatively low cost, practical approach, which is compatible with presently conducted functional, EMC/EMI, and SGEMP component electrical tests. However, this approach has two major technical limitations. First, there is little quantitative data which relates discharge-induced external transients to internal signals produced on wires and at the interfaces to electronic boxes. Therefore, it is difficult to specify realistic drive levels. Second, the approach will not test many of the design features such as structure, box and cable shielding, and cable placement which form part of the total design package to protect spacecraft against EID and other externally generated electromagnetic transients.

3. The approach which seems most attractive from a combined technical risk, cost, schedule, compatibility and simulation fidelity point of view is global external electrical injection at likely discharge points. Model studies

indicate that it appears feasible to simulate the external electromagnetic environment, at least over limited regions of the spacecraft and excite points of entry (POE's) for electromagnetic energy in a manner similar to that by EID.

Therefore, a feasibility study was performed to evaluate various specific electrical injection schemes based on similar testing which has been performed to electrically simulate the electromagnetic currents and fields generated on the surface of spacecraft by the nuclear weapon produced X-rays (SGEMP). Part of this evaluation included a review of relevant features of representative SGEMP and EID electrical testing of satellite models including the STARSAT (a DSCS-III Model), the CAN, SCATSAT, and the VOYAGER spacecraft.

The following electrical excitation approaches were evaluted through model calculations:

1. Low level, narrow pulse, capacitive discharge, capacitive coupling between pulser and test object (few amps, peak amplitude, 20-40 ns FWHM pulse widths)
2. Low level, wide pulse capacitive discharge, capacitive coupling (few amps, 1 μs FWHM)
3. High level, wide pulse capacitive discharge, capacitive coupling (200A, 1 μs FWHM)
4. Capacitive discharge, direct coupling between pulser and test object and test object and pulse ground (hundreds of amps, 1 μs FWHM)
5. MIL-STD 1541 Arc (10-50A, 10-50 ns FWHM)
6. MIL-STD 1541 Arc (200A, 1 μs FWHM).

The wide-pulse, high-level injection currents were taken to be representative of those induced on the surface of spacecraft as a consequence of discharging large area (0.5 to 1 m^2) dielectrics.

The results of the model calculations can be summarized as follows:

1. Low level, subthreat excitation of any type was rejected because of problems associated with
   a. Scaling results to threat level (feasibility, accuracy)

b. Requirement for significant additional internal monitoring instrumentation

c. Sensitivity and noise problems.

2. Conventional capacitative direct injection employed during the SCATSAT tests was rejected because

   a. Attainable pulse widths are too narrow (tens of nanoseconds)

   b. Amplitudes attainable are too low (by about a factor of 10-100) unless extremely high charging voltages are used (1 MV)

3. The present MIL-STD 1541 arc was rejected because it is a poor simulation of the blowoff of electrons.

4. The most realistic practical approach capable of generating sufficiently large pulse amplitudes and pulse widths is a direct injection with a capacitive discharge source and direct connections between pulser and test object and test object and pulser return. This approach can provide a simulation of the body currents which flow over the surface of the spacecraft.

5. It is also desirable to perform a capacitive discharge current injection with capacitive coupling with wide pulses and threat level drive to simulate some aspects of the EID excitation (normal displacement fields, spacecraft resonant modes) not well simulated by direct injection. However, the model studies indicate that this approach is technically difficult to implement using practically attainable values of circuit parameters because of the high charging voltages required (~600 kV). However, if more modest drive currents (<50A) and pulse widths (<250 ns) are required, then a pulser of about 50 kV would suffice. However, what is excited is the combined pulser, coupling network, test object system. The fidelity of the simulation is diminished compared to capacity coupled injection (CDI).

Based on the modeling studies a qualification test procedure was devised which is described in Section 3. Its basic element is the elecrical excitation of the spacecraft by a high level, wide pulse direct drive scheme supplemented, where necessary, by capacitively coupled injection. Based on available ground test discharge data, rules are given for determining the critical test or injection points and how to select pulser characteristics to achieve desired injection levels and pulse widths. The test configuration is basically one in which the pulser and test object are isolated from

the external surroundings through the use of battery driven pulsers, analog fiber optic links for the transmission of electromagnetic environment and monitor point data, and dependence on the vehicle telemetry for spacecraft status during electrical testing. The vehicle would be in its flight configuration and isolated from external grounds and extraneous conductors.

The test procedures specified should be taken as provisional. They need system validation for the following reasons:

1. While similar electrical testing has been performed on spacecraft or spacecraft models, the particular tests proposed have not been tried out either on a real spacecraft or on a reasonably complex electrical model like the SCATSAT. Proof testing is required.

2. There is insufficient quantitative data produced either by model analysis or testing with which one can compare the kinds of simulation produced electrically with the electromagnetic responses invoked by EID (especially for the normal displacement fields created on the surface of the spacecraft). For this reason further coupling analysis as well as model testing in a simulated charged particle environment are required.

In addition, there are fundamental gaps in our knowledge of EID which impact the specification of an electrical qualification test. These include:

1. Our knowledge of the discharge process is limited. No adequate, comprehensive discharge models exist by which one can predict with confidence the discharge characteristics given the charging environment, material properties and sample configuration.

2. A quantitative analysis has not been made infers discharge characteristics from the magnitude of the P78-2 transients recorded by the SCI-8 and TPM experiments. The P78-2 coupling model begun under this program should be completed in order to facilitate this analysis.

3. Limited experimental evidence indicates that the components of the space radiation environment such as high energy penetrating electrons, UV and ions tend to diminish or eliminate discharges in many materials. It is important to complete item (2) so that a quantitative comparison between the ground test discharge data and that obtained from the P78-2 may be made. It may be that the scaling laws used as a basis for specifying electrical injection pulse

amplitudes and pulse widths provide for much more severe stresses than those to which real spacecraft are subjected.

4. If the required pulse widths and amplitudes could be reduced, then it would make capacitively coupled injection more feasible. In addition, it might be possible to use an alternate scheme of vehicle isolation based on inductive loading of power cables and signal return conduits attached to the spacecraft. This would simplify test conduct.

5. These test procedures are not designed to qualify spacecraft against electron caused electromagnetic pulse (ECEMP) effects produced by the charging and discharge of interior dielectrics such as cables or printed circuit boards by high energy, penetrating electrons. More work is needed to understand the severity of this problem for spacecraft in the natural and nuclear weapon environments.

2. SELECTION OF AN EID SYSTEM QUALIFICATION TEST TECHNIQUE

2.1 APPROACHES TO QUALIFICATION

In identifying a procedure for qualification of spacecraft against the harmful electromagnetic effects of EID, there are two key issues which are related. The first is test technique; i.e., by what means is the spacecraft to be stressed. The second relates to test conduct, how is the test to be performed. The question of pulsers will be addressed in this section, test conduct in the next.

Section 5.1.1 of MIL-STD 1541 prescribes that the complete spacecraft electrical/electronic system be tested to demonstrate qualification. Compliance is to be demonstrated by showing that critical system points have a 6 dB (energy) safety margin (20 dB's for EED-electroexplosive devices). Critical system points are those which are chosen to monitor the performance of the system; i.e., to determine whether the system will perform according to system functional and operational requirements. These critical test points are further identified as:

1. Susceptible to interference because of sensitivity, inherent susceptibility, mission significance, or exposure to the stressing environment.
2. Part of an electrical circuit, generally before the output stage.
3. A subsystem stress point.

The performance of the system is monitored for improper response at monitoring points which are:

1. Either electrical or mechanical
2. Generally at the subsystem output or internal to the subsystem.

For the EID qualification of the P78-2, Martin chose critical test points to be those on the exterior of the spacecraft likely to suffer on-orbit discharges. Monitoring was performed using the AGE to identify improper system performance, supplemented by directly observing the behavior of 12 critical electric circuit points (Ref 1). Section

6.2.1 of MIL-STD 1541 specifies that the AGE or vehicle telemetry is not to be used as the sole monitor of system performance during testing. These points included several which are part of the spacecraft system and several related to the engineering experiments (SCI-8B, TPM) designed to measure transients. In addition data was recorded by the SCI-8B and TPM transient monitors. Thus, the excitation points were chosen because of their inherent susceptibility to arc discharges, although not part of an electronic circuit. The monitoring points were chosen because of their significance to the system electrical performance, sensitivity, because they were representative of typical interface circuits, or to provide a baseline for the response of the transient measuring experiments.

Of course, the MIL-STD 1541 arc used to excite the P78-2 has been shown in the work described in References 2 through 4, to be a grossly inadequate simulation of the principal driver for the inducement of electrical transients, namely the blowoff of charge. That the P78-2 has not suffered a significant number of environment induced upsets is due in large part to the heavy shielding (double Faraday cage) incorporated into the P78-2. This has been reviewed in References 5 and 6. It is the objective of this chapter to identify a more realistic, viable system test procedure.

MIL-STD 1541 specifies three generic approaches to demonstrating compliance. These include:

(1) Providing a 6 dB overstress of critical points (20 dB for EED)

(2) Measurement of the noise environments at the critical test points and comparing them to subsystem susceptibility levels as determined through test or analysis (as required by Section 5.1.2.1.6 of MIL-STD 1541).

(3) Increasing the sensitivity of critical points by 6 dB to demonstrate satisfactory performance in the noise environment.

It is clear that the most technically sound approach to demonstrate survivability in the EID environment is Approach 1 The second method is not really practical as the actual EID stressing environment is only observed on orbit. There is essentially no space data on the characteristics of discharges which occurs in surface dielectrics. It is possible to infer some characteristics from the transient sensor data (SCI-8B, TPM) recorded by the P78-2. However, the response of a spacecraft to electrical excitation is highly configuration dependent. In extrapolating for the P78-2 sensor data to source terms, it is important to have an accurate coupling model. Hence, maximum utilization of this space data is dependent on completion of the P78-2 coupling model.

In principle, one can calculate the electromagnetic coupling produced by EID for particular satellite configurations, predict the transients induced at critical points and compare them to upset thresholds. However, such an approach is bound to introduce errors which are larger than the 6 dB margin. There are two principal reasons for this - First, the necessary discharge source terms are not well known. This issue has been reviewed in Section 6 of Reference 2. Second, experience gained in applying conventional system modeling approaches such as SEMCAP or IEMCAP (Ref 7) indicate that 20 dB uncertainties are not uncommon if experimental test data produced by well characterized electrical sources are compared to prediction. Based on IRT experience in SGEMP coupling analysis of satellite structures, the analysis uncertainties are comparable. For example, predictions were made by various groups of the response of various components of the STARSAT, a DSCS-III model, exposed to the output of a nuclear weapon in the Huron King UGT. It was found that the average discrepancy between prediction and measured response was 12 dB (amplitude). The range of discrepancies was from -12 dB to greater than +28 dB.

The third approach is also not practical for EID qualification. Many of the specified design practices which increase the electron induced discharge safety margins (EIDSM) depend on electromechanical hardening rather than on specific circuit parameters. The former include structural, cable and box shielding and grounding. It is desirable that any system test validate these design features. In any case, their removal for testing is probably impractical.

In Table 1, we have presented a summary of the generic test methods for satellite EID qualification. The methods are arranged according to simulation fidelity with a test flight being best in this regard and box testing worst. Unfortunately, cost and risk are directly correlated with fidelity. As we will discuss in more detail in this section, no one technique best satisfies all the possible evaluation criteria. The radiation tests rank highest in terms of simulation fidelity and confidence in the result. They also are the most expensive and present the greatest technical risks in performance and have the greatest potential schedule impact.

At the other extreme, box and subsystem electrical testing is technically mature, quite compatible with existing spacecraft design, development and test practice, and presents a relatively low risk. However, given our present state of knowledge about external EID efforts, the confidence that such tests inspire is relatively low. This is true for two reasons. First, specification of test levels, pulse amplitudes and waveshapes depends on a coupling analysis. As we have pointed out above, our

knowledge of source terms and our ability to do an accurate coupling analysis of a system as complicated as a spacecraft is limited. This can lead to inclusion of extra safety margins to cover analysis uncertainty with possible overdesign. Second, box and subsystem testing is not a true system test. Design features such as shielding, grounding and cable routing are not tested.

In between the two, stands global electrical testing. It is a true system test, can be performed at threat levels (for some hardware configurations), simulates many of the electromagnetic effects produced by excitation schemes and surface EID, and is relatively compatible with present EMC test practices. The key issue here is providing an optimum EID simulation. We feel that on balance, global electrical testing in accordance with the procedure described in Section 3, is the optimum method for performing EID system qualification testing. The rationale for this choice is developed in the balance of this chapter.

It is to be noted that the test procedures to be specified are designed to qualify spacecraft against external surface EID. MIL-STD 1541 in its present version and near term modification do not address the question of ECEMP, electron caused electromagnetic pulse effects. ECEMP occurs as a consequence of the charging and discharging of interior dielectrics; i.e., cables and printed circuit boards by the penetrating, high energy (>100 keV) component of the trapped electron population.

Relatively little is known about this phenomenon. The emphasis of the SCATHA program has been on surface charging of spacecraft dielectrics in the magnetic substorm environment. There is little direct evidence from flight behavior that natural environment produced ECEMP is a serious problem. It has been noted that a fraction of the spacecraft anomalies associated with spacecraft charging did not occur during the midnight-to-dawn quadrant of local time associated with substorm induced charging. About 5 of 19 SCI-8B EID transients on the P78-2 occurred about 48 hours after a substorm when the trapped electron belts would be pumped up (Ref 8). The GPS spacecraft suffered at least one anomaly in which the solar energy power drive malfunctioned which has been attributed to ECEMP (Ref 9).

Of much more potential significance are ECEMP effects associated with the pumped up electron belts consequent to exoatmospheric nuclear explosions. Limited ground tests (Refs 10,11) indicate that the fluences associated with a saturated electron belt can induce discharges in cable dielectrics and printed circuit boards. The problem is more severe in some nuclear electron environments in that the charging environments for some scenarios are one to two orders of magnitude more intense than those

associated with the average natural environment. As exoatmospheric nuclear testing ended in 1962, when only a few, relatively poorly instrumented satellites were flying, there is no published information about spacecraft nuclear ECEMP induced anomalies.

A second area of potential concern are planetary environments. For example, that associated with Jupiter presents a much more severe charging environment than that associated with the earth.

On the other hand, it has been shown that the radiation conductivity induced by the penetrating electron component can minimize or eliminate discharges in outer surface dielectrics. (Ref 2).

Thus, the limited amount of evidence which presently exists indicates that ECEMP is potentially a problem to USAF, NASA, and commercial spacecraft. However, it is premature to specify qualification procedures based on our limited knowledge of the phenomenon. At any rate, it is likely that ECEMP will have to be dealt with at the component level with qualification through subsystem and box testing. When the problem is better defined, it will properly be dealt with in a future revision of the section of MIL-STD 1541 devoted to subsystem EID testing. Meanwhile, it is best handled on a system by system basis as the operational requirements and environments to be evaluated are different for military, scientific and commercial spacecraft.

2.2 EVALUATION OF QUALIFICATION APPROACHES

2.2.1 On-Orbit Testing

Broadly speaking, the five test methods shown in Table 1 can be grouped into three categories. These are:

1. Test in the real radiation environment.
2. Test in a simulation of the orbit appropriate ionizing and electromagnetic radiation environment.
3. Test by reproducing the electrical responses evoked by the radiation environment. This may be further subdivided according to the level at which the simulation is attempted: system, subsystem, or component.

The flight test falls into Category 1, electron spraying tests in Category 2, and the various electrical injection schemes into Category 3.

Clearly, the best test from the point of fidelity is the flight test of a qualification spacecraft. This is actually an example of the second of the MIL-STD 1541 system

Table 1. Generic Test Methods

METHOD	IMPLEMENTATION	SYSTEM EXAMPLES	ADVANTAGES	DISADVANTAGES	COMMENTS
1. Real Environment	1. Fly qualifying spacecraft to demonstrate survivability	1. None directly - Successful within Block flight experience validates design	1. Most realistic test 2. Lowest impact on production schedule 3. Compatible with present practice	1. Obvious high risk if not combined with alternate ground tests 2. Typical spacecraft not well instrumented for diagnosis	1. As present qualification procedures are evidently technically inadequate, a flight test is actually the way in which current systems are qualified 2. Survivability depends on adequacy of design
2. Simulated Environment	1. Test spacecraft in simulated environment with particle sources in vacuum tank.	1. Meteosat (Passive Test) 2. Components such as solar arrays, thermal blankets have been tested 3. Model tests on CAN 4. SKYNET (Passive Test) objects	1. Moderately realistic in that discharge susceptibility is tested directly 2. Relatively high confidence in the result (probably an overtest with typical ground test simulations). 3. Is a true system test - tests total design including structural/component/cable shielding	1. Key elements of radiation environment may be left out 2. Based on SXTF evaluation, substantial cost ($1M?) and schedule impact (6 mo?) for full system test 3. Relatively high risk of damage 4. Facility and instrumentation not available - must be assembled on an ad hoc basis - requiring substantial additional cost - long lead schedule.	1. Should examine the limited experience in SGEMP testing of satellites (STARSAT, FLTSAT) to better define cost, schedule, implementation difficulties 2. No experience base exists, for (active) system test of satellite in EID environment.
3. Global Electrical Test	1. Electrical excitation simulates the external currents, surface change produced by EID 2. Excite all likely external discharge points or penetrations	1. SCATSAT (EID) 2. Mil-Std-1541 EID tests (P78-2, DSCS-III, Voyager Meteosat) 3. Capacitive Discharge - Voyager 4. STARSAT	1. Is a system test 2. Can get threat level responses 3. Mimics the primary effects produced by blowoff 4. Purely electrical - can raise levels gradually 5. Need for supporting coupling analysis minimized 6. Can use system telemetry for diagnostics 7. Compatible with present system electrical testing	1. Realism of simulation - no one electric technique simulates all aspects (skin currents/charge distributions/external fields) 2. Must depend on analysis for drive points, external levels 3. Possible improper internal excitation 4. Test configuration not standard EMC 5. Possible safety problem - high voltage, currents 6. Does not test surface material design features.	1. Proposed generic approach

Table 1 (Continued)

METHOD	IMPLEMENTATION	SYSTEM EXAMPLES	ADVANTAGES	DISADVANTAGES	COMMENTS
4. Subsystem	1. Electrical drive directly excites the critical points in subsystem by a simultaneous multipoint cable excitation	1. STARSAT (DSCS-III) 2. FLTSAT 3. Voyager (Arc Discharge)	1. Direct unambiguous excitation of critical test points 2. Can be done on a subsystem by subsystem basis as systems are built up. 3. Compatibility with subsystem development testing 4. Design flaws can be identified early in program 5. Can use subsystem diagnostic instrumentation 6. Compatible with other functional checkout 7. Can be used to establish subsystem susceptibility levels 8. Can be done for range of excitations from below to above threat	1. Not a true system test 2. Mechanical design features not tested 3. Must infer individual wire responses on the basis of a coupling analysis 4. Does not test subsystem interactions 5. Because of analysis uncertainty may lead to over test, over design. 6. Requires development of pulser	1. Combined with coupling anaysis can be used for validation approaches (1) or (2)
5. Individual Box	1. Electrical excitation of individual pins (either singly or entire input). System response inferred.	1. Standard EMP test procedure 2. MilStd 1541 procedure for subsystems	1. Box testing procedure, pulsers well developed. 2-7. Similar to subsystem testing - except done at box level.	1-5 Same as for subsystem testing	1. Combined with coupling analysis can be used for validation approaches (1) or (2). 2. SGEMP qualification of satellites typically based on box tests.

qualification test approaches; i.e., comparison of the real stressing environment to the critical points EIDSM. This approach carries the highest potential risk, cost and schedule impact because of the consequences of an on-orbit failure necessitating redesign. However, it is compatible with existing procedures. If in fact, the present MIL-STD 1541 arc test is a gross undertest as indicated by the ground test data, then actual vehicle qualification occurs on orbit. The burden is placed on careful electromagnetic design. Similarly, the confidence level generated by flight experience is also relatively high. Unfortunately, real spacecraft are not well instrumented to record internal transient levels which may be quantitatively compared to upset thresholds. Typically, if uncommanded changes of state occur, no information is available on the size of the discharge which produced the electrical transient, where in a subsystem the transient was generated, and how large was the negative safety margin. Hence, little information is available to correct the design flaw. For this reason, and because of the potentially large risks and cost involved, this approach is unacceptable for spacecraft EID qualification.

2.2.2 Test in Simulated Radiation Environment

The second approach attempts to provide those elements of the electromagnetic and ionizing radiation environments thought to be significant in producing discharges. The satellite is exposed to these sources in a large vacuum tank and its responses monitored. The elements of this environment for geosynchronous orbits are given in Table 2. It is clear that as a minimum, such a radiation simulation must include the electron component of the substorm plasma which is responsible for surface charging. The principal determinant of the EID electromagnetic response is the blowoff of these electrons and their subsequent motion in the electromagnetic fields whose sources are the remaining charges embedded in the dielectric, replacement charge induced in the rest of the spacecraft structure, and the emitted electrons themselves. The other components of the environment act to determine the equilibrium charging potentials on the spacecraft and, in a manner which is not really well understood, evidently limit the magnitude of, or eliminate the occurrence of discharges. This issue has been reviewed in Sections 5 and 6 of Reference 2.

However, there are other aspects of the space environment whose simulation is also important for valid qualification testing. In space, the satellite is loosely coupled to the surrounding plasma and trapped electron belt. Given the level of the charging currents due to electrons, protons, UV ($\sim$1 na/cm^2 or less), differential charging of the

Table 2. Components of Geosynchronous Space Radiation Environment Responsible for Charging

Component	Characteristics	Effects Produced	Comments
1. Solar electromagnetic	0.14 w/cm^2 total flux. Visible, IR like 6000^{0}K blackbody. UV comprised of discrete lines, of which H(Lyα) is most important, superimposed on a continuum.	Photoemission (UV,x-ray), heating (visible, IR) Photoconductivity (UV, visible)	Photoemission controlled by surface properties
2. Natural trapped electron	Outer zone specified in AEI-7. Energies ca. 0.1-5 MeV. Integral omnidirectional flux ca. 10^8 e/cm^2/s at geosynchronous altitudes	Charge and dose deposition, secondary emission, backscatter, semiconductor damage, leakage currents, currents, discharges	Primary effects in spacecraft dielectrics include enhancement of bulk charge leakage, charging of internal dielectrics
3. Magnetic Substorm	Characterized by single or double Maxwellian Provisional Spec: $n_{e,i} = 2cm^{-3}$; $J_e = 0.54$ na/cm^2, T_e=10keV; $J_i = 18$pa/cm^2, T_e =20keV.	Charge and dose deposition secondary emission, backscatter, leakage currents, discharges.	Weighted Average Typical Environments: ATS-5 / ATS-6 / Worst Case (10% Occurrence) — J_e(pa/cm^2) 63 / 87 / 275; T_{1e}(keV) 1.8 / 2.3; T_{2e}(keV) 3.3 / 5.8; J_{1i}(pa/cm^2) 4.1 / 2.3 / 7.6; T_{1i}(keV) 4.6 / 7.9; T_{2i}(keV) 8.7 / 16.3
4. Nuclear trapped electron	Fission electron spectrum. Integral fluxes ca. 10^9 e/cm^2 • s (minutes), ca. 7 x 10^7 e/cm^2 • s (long term)	Charge and dose deposition, secondary emission, backscatter, semiconductor damage, leakage currents, discharges	Same as item 3, but charging rates are faster because of higher fluxes

spacecraft occurs essentially as a DC process. However, when a discharge occurs, it happens in a short time (less than a few microseconds) compared to charging times (upwards of 1 second to hours). Thus, the spacecraft is essentially electrically isolated from the surrounding environment during a discharge. Such isolation is especially important in limiting and controlling the trajectories of the emitted blowoff electrons. Ground testing clearly shows that for an isolated spacecraft, nearly all of the emitted charge is returned to the spacecraft (Refs 2,4), although this charge can travel over distances comparable to a spacecraft dimension before returning to the structure. Thus, it is important to electromagnetically isolate the spacecraft during a discharge. This can be done most conveniently by dielectrically isolating the spacecraft from the tank by the use of a nonconducting pedestal or support straps. During charging, the model will rise to a net negative potential relative to tank ground. Another manner in which isolation can be accomplished is to ground the structure to the tank through a resistor string capable of withstanding potential differences which approach the accelerating potential of the electron guns. The magnitude of such resistances are typically 10^5 to 10^6 ohms, which when combined with the capacitance between

spacecraft and vacuum tank (ca. 100 pF) give RC time constants of 10-100 μs, long compared to the observed discharge pulse widths (ca. 1 μs) for meter sized dielectrics.

In order to maintain electrical isolation of the spacecraft during testing it is important to eliminate stray coupling paths. This must be done for real satellites by monitoring the performance through on-board telemetry or through the use of special sensors whose output is patched into the telemetry or brought out via dielectric data links (fiber optic or microwave). The spacecraft must also be operated on battery during the testing. If the tests are performed in a typical spacecraft thermal vacuum chamber which contains blackened cold walls to simulate the heat sink of deep space, then provision must be made to maintain the proper thermal environment for the spacecraft.

In many ways, a simulated environment tank test of the spacecraft qualification model is technically the most attractive approach. Clearly, it would be a true system test. The excitation mechanism, EID, is the same as that in the space environment. The stress would be applied at the same points; i.e., external dielectrics which are discharge foci so that one could hope to achieve a reasonably faithful excitation of the electromagnetic energy points of entry (POE's). A major unresolved problem is that it is clearly costly and in some cases beyond the state of the art to provide a high fidelity simulation of the space environment. To simulate the components of the space environment, one might include:

1. 0-30 keV electrons (1 na/cm^2)
2. High energy (hundreds of keV) electrons with energies sufficient to penetrate the satellite surface (1 - 50 pa/cm^2)
3. Vacuum UV to produce photoemission
4. UV/Visible
5. Ions.

In addition, it is desirable to simulate the isotropy or lack of same for the individual sources. One technical problem makes performance of a simulation fidelity/cost tradeoff difficult. No clear correlation between discharge characteristics for the space environment and those for ground testing under various simulations has been established. To date, simulation fidelity has been driven largely by cost considerations.

A second set of problems to be faced are those involved in handling the spacecraft, ensuring its safe operation in the tank under test conditions, and providing for power, housekeeping telemetry and special sensor outputs while maintaining thermal balance and dielectric isolation. A sufficiently large vacuum tank with cold walls and

possibly solar simulators or other heat sources must be available for a test of a fully powered system. Most spacecraft manufacturers have vacuum tanks which are large enough to handle at least satellite center bodies for required thermal vac testing. It may be more difficult to find a tank large enough to handle a fully deployed satellite with solar panels while providing adequate room for source illumination. No existing facility is presently instrumented to perform such tests.

Care must be taken to maintain the thermal balance in the spacecraft. In order to satisfactorily operate the electron and ion sources tank pressure must be sufficiently low ($<10^{-5}$T). Pumpdown and maintenance of such low pressures in large vacuum tanks typically requires the use of cold walls. Such blackened cold walls also serve as sinks for the radiatitive transfer of heat generated by spacecraft electronics. The system thermal balance must be carefully controlled so that external components such as the solar panels and antennae are not cooled below low temperature limits, while the electronic components are kept below upper operating temperatures. A study performed by TRW which addressed the feasibility of performing an SGEMP test on FLTSATCOM in a large vacuum tank under similar operating environments, indicates that a proper thermal environment can be maintained (Ref 12).

The requirement that the spacecraft be isolated from the tank during discharge imposes stringent requirements on power and data transmission. During radiation testing, spacecraft power would have to be provided by battery. Because the pumpdown and warmup times in large vacuum tanks are long compared to the times that satellites are typically in eclipse, provision must be made to provide power through a retractable umbilical. Monitoring of satellite functional and special response data would have to be performed with the RF telemetry system and with specially provided dielectric data links. It does not seem feasible to use the ferrite isolation techniques employed for SGEMP testing (Ref. 13) if the results of ground test data which imply that EID pulse widths are much wider (hundreds of nanoseconds to microseconds) that those associated with SGEMP (less than 100 ns) hold for space electron-induced discharges. To minimize reflection of electromagnetic radiation produced by the discharge from the tank walls, an electromagnetic damper coaxial with the tank's inner surface should be provided.

The number of system radiation tests performed on satellites or satellite-like models has been extremely limited. Table 3 describes a representative set of tests. In that table, only the STARSAT test conducted in 1980 and the recently concluded FLTSATCOM tests are comparable in comprehensiveness to what might be involved in performing a system EID satellite qualification test in the simulated radiation environ-

Table 3. Representative Satellite System/Model Tests

Test Object	Type of Test	Radiation Sources	Active Spacecraft Electronic	Thermal Balance with Cold Walls	EM Dampers	Electrical Isolation	References
1. STARSAT (DSCS-III Model)	SGEMP	Nuclear Weapon	Yes	No	Yes	Partial, Signal cables brought out through ferrite loaded stinger.	(13,30,31,)
2. DIABLO HAWK	SGEMP	Nuclear Weapon	No	No	No	Like STARSAT	(14)
3. METEOSAT	EID	Substorm Electrons	No	No	No	Isolating Support	(15)
4. CAN (IRT/NASA)	EID	Substorm Electrons	No (active diagnostic electronics)	Yes	No	Isolation resistor + fiber optics	(2)
5. CAN (JAYCOR/AFWL)	EID	Substorm, ECEMP electrons	No (active diagnostic electronics)	Yes	No	Isolation resistor + fiber optics	(4)
6. SCATSAT	EID	Substorm electrons, ions, UV,CDI, Arc Discharge	No (active diagnostic electronics)	Yes	No	Isolation resistor + fiber optics	(3,5,16,17)
7. FLTSATCOM	SGEMP	Flash X-ray	Yes	Probably Not	No	Fiber Optics	(18)
8. VOYAGER	EID	Arc Discharge	Yes	No	No		(7,33)

ment. A number of issues in regard to instrumentation, provision of power, data recording, and ensuring satellite safety must be solved. Some of these have been addressed in a program whose objective was the planning of a proposed Satellite X-ray Test Facility (SXTF) (Ref. 19). This proposed facility was designed to qualify spacecraft against SGEMP. The facility design provided for a spacecraft charging test capability. However, it does not appear likely that such a facility in which both SGEMP and spacecraft chargin qualification tests could be performed will be constructed in the near future. Thus, on the basis of technical uncertainty, limited test experience, possible spacecraft damage, this qualification approach is one of high risk.

The potential cost of such a test is also high. Up front, one would have to provide the radiation sources, data links and satellite handling equipment and integrate them into a particular test facility. It is hard to quantify these costs because no prior experience is available to draw upon. However, as part of the SXTF program, TRW estimated that the cost for an SGEMP system test of one month duration at an external facility might run as high as $2.3M (in 1980 dollars) (Ref 20). Such a test is probably more complicated to execute than one for EID. However, the cost breakdown provided indicates that actual test conduct (at $11.4K per day) is only about 15 percent of the total cost. More than half of the total cost is due to shipping, equipment preparation, setup, installation and checkout of spacecraft and AGE at the test facility and a repeat of this process at the manufacturer's facility after test. Not included in this cost estimate is the extra analysis and component testing likely to be performed by the manufacturer to ensure satisfactory performance during the test. Also not included is the cost of test fixtures, adapters and equipment unique to the performance of the test.

Such a test would also have a considerable program schedule impact because of the need for pre and postradiation testing functional checkout, shipping, test planning and analysis. These activities, would be made more difficult because many of the aspects of test conduct are not compatible with presently conducted electrical or thermal vac tests. Thus, there would be time delays associated with developing, learning, and validating nonstandard test procedures.

On balance, a qualification test based on exciting a spacecraft with a simulation of the charged particle environment is feasible. Given the present state of the art such testing would present high technical risk, cost and schedule impact and is not likely to be looked on with favor by either manufacturers or System Program Offices (SPO's).

2.2.3 Global Electrical Testing

The essence of this technique is to reproduce the electromagnetic responses evoked by the discharge. One may directly simulate the emission of electrons produced by blowoff in EID or generated by X-ray induced photoelectron emission in SGEMP with the capacitive direct drive technique (CDI). It may also be done by a direct current injection in a manner which mimics the replacement currents which flow on the satellite surface. The role of electrical testing in SGEMP hardening is discussed in References 22 and 23.

The objective is to reproduce as faithfully as possible the external electromagnetic environment around the POE's. An alternative approach is to inject directly into cables or pins current pulses which are similar to those produced by the coupling of external electromagnetic fields into the interior of the spacecraft.

Typically, simulation fidelity for global excitation is measured by how well the tangential magnetic field ($\vec{H}_t$), related to surface currents, and the normal displacement field ($\vec{D}_n$), related to surface charge density, are reproduced as a function of time over the surface of the spacecraft. These fields represent the response of the object to the exciting discharge. They are, in a sense, the electromagnetic boundary conditions for the fields generated by electron emission through the following equations:

$$\hat{n} \times \vec{E} = 0$$

$$\hat{n} \times \vec{H} = \vec{K},$$

$$\hat{n} \cdot \vec{E} = \sigma/\epsilon_o, \qquad (1)$$

for ideal conductors. $\vec{K}$ is the induced surface current density in amps/m, σ is the surface charge density (C/m^2) and $\hat{n}$ is a unit vector normal to the satellite surface. It is to be noted that $\vec{K}$ most clearly corresponds to the concept of replacement current, typically used to evaluate the simulation fidelity of global electrical excitation schemes. However, there are cases where the normal electric fields are more important in coupling energy into POE's.

In order to evaluate various simulation approaches, it is useful to briefly summarize the existing data base. These serve as a baseline for the evaluation of proposed practical electrical injection schemes. The bulk of the EID coupling data for satellite like objects has been obtained in two simulated environment tests of right circular cylinders, covered on one end with a dielectric, described in References 2 and 4. For the latter series of tests, data was also obtained for two reentrant geometries

attached to the cylinder. One was a small solar array panel mounted on a boom attached to the end of the cylinder. The second was a mesh antenna mounted on the end of the cylinder facing the elecron sources. In addition, some information on the external electromagnetic fields produced by discharges is presented in Reference 21. Unfortunately, the P78-2 is not well instrumented to provide a direct measure of $\vec{K}(\vec{r},t)$ and $\sigma(\vec{r},t)$ for discharges produced on surface dielectrics by the space charging environment. All but one of the transient monitoring sensors are separated from the exterior surface by one or more conducting interfaces. Interpretation of the transient data is made difficult because the coupling between the surface electromagnetic fields and the transient sensors depends not only on the specific geometry but also on the discharge location. Electrical testing of the SCATSAT (Ref 3) has shown that the transfer function which couples discharges produced at various dielectric surfaces on the satellite into a particular internal sensor can vary by factors of 10 or more. Thus, it is difficult to infer discharge amplitudes from these sensors.

The EID coupling data has been discussed in Reference 2 and will only be reviewed here. There are two key issues: what is the nature of the discharge driver; what are the responses produced. Based on the ground test data the following picture has emerged.

1. When a dielectric is irradiated by nonpenetrating electrons (those whose range is less than the dielectric thickness, the material will reach charge equilibrium or will breakdown at a threshold voltage V_B. Experimental evidence indicates that V_B depends on material, geometric configuration, especially the location of ground planes and edges, and the charging environment in a manner which is not well understood.

2. Should discharge occur, a fraction of the embedded electron charge is blown out the front surface of the dielectric, and a fraction may flashover to a conducting edge or substrate.

3. In nearly every case studied, the predominant generator of electromagnetic effects, replacement currents and surface charge, is the blowoff electrons. The primary effect of flashover and punchthrough are to decrease the dielectric surface potential relative to the conducting frame of the spacecraft. Based on electrical testing reported in Reference 3, in which the effect of blowoff was simulated with the capacitive direct drive technique described below, the blowoff component of the discharge also produces the

largest internal wire responses in most cases. One exception to this observation is that strong coupling can occur when a punchthrough or flashover discharge occurs in close proximity to the wire into which energy is coupled.

4. The emitted electrons move in the electromagnetic fields whose sources are electrons trapped in the dielectric, structural replacement currents and charge and other emitted electrons.

5. The electrical isolation of the spacecraft during discharge leads to space-charge limiting of emission for discharges occuring in all but the smallest area dielectrics. Most of the blown-off electrons return to the structure although they may travel over distances comparable to a spacecraft dimension before doing so.

6. Based on ground testing of edge grounded planar samples, a series of scaling laws have been developed which relate dielectric area to charge removed in a discharge (Q_p), peak blowoff current (I_p) and discharge pulse width (τ_p). These laws are

$$\begin{aligned} Q_p &\propto A, \\ I_p &\propto A^{1/2}, \\ \tau_p &\propto A^{1/2} . \end{aligned} \tag{2}$$

The scaling laws for particular dielectrics were derived primarily by measuring the response of circular, edge grounded samples exposed to electron beams of energies of ca. 20 keV, and include fluxes of ≥ 1 na/cm^2 and are summarized in Table 4. As the data presented in Reference 2 shows, the response of individual samples display fluctuations of an order of magnitude or more about the mean depending on sample configuration and exposure conditions.

7. The implication to be drawn from the ground tests are that EID in large dielectric structures can involve peak currents of hundreds of amps and pulse widths of the order of 1 μsec or greater. Such pulses are much greater in pulse width and amplitude than the MIL-STD 1541 arc. A key unresolved issue is whether similarly large discharges occur in spacecraft dielectrics exposed to the actual space environment. As we have pointed out in

Table 4. Summary of Discharge Scaling Laws

Material	$I_p(\text{amps}) = K_I A(\text{cm}^2)^{n_I}$		$\tau_p(\text{ns}) = K_p A(\text{cm}^2)^{n_p}$		$Q_p(\mu\text{C}) = K_Q A(\text{cm}^2)^{n_Q}$	
	K_i	n_I	K_p	n_p	K_Q	n_Q
Teflon[a]	10	0.58	16.5	0.48	0.18	1.06
Kapton[a]	5.6	0.51	21.9	0.59	0.15	1.00
Mylar[a]	10	0.59	18.2	0.46	0.21	1.05
Fused Silica[b]	0.81	0.6				

[a]From Reference 24.

[b]From Reference 2.

Reference 2, most of the elements of that environment typically not included in ground simulations such as distributed low-energy and high-energy (penetrating) electrons, ions and vacuum UV tend to diminish or even eliminate discharging in most surface dielectric structures tested to date.

8. The discharge-induced response of simple CAN-like objects is reasonably well understood and therefore an electrical simulation can be developed with reasonable confidence in its fidelity. The observed surface replacement currents are comparable in magnitude and pulse width (although narrower and lower in amplitude) to those of the exciting pulse. The CAN is a nonresonant low-Q object. The body modes of this object which have resonant frequencies ≥70 MHz are only weakly excited. However, the important case is a highly resonant satellite containing booms, solar panels, and antennae. As these objects typically have resonant modes above 20 MHz, they too may only be weakly excited by the relatively low frequency content of the large amplitude discharges. The experimental data can be reproduced in a model in which the response of the object is generated by the self-consistent motion of blowoff electrons in external electromagnetic fields. A worst case occurs for the test object grounded to the surrounding environment (plasma or tank). Here, the surface replacement currents generated can be taken to be identical to the blowoff discharge current pulse.

9. There are significant gaps in our knowledge of the details of the discharge emission process in terms of emission energy distribution, spatial distribution, plasma effects, and configuration effects which make it difficult to predict the response of a typical spacecraft configuration to an arbitrary EID excitation. There is little ground test data for realistic spacecraft structures, i.e., those with booms, antennae, solar array panels, etc., on which to

develop a more accurate model. Attempts to reproduce the observed EID responses for a structural model with reentrant geometries such as antennae, have required ad hoc assumptions about the emission characteristics of the discharge which are not consistent with those made to model the response of more simple structures. Both the electron spraying experiments reported in Reference 4 and the electrical testing of the SCATSAT reported in Reference 5 demonstrate in a quantitative manner how the addition of such reentrant geometries alters the basic body response.

10. This gap in our knowledge has two implications for the development of validated electrical test procedures for the EID qualification of spacecraft. First, a lack of valid discharge models makes it difficult to predict discharge thresholds for specific material and geometry configurations. One must depend on poorly validated empirical scaling laws to predict the magnitude of the discharge drivers which determine the EID responses. Second, there is a lack of both a validated coupling model and a detailed experimental data base by which we can estimate $\vec{K}(\vec{r},t)$ and $o(\vec{r},t)$ on realistic spacecraft structures as a basis for development of a comprehensive set of test techniques. Yet this is the real case of interest.

However, on the basis of electrical and electron spraying tests performed to date the following seems clear:

1. The present MIL-STD 1541 arc is a poor simulation of the effects produced by blowoff as measured by the amplitudes, pulse widths and distribution of the surface replacement currents generated and the magnitude of the internal wire responses evoked. The existing test data indicates that the surface current pulse widths are much too narrow (50 ns or less versus 0.1-5 s for EID) and the amplitude of the replacement currents generated are two orders of magnitude too low, except possibly close to the exciting arc. Similarly, the SCATSAT electrical test data indicates that the amplitude of the internal wire responses evoked by a capacitative direct drive excitation (CDI) simulation of blowoff are typically much larger per amp of drive current than those evoked by a MIL-STD 1541 arc, though the difference observed is smaller than those found for surface currents. It is to be noted that this finding remains to be validated by electron spraying of a complex satellite-like object (or real satellite) containing realistic structural

shielding, cable bundles and electronic box layout.

2. In principle, CDI provides a better simulation of the surface current patterns produced by a blowoff discharge in a simple symmetric object. The implications of the electrical testing of the SCATSAT reported in Reference 3 are that CDI also produces more valid internal cable responses. Whether it is possible to develop a practical implementation of the CDI technique which gives proper pulse widths and current amplitudes or whether some other technique such as direct injection will be examined in Section 2.3.

For a more detailed discussion of these points the reader is referred to References 2 through 5 and Reference 10.

One may summarize the relative advantages of a global system electrical test. First, if conducted at a high level, it is a true system test which can test the validity of all of the design features including structural, cable and box shielding, and current interface protection. The simulation fidelity of a high level test is only fair with the available practical test techniques for global simulation, but can be good around particular local POE's. However, these tests provide a better simulation of EID electromagnetic responses than any of the presently utilized approaches. The technical risk involved in such testing is that the specific procedure has not been tried on satellite models or real satellites. However, similar electrical tests have been performed successfully for SGEMP qualification. A key test issue is the need for high voltage pulsers ($\leqslant$50 kV), capable of being operated in a mode in which they are isolated from ground, and the need for isolated data links. Both of these are required because the interaction between the satellite and the external environment must be minimized. However, suitable pulsers and data links exist. These electrical tests are relatively compatible with standard EMC testing. One possible difference is the requirement to dielectrically isolate the spacecraft. This means that the spacecraft must be run on battery power, and that the AGE must be disconnected from the S/C during tests. Data must be taken with special dielectric isolated sensors and data links and through the S/C telemetry system. Because these tests are purely electrical, they can be performed as part of the manufacturers EMC testing with relatively moderate cost and schedule impact. In addition to the costs and time devoted to the actual test, some effort will have to be devoted to developing a pulser, data links, and a test stand. Given the progress in the development of test hardware of this type, it is likely that by

the time the test standard is implemented, suitable pulsers and data links will be available commercially.

2.2.4 Subsystem and Component Tests

Two additional methods of performing qualification testing are by electrical excitation of complete subsystems comprising several functional units or "boxes" connected together by their cabling and by the test of individual boxes. In box testing one may drive all of the box pins simultaneously, or one by one.

The idea behind the use of box testing as a qualification technique is the following. Surface electron discharges generate electromagnetic fields. These fields enter the interior of the spacecraft through POE's where they can couple into wires in the cable bundles and into the boxes themselves. For well shielded boxes, the primary method of coupling is into cables and connectors. This is somewhat different than the case for SGEMP where the exciting x rays penetrate the interior of the spacecraft, generate internal fields through x-ray-induced photoemission (Internal Electromagnetic Pulse Effect or IEMP) which can then couple into cables or boxes. The x rays can also directly inject charge into cables or electronics. In this sense, ECEMP is a similar effect in that it is due to the direct injection of the penetrating high energy electrons with cable dielectrics or printed circuit boards.

The idea behind subsystem and component testing is that one directly excites the vulnerable elements, the cables leading to interface circuits and the interface circuits themselves.

To perform box and component testing the following steps must be taken:

1. Discharge source terms must be developed for possible points of excitation. This may be done by analysis, by using the guide given in Sections 3.5 and 3.6 or by testing of sample panels.

2. A model must be developed which predicts the response of the spacecraft to the EID and provides the external electromagnetics field environment. This may be done either analytically using a lumped element approach with an SGEMP code, or with an EMC code such as IEMCAP.

3. The signals generated on individual wires must be calculated based on the predicted internal EM environment. One means of performing this analysis is by modeling the cable bundles and wires in terms of lumped-element transmission lines and solving with a network analysis code such as TRAC. It may

be possible to combine the modeling effort of Steps 2 and 3. Alternatively, electrical transfer functions which relate wire responses to external excitations may be determined experimentally.

4. Based on the cable and pin specs computed in Step 3, current injection techniques (waveshapes, levels, phasing) must be developed to produce the correct signal levels including the necessary 6 dB overstress. Note that any analysis uncertainties must be taken into account. Thus, if an analysis approach has an uncertainty of $\pm$ 12 dB, critical test points must be driven by 18 dB above the estimated internal environment.
5. Pulsers to provide the necessary drive levels must be designed and constructed or procured.

Subsystem or functional electrical testing is on its face a very attractive method of verifying survivability. Such electrical testing is now routinely performed to demonstrate the SGEMP hardness of satellite electronics. Its major advantages include:

1. Functional simplicity
2. Compatability with other subsystem electrical testing
3. Can be an engineering development test so that design faults in components may be detected and corrected before the entire system is assembled.
4. Critical electrical test points are stressed directly with known signals.

There are several major disadvantages inherent in depending on subsystem tests for system qualification. Two of these are inherent and two relate to the technical immaturity of the state of our knowledge about internal EID effects. The major technical deficiencies include:

1. Subsystem and component testing does not test those electromechanical design features such as box, cable and structural shielding, box and cable placement, and cable routing which are an important part of electromagnetic hardening.
2. Subsystem, and, more importantly, box testing may not show upsets which depend on the interaction of the system as a whole.

The difficulties relating to our state of knowledge about EID coupling include:

1. There is little direct data on the kinds of interior wire responses produced by EID. While there is a growing but still small transient data base for the

P78-2, there are two problems in evaluating this data. First, the satellite has only one sensor (the SC1-4 dipole) which can provide information about the nature of the discharges or the external transient surface electromagnetic fields generated. Thus the space environment discharge sources are not well characterized. The transient response produced on interior circuitry depends on the details of the satellite electromagnetic configuration. A detailed coupling model has not been prepared for the P78-2 to permit maximum use of this data.

2. These are inherent and potentially large uncertainties inherent in the coupling analysis of systems as complicated as a spacecraft. These uncertainties are related to the fact that relatively complicated systems are modeled with relatively simple coupling models. The dependence on such analysis increases the error budget associated with determining EID safety margins. This requires testing and design to survive levels of stress higher than actually necessary. Specific subsystem test approaches are presented in References 23, 25, and 26.

Thus, while subsystem and box testing is an alternative method of ensuring system compliance, it does not provide a true unambiguous system test.

2.3 REVIEW OF GLOBAL ELECTRICAL EXCITATION TECHNIQUES

2.3.1 Introduction

The objective of this section is to define a practical electrical injection technique which can provide a valid worst case electrical stress of a satellite to simulate the effects of electron induced discharge. To arrive at the optimum test methodology, a variety of previous test techniques and test results were reviewed. These included EID simulation tests as well as SGEMP current injection methods and tests.

From the above, the basic test options available for EID simulation are extracted. Their relative advantages and disadvantages are characterized. This calculation has used the limited quantitative data base for the EID response of satellite objects, based on the ground test data presented in References 2 and 4, and the electrical test data of Reference 5 and summarized in the preceding section. These data provide a worst case based on the amplitude, pulse widths and spatial distributions of the surface currents generated by EID. The output of the feasibility calculations described below have yielded test methodologies described in Section 3 which, it is felt, will provide the best

tradeoff between known response characteristics and practical test techniques. We must reiterate that the existing data base on which the test procedures have been generated is extremely limited and should be extended by measuring the response of highly resonant satellite structures with reentrant geometries and by quantitatively comparing the P78-2 and SCATSAT EID and electrical testing responses.

2.3.2 Comparison with SGEMP

In an attempt to extend the available data base it is valuable to review some of the testing performed to simulate system generated electromagnetic pulse (SGEMP) effects in satellites. This testing has been used to simulate the replacement currents and charges induced on a satellite surface when the X-ray pulse created consequent to the exoatmospheric detonation of a nuclear weapon interacts with the satellite to cause the expulsion of electrons from its surface. This process is similar in many ways to EID coupling because in both cases the electromagnetic driver is the electrons emitted from satellite surfaces that subsequently move in the fields whose sources are replacement charge induced in the satellite structure and the other emitted charge. In the case of EID, the satellite dielectric may be initially charged and these embedded charges themselves also serve as a source for the accelerating fields. Of course, precharging by space electrons may also affect SGEMP photoelectron motion.

However, there are significant differences in the electron emission characteristics for SGEMP and EID which bear on attempts to develop an electrical simulation. These differences are summarized in Table 5. It is to be noted that in both cases spacecharge limiting can occur to diminish charge emission amplitudes and pulse widths. One of the more significant differences is that the pulse widths characteristic of SGEMP are less than 100 ns, while ground tests imply that those associated with EID are upward of 100 ns to microseconds for discharges occuring on dielectrics of sizes typical of that found on spacecraft. A second major difference is in the rate of rise of the exciting pulses. For EID, these are typically of the order of 10^8 A/s. For SGEMP, rates of rise are typically two orders of magnitude higher.

The basic methods of response testing for both SGEMP and EID fall into the five categories described earlier in this chapter. Several of the tests described in Table 3 were phenomenology tests to study the SGEMP response of satellites and satellite models. A great deal of work has been carried out to evaluate and define electrical simulation techniques for SGEMP structural current excitation. A theoretical evaluation of the fidelity of various approaches to electrically simulate SGEMP replacement

Table 5. Comparison Between SGEMP and EID

	EID	SGEMP
1. Exciting Source	Electrostatic Discharge	X-ray photoelectron emission
2. Approximate Scaling Laws for Emission		
a. Emitted Charge	$Q_p \propto A$ (175 μC for 1m^2 SiO_2)	$Q_p \propto \Phi$, incident X-ray fluence (~1.4 μC for 1 cal/m^2, 2 keV BB incident on SiO_2)
b. Peak Emitted Current	$I_p \propto A^{1/2}$ (200A for 1 m^2 SiO_2)	$I_p \propto Q_p/\tau_x$, where τ_x is X-ray pulse width I_p = 1400A for 10 ns pulse
c. Emission Pulse Width	$\tau_p \propto A^{1/2}$	$\tau_p \propto \tau_x < 0.1$ μs.
3. Electron emission Characteristics		
a. Energy Distribution	Unknown (E<10 eV?)	Backemission: $n(E) \propto e^{-E/\bar{E}}$ where $\bar{E} \leq k_B T$, X-ray blackbody temperature
b. Angular Distribution	Unknown (Isotropic?)	Backemission: $n(\theta) \propto \cos\theta$, where θ is measured relative to surface normal
c. Other features	Plasma evidently emitted along with blowoff electrons	
4. Parametric dependence	Material Geometry (location of ground planes & grounded edges) Charging environment Flux	Material X-ray spectrum Fluence Flux

currents is given in References 27 through 29. Because it was realized that in many ways EID is similiar to SGEMP, it was natural to modify and utilize as many of the analyses and test techniques developed for the latter in this program. For example, the CDI technique was developed to simulate the spacecharge limited emission and subsequent motion of X-ray generated photoelectrons. As we have shown in Reference 2, CDI in principle also simulates reasonably well the surface currents generated in an isolated satellite driven by the blowoff of electrons. The difficulty, as we shall see, lies in development of a practical CDI excitation scheme capable of producing the required pulse widths and amplitudes.

As a background, it is useful to review briefly some of the recent SGEMP and EID electrical tests which have been conducted on satellites and satellite models. All of the schemes which have been employed to globally excite spacecraft or spacecraft models fall into two basic categories. In the first, the discharge pulse is capacitively coupled into the test object. In the second, current is directly driven onto the body of the satellite (direct drive) through one or more conductors. Current is returned to the common ground plane either through the capacitative coupling between the test object

and that plane or by a direct conducting path. Generally, the pulser is based on charging a capacitor which is rapidly switched into the coupling network. Pulse shaping is determined not only by the charging switch but also by the electrical characteristics of the coupling network and the test object.

There is a third category of electrical excitation produced by coupling electromagnetic fields onto the object. One example of this is exposure to a plane wave. More relevant is the MIL-STD 1541 test in which the satellite is excited by the arc generated electromagnetic fields. Such excitation in both cases produces a relatively poor simulation of the electromagnetic fields induced on the satellite surface by either EID or x-ray-induced electron emission Reference 28.

The conclusion of these SGEMP related model studies is that it is very difficult, if not impossible, to reproduce $\vec{H}_t$ and $\vec{D}_n$ everywhere on the satellite surface using a local excitation. It is possible to reproduce some aspects of these fields reasonably accurately over limited areas of the satellite surface. The choice of which simulation approach to take then depends on which aspect of the electrical response is important in determining coupling into particular POE's (Ref 30). For example, the data presented in Tables 10 and 11 of Reference 2 indicate that a capacitative discharge excitation of the dielectric covered surface of the CAN with a pulse shape and amplitude similar to that for the blowoff discharge reproduces the surface current pattern reasonably well (factor of 2 or better in amplitude) at points away from the drive wire provided that one adjusts the drive plate to CAN distance to approximate that over which the blowoff electrons travel before returning to the CAN. A similar result applies for the simulation of the SGEMP excitation of a satellite center body. Less well simulated in the latter case are the body $\vec{E}$ fields. In both the EID case, and for SGEMP the tangential $\vec{H}$ fields will be much too large while the normal $\vec{E}$ field will be too small near the drive wire. The reason that the CDI injection with a pulser isolated from external ground provides a good simulation of the tangential magnetic fields is that this electric injection technique provides a reasonable simulation of the exciting process, which is a combination of electron emission and the displacement current created by the transfer of charge from the satellite surface to the electron cloud; i.e., the surface currents generated and the charge density on the emitting surface both have the correct polarity.

For other cases, such as field penetration into small apertures, it may be more important to simulate the normal electric fields at the aperture to obtain the best simulation of coupling to the interior of the spacecraft.

Clearly, considerably more work is required in both the areas of testing and modeling of both EID and electrical injection responses invoked in a variety of satellite geometries containing representative POE's. The approach taken here is that the limited data base available indicates that it is important to best simulate the electromagnetic response evoked by the blowoff of electrons and that the present MIL-STD 1541 are a poor simulation of this.

2.3.3 Representative Current Injection Tests

To assess the current state of the art in the global electrical testing of satellites it is useful to look at some of the recent tests performed. We have taken examples from three programs. An extensive series of electrical testing was performed on the STARSAT, a simplified version of the DSCS-III satellite as part of the program which culminated in the Huron King UGT described in References 13 and 30 through 32. Also briefly reviewed are the electrical excitations of the SCATSAT and CAN designed to simulate EID blowoff with the CDI techniques (Refs 2,5). As an example of a system electrical test designed to qualify a spacecraft against EID, the Voyager tests are described in References 7 and 33. In the discussion which follows, each test setup has been modeled using the basic circuit shown in Figure 1. In some cases, complete test reports were not available and as a result, some pertinent test parameter values are not known.

General Electric performed CDI testing on the STARSAT satellite mockup while it was installed in the vacuum tank used in the Huron King Underground Test (Refs 13,32). The basic excitation was produced by discharging a capacitor onto the south solar array paddle through a low impedance current path. The pulse generator was capacitively coupled to the test object, and the test object was capacitively coupled to the ground of the pulse generator. Figure 2 shows the basic test setup, the equivalent electrical circuit, and pertinent test information. The noteworthy points for this case are:

1. The injected current waveform was determined by the interaction of the pulse generator electrical parameters and the equivalent electrical parameters of the test object.

2. To drive threat level currents onto the solar array, a low impedance coupling path was necessary. This changed the ringing frequency of the STARSAT

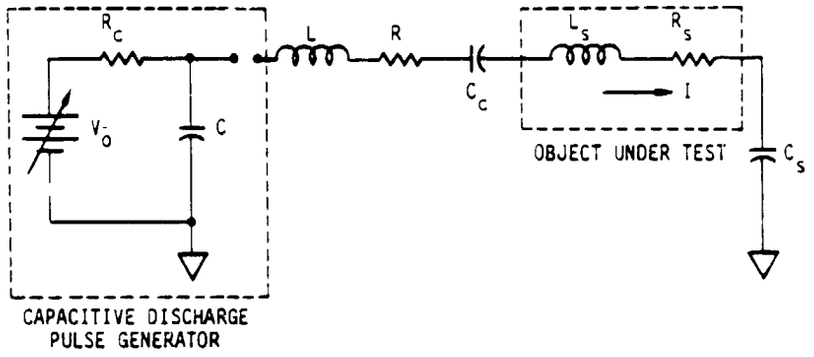

ADJUSTABLE CIRCUIT PARAMETERS

- V_O = ADJUSTABLE CHARGING VOLTAGE
- R_C = CHARGING RESISTOR
- C = DRIVE CAPACITOR
- L = ADDED INDUCTANCE FOR WAVESHAPING
- R = ADDED RESISTANCE FOR WAVESHAPING
- C_C = CAPACITIVE COUPLING BETWEEN PULSE GENERATOR AND TEST OBJECT
- L_S = NOMINAL INDUCTANCE OF TEST OBJECT
- R_S = NOMINAL RESISTANCE OF TEST OBJECT
- C_S = CAPACITANCE BETWEEN TEST OBJECT AND PULSE GENERATOR GROUND
- I = BODY CURRENT OF TEST OBJECT WHICH IS CHARGING CURRENT FOR C_S

FOR DIRECT DRIVE, C_C AND C_S ARE REMOVED FROM CIRCUIT.

RT-20911-1

Figure 1. General discharge injection model

mode of response excited from 1/2 wavelength or about 19 MHz for the 7.9 M (tip to tip) long satellite to 1/4 wavelength or about 10 MHz.

3. Isolation of the spacecraft structure during the pulse (except for capacitive coupling between the S/C and tank) was provided by loading the boom through which signal cables were run with ferrite chokes.

4. A direct injection test was performed on DSCS-III in which a 10-ns rise-time, 40-ns wide, 300-A peak/peak pulse was driven between points A and B in the figure, which was viewed as both an ESD and SGEMP qualification test. No telemetry upsets or state changes were observed or damage detected.

JAYCOR (Ref 30) performed several subthreat level electrical tests on the STARSAT to excite various POE's. Two of the test configurations are shown in

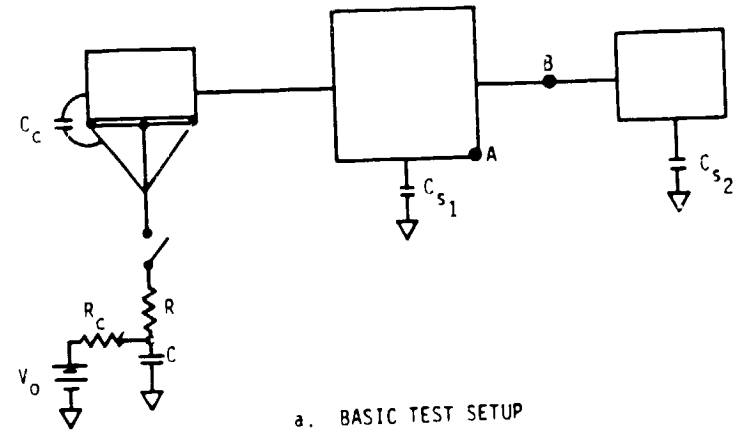

a. BASIC TEST SETUP

R_c: CHARGING RESISTOR
C: DRIVE CAPACITOR, UNKNOWN VALUE
R: DAMPING RESISTOR, 50Ω
C_c: COUPLING CAPACITANCE, UNKNOWN VALUE
C_s': EQUIVALENT CAPACITANCE TO GROUND $C_{s1} + C_{s2}$, ≈150 pf
L: TEST OBJECT INDUCTANCE, UNKNOWN VALUE

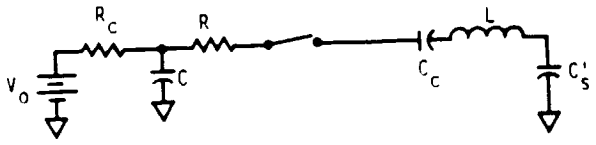

b. SIMPLIFIED EQUIVALENT ELECTRICAL CIRCUIT

TYPE OF TEST: CAPACITIVE DISCHARGE WITH CAPACITIVE COUPLING
CHARGE VOLTAGE, V_o: ≤25 kV, EXACT VALUE UNKNOWN
PEAK CURRENT DRIVEN: 137 A, ZERO TO PEAK
WAVEFORM: DAMPED SINUSOID, 350 ns LONG, τ_r ≈10 ns, RINGING FREQUENCY PREDICTED TO BE 10 MHz
INSTRUMENTATION: HARDWIRE WITH FERRITE CORES FOR LIMITED ISOLATION, S/C TELEMETRY
OTHER INFORMATION: UGT TANK HAD ELECTROMAGNETIC DAMPER. ELECTRONICS ACTIVE DURING TEST.

RT-21031

Figure 2. Setup for General Electric test of STARSAT in the Huron King Underground Test tank

Figures 3 and 4. In the first, the intent was to selectively excite a solar panel and preferentially drive the solar array power line penetration into the center body which is the major POE on the STARSAT. To decouple the pulses from the test object to excite the natural body resonance, a 1 kΩ isolation resistor was inserted in series with the output of the pulser. This significantly reduced the amplitude of the currents on the boom by about a factor of 7.5 compared to the high level test if scaled to equal exciting pulser voltages. To drive a similar amount of current on the solar array boom with a high impedance source of the type used would require a pulser capable of producing 200 kV.

In the second test, the center body was excited via the CDI technique. The exciting pulse width was not described in Reference 30 but is probably about 10 ns. The

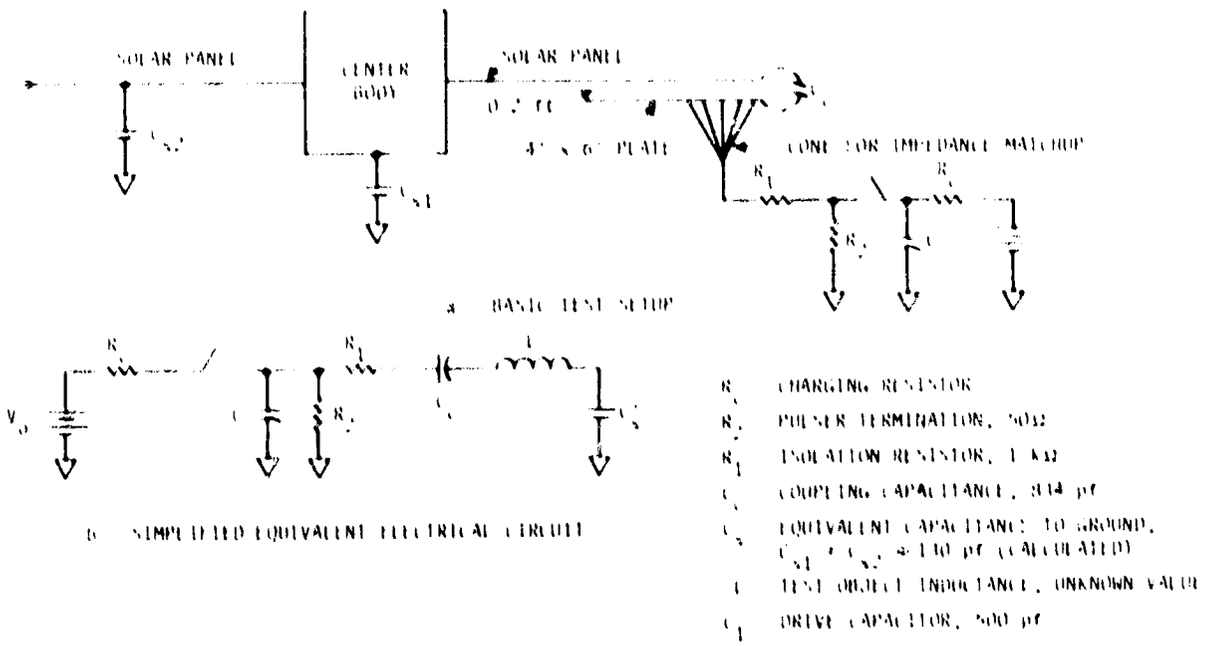

TYPE OF TEST — CAPACITIVE DISCHARGE WITH CAPACITIVE COUPLING

CHARGE VOLTAGE — ca 1 kV, NARROW PULSE (EXACT CHARACTERISTICS UNKNOWN)

PEAK CURRENT DRIVE — ca 1.5 amp ON BOOM (BASED ON G.E. DESCRIPTION OF JAYCOR RESULTS)

WAVEFORM — DAMPED SINUSOID, RINGING FREQUENCY ≈ 20 MHz, 250 ns LONG

INSTRUMENTATION — FIBER OPTIC AND FERRITE ISOLATION (LITTLE DIFFERENCE IN TEST DATA NOTED AT EARLY TIMES, BUT FERRITE DID AFFECT LATE TIME)

OTHER INFORMATION — EXACT PULSER CHARACTERISTICS UNKNOWN, BUT APPARENTLY A VARIATION OF MERCURY WETTED SWITCH WITH A CIRCUIT ADDED TO SLOW THE VERY FAST RISE TIME OF SUCH SWITCHES. TEST OBJECT IS SUSPENDED OVER ca 40 SQ GROUND PLANE 4 FEET FROM BOTTOM OF CENTER BODY

Figure 1. Low-level electrical test of STARSAT (solar panel excitation)

current induced in the solar array booms is probably less than 5 amps based on IRT's experience with pulsers of this type. To drive a threat level boom current (270 A), the pulser charging voltage V_o would have to be in excess of 50 kV.

For both current injection schemes, the effect of dielectric isolation was investigated. Dielectric isolation was achieved by using a battery operated pulser and fiber optic link to record data. Ferrite core isolation was implemented by wrapping the power cords of both the pulser and oscilloscopes around several ferrite cores. It was found that the peak amplitudes of currents coupled to interior cables were equal for both isolation methods. Waveform agreement for external and large internal currents was good for the first 100 to 150 ns. In later times a frequency shift or damping increase was showed by the ferrite isolated signals. Small internal currents showed good waveform agreement at longer times. Thus, it appears feasible to conduct SCATHP

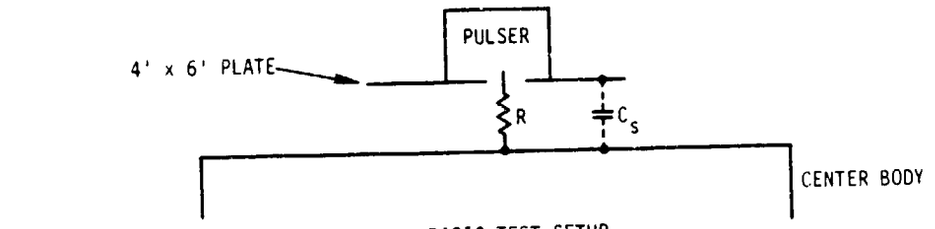

a. BASIC TEST SETUP

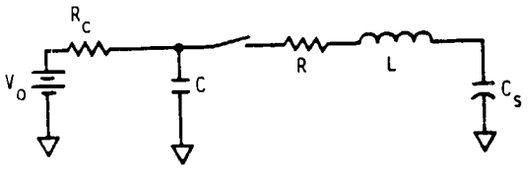

R_c: CHARGING RESISTOR
R: DAMPING RESISTOR, 200 Ω
L: WIRE AND TEST OBJECT INDUCTANCE (UNKNOWN VALUE)
C_s: RETURN PATH CAPACITANCE (UNKNOWN VALUE)
C: DRIVE CAPACITOR (UNKNOWN VALUE)

b. SIMPLIFIED EQUIVALENT ELECTRICAL CIRCUIT

- TYPE OF TEST: CAPACITIVE DISCHARGE, CAPACITIVE DIRECT DRIVE (CDI)
- CHARGE VOLTAGE: V_o ca. 1 kV PEAK, NARROW PULSE, EXACT CHARACTERISTICS UNKNOWN
- PEAK CURRENT DRIVEN: UNKNOWN (BUT $\leq$5 amps)
- WAVEFORM: DAMPED SINUSOID, RINGING FREQUENCY $\simeq$20 MHz, 250 ns LONG
- INSTRUMENTATION: FIBER OPTIC AND FERRITE ISOLATION (LITTLE DIFFERENCE IN TEST DATA NOTED AT EARLY TIMES, BUT FERRITE DID AFFECT LATER TIME)
- OTHER INFORMATION: EXACT PULSER CHARACTERISTICS UNKNOWN, BUT APPARENTLY A VARIATION OF MERCURY WETTED SWITCHING PULSE GENERATOR, CIRCUIT ADDED TO SLOW VERY FAST RISE TIME.

RT-21027

Figure 4. Center body excitation test of STARSAT

electrical testing usng ferrite isolation of pulsers, and data channels. However, the EID exciting pulses are typically much wider than those associated with SGEMP and it is not believed that the ferrite isolation approach would work for EID testing unless the exciting pulses are narrower than believed. However, as the need to dielectrically isolate the spacecraft and data recording channels significantly increases the difficulty of performing the qualification test, the degree to which such isolation is necessary to preserve correct internal responses should be futher investigated. In the absence of firm experimental evidence, the conservative approach is to maintain dielectric isolation of the system under test. This in turn makes the selection of a pulser more difficult if it is desired to perform a threat level test. As the model studies discussed later in this section indicate, one would have to specially design a pulser with the desired characteristics of compact size and dielectric isolation, yet capable of outputting more than 100 kV.

In support of the SGEMP Analysis Verification and the SCASAT tests, IRT and NASA LeRC performed both CDI injection and arc excitation of the CAN and SCATSAT

which are described in detail in References 3, 5, and 34. The basic test setup for the CDI injection is shown in Figure 5 and for arc injection is shown in Figure 6. The following points are to be noted:

1. Away from the location of drive wire, larger responses were produced for the narrow (10 ns) CDI pulse than wide pulse (30 ns) CDI. This effect can be seen qualitatively in the data presented in Table 11 of Reference 2. The reason for this is that as plate spacing is decreased to increase plate to CAN capacitance (C_s), the CDI drive becomes more like that of current injection by a single wire or an arc discharge. Such direct injection typically produces a surface current response which is large near the exciting wire or arc but much smaller elsewhere. This is evident in the arc discharge data summarized in Table 11 of Reference 2.

2 The CDI excites resonant frequencies on the SCATSAT configured with booms (which makes it a more resonant or higher Q object than a simple cylinder). The relative strength of the mode excited depends on drive point. It is possible to relate some of the observed modes to structural features of the model. However, the electrical tests which were performed utilized a relatively narrrow pulse with significant frequency content in the range between 35-200 MHz which covers most of the observed structural resonances for the SCATSAT. The observed EID pulse is much wider, and has significantly less energy in that frequency band. Therefore EID or an electrical simulation thereof is expected to excite these modes much more weakly. This was evident in the CAN tests in which it was observed that the basic body responses followed the exciting pulse. The high frequency component between 50-70 MHz associated with the excitation of the fundamental circumferential mode of the CAN had an amplitude estimated to be only a few percent of the total pulse.

3. When the capacitance between the return plate and the test object was increased by decreasing the plate-to-test-object spacing, resonances were observed which are associated with the combined pulser-test object system rather than the test object itself.

4. For the arc discharge excitation of the CAN the basic wave shapes observed using fiber optic and hardwire transmission of $\dot{B}$ data were similar. Measured amplitudes differed by up to a factor of 2.

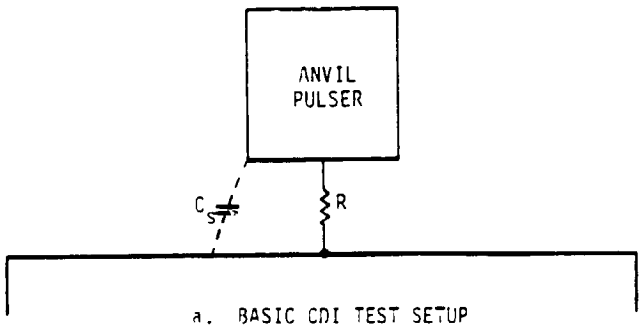

a. BASIC CDI TEST SETUP

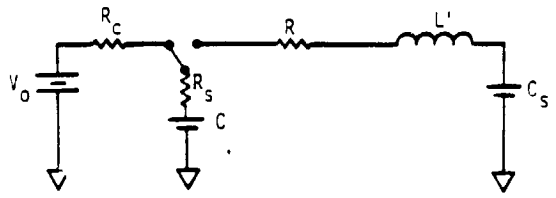

b. SIMPLIFIED EQUIVALENT ELECTRICAL CIRCUIT

TYPE OF TEST: CAPACITIVE DIRECT DRIVE (CDI)
V_o: 320 V
R_c: CHARGING RESISTOR, UNKNOWN VALUE
C: DRIVE CAPACITOR, 1100 pf
R_s: SOURCE IMPEDANCE, 50 Ω
R: DAMPING RESISTOR, 100 Ω
L': TEST OBJECT AND DRIVE WIRE INDUCTANCE (CALCULATED TO BE 0.1 μH FOR NARROW PULSE AND 2.1 μH FOR WIDE PULSE)
C_s: CAPACITIVE RETURN (CALCULATED TO BE 10 pf FOR NARROW PULSE AND 200 pf FOR WIDE PULSE)
DRIVE PULSE: NARROW PULSE (MEASURED) $\tau_r \approx 3$ ns, 20 ns FWHM
WIDE PULSE (MEASURED) $\tau_r \approx 10$ ns, 45 ns FWHM
DRIVE CURRENT: NARROW PULSE ≈0.9 amp, WIDE PULSE ≈1.4 amp

RT-21028

Figure 5. IRT CDI test of the CAN and SCATSAT

The Jet Propulsion Laboratory performed an extensive series of tests on the Voyager Physical Thermal Model (PTM) and the actual flight model. These tests represent the most comprehensive satellite EID program reported in the literature as it included extensive analytical predictions of the response of critical circuits to both laboratory and predicted space discharges, materials testing in a charged particle

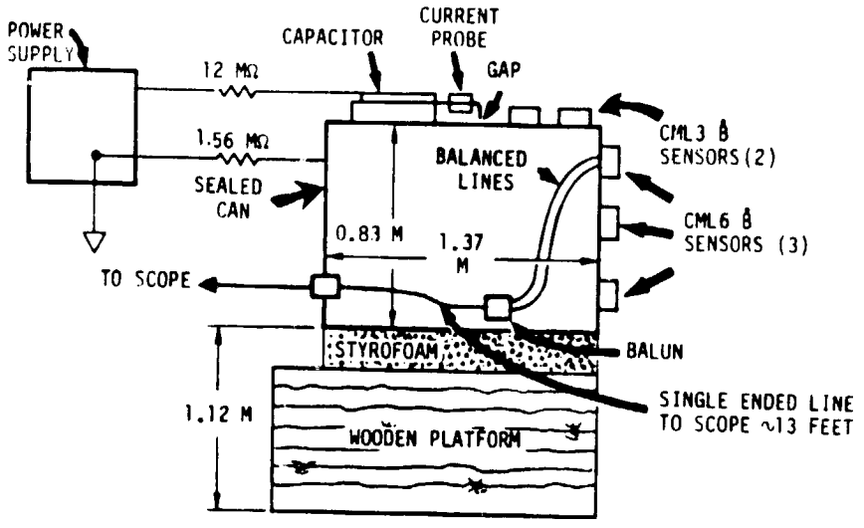

(a) EXPERIMENTAL SETUP. THE THICKNESS OF THE CHARGING CAPACITOR AND GAP SIZE ARE EXAGGERATED TO SHOW DETAIL.

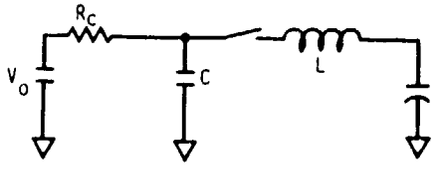

R_C: CHARGING RESISTOR, 13.56 MΩ
C: CHARGING CAPACITOR, 60 nF
L: INDUCTANCE OF SPARK GAP AND TEST OBJECT, VALUE UNKNOWN

(b) EQUIVALENT ELECTRICAL CIRCUIT

TYPE OF TEST: CAPACITIVE DISCHARGE, DIRECT DRIVE (ARC)
CHARGING VOLTAGE: V_o = 1.4 kV
PEAK CURRENT DRIVEN: 1000 A
WAVEFORM: BIPOLAR, PEAKS -1000 A, +750 A, CROSSOVER AT 80 AND 240 ns
INSTRUMENTATION: FIBER OPTIC, HARDWIRE

RT-16397-1

Figure 6. Arc discharge excitation of CAN

environment, and electrical testing of the entire spacecraft as well as individual components (Refs 7,33).

Several types of system tests were performed. These included excitation by a MIL-STD 1541 arc whose characteristics are shown in Figure 7a where the spacecraft was excited by arc generated radiated fields, a contact arc with direct return, and a contact arc with a remote ground return. The latter procedure was similar to that used for SCATSAT testing (Ref 3). The second type of excitation was an arc discharge of a capacitor as shown in Figure 7b. This form of current injection was similar to that used for the CAN electrical tests reported in Reference 5.

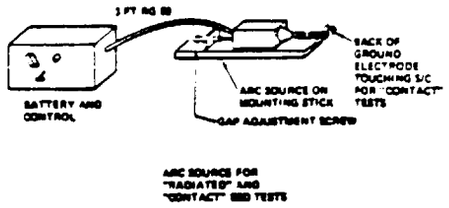

PULSE CHARACTERISTICS

TYPE: CAPACITIVE DISCHARGE; RADIATED OR INJECTED ARC
V_o: 12 kV
SOURCE: t_r=2 ns, $W_{1/2}$=20 ns, I_p=ca. 30 A

a. ARC SOURCE FOR "RADIATED," "CONTACT," AND "STRUCTURE CURRENT" ESD TESTS

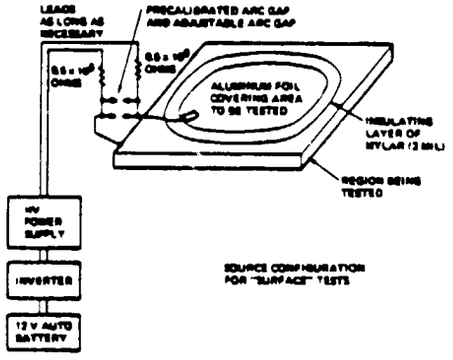

PULSE CHARACTERISTICS

TYPE: CAPACITIVE DISCHARGE, ARC INJECTION
V_o: 5 kV
SOURCE: t_r=10 ns, $W_{1/2}$=10-20 ns, I_p=12-37.5 A
C: 12-150 pf
REPLACEMENT CURRENTS: 2.8-6 A

b. SURFACE DISCHARGE SOURCE

RT-21029

Figure 7. Voyager ESD arc discharge sources

The pulsers and scopes were isolated from ground, the former through the use of batteries as the primary source of power, the latter by an isolation transformer. The spacecraft was powered through an external line. Spacecraft diagnostics were accomplished via telemetry and monitoring of internal points with high impedance probes.

The following points are significant:

1. During a test of the PTM in which the MIL-STD 1541 arc was remotely returned, the spacecraft suffered extreme failure due to ESD induced latchup in interface circuits. While upsets were noted for radiated and contact arc excitation, no circuit failures were noted. This is not surprising as the electron spraying and electrical tests performed on the CAN and SCATSAT indicate that the creation of surface currents and associated fields on

relatively large areas of the spacecraft are more likely to excite POE's and produce correspondingly large wire responses than those produced by a localized arc excitation or radiated field coupling. This is why blowoff and its CDI electrical simulation produce larger internal responses per amp of drive current than does a MIL-STD 1541 arc, even if the arc current is remotely returned.

2. The observed failure during ESD testing led to an extensive redesign program to eliminate perceived susceptibility.

3 The final test on the Voyager flight spacecraft was not a true qualification test as excitation levels at critical points were kept at least 3 dB lower than upset levels.

4. A SEMCAP model calculation was performed in which the response of the spacecraft was predicted at various monitoring points for excitation with known electrical sources at specific critical injection points. The mean error in the predictions (predicted level/measured response) was -12 dB (underprediction). The standard deviation was 20 dB. Thus, even in this case where the sources were well characterized, the observed average error was twice the required safety margin. One can expect, that for an EID coupling analysis in which the characteristics of the exciting sources are not well known, the uncertainties in the analysis would be much larger. Based on the scatter observed in ground test data for discharges induced in different samples of the same material and area, source uncertainty might add another 20 dB to the analysis error budget. Hence, it does not seem technically sound to rely on subsystem or box current injection testing, where the drive levels are determined by analysis, to determine EIDSM. By performing a global excitation one at least eliminates those uncertainties due to inaccuracies in the analytical modeling.

2.4 EVALUATION OF PULSERS

The problem to be addressed is how to simulate the levels of discharge responses produced by EID as represented by available test data. This means that one would like to produce the correct $\vec{H}_t(\vec{r},t)$, or surface current, and $\vec{D}_n(r,t)$, surface charge, distributions on the structure. To evaluate the various possible schemes for driving satellites the generalized circuit model shown in Figure 1 is used. This circuit has two

principal subsystems, a capacitive discharge pulse generator and a generic test object. All of the proposed or previously utilized excitation sources use such a pulser as it is conceptually simple, can be used to store large amounts of electrical energy which can be dumped through a pulse shaping network, and can be run as an isolated source provided that the charging voltage required to produce the necessary output voltage is not too high. There are two basic coupling schemes of importance. In the first, the pulse generator and the test object are capacitively coupled. In the second, this coupling is replaced by a direct connection between the test object and the pulse generator ground. This permits the direct injection of current into the test object, typically at higher current levels per unit charging voltage than for a capacitively coupled injection.

The following criteria have been used to evaluate candidate EID simulation testing techniques.

1. The worst-case electrical stress on a satellite results from charge blowoff. Simulating the kinds of responses produced by this aspect of the discharge process is given first priority.

2. Of the various electromagnetic effects induced on a satellite due to blowoff (which includes generation of replacement currents, generation of external EM fields, excitation of the resonant modes of the satellite, etc.), the most important is typically the replacement currents. Primary emphasis should be placed on simulating these currents. Secondary emphasis is placed on exciting normal electric fields. While it is realized that they may be important in some cases such as aperture coupling, no quantitative data is available about their magnitudes and distribution.

3. An upper bound on the magnitude of the replacement current is derived from the response for EID excitation excitation of the grounded test object. A goal of injecting 200 amperes onto the satellite was chosen based on test evidence available to date. It is realized that available ground test data measured on large area samples indicate that discharges as high as 1000 A might be seen on meter sized dielectrics. On the other hand the limited data available from the P78-2 and multicomponent ground testing, imply that the scaling laws presented in Table 4 are too stringent. This value has arbitrarily been used as a baseline worst case for simulation. Since the electrical response will depend on the charging voltage, the results can be scaled.

4. The time history for this replacement current is a pulse having about a one microsecond rise and fall time (i.e., one microsecond FWHM) and the simulation should reflect this. Again it is realized that the pulse width scales with discharge amplitude. The important point is that ground test data indicates that large area discharge pulse widths are about 1 μsec rather than 10-50 nsec.

5. It is desirable to minimize the need to add additional sensors by making maximum use of S/C self-diagnosis capability, supplemented by that provided by the aerospace ground equipment.

6. The ambiguity about test results introduced by a need to scale the test results should be minimized; i.e., a threat level test is desired.

7. It is desirable to isolate the test system (test object, pulser, data recorders) from the external world to minimize stray coupling paths and also minimize perturbations due to the modification of the test object electrical characteristics because of coupling to its surroundings. In space, the satellite is isolated from the surrounding plasma during the discharge.

The following approaches summarize the various simulation techniques that have been theoretically considered.

1. Capacitative discharge with capacitive coupling between pulser and test object and test object and pulser ground. Test setup to generate a low level (few amperes), narrow (20-40 nanoseconds FWHM) pulse. This is the present manner in which the CDI test is performed.

2. Capacitive discharge as in Technique 1, except generate a wide pulse (one microsecond FWHM) at a low level.

3. Capacitive discharge as in Technique 1, except generate a wide pulse at the full threat level (200 amperes).

4. Capacitive discharge using only direct connection (no capacitive coupling) between the pulser and the test object and between the test object and the pulser ground. Test setup to generate wide, high level pulse.

5. Arc discharge yielding a narrow pulse (20-60 nanosecond FWHM) as per current MIL-STD 1541.

6. Modification of Technique 5 to yield the wide pulse.

The feasibility, relative advantages and disadvantages of these test techniques are briefly summarized in Table 6. Note that the capacitive direct injection scheme is a subset of the capacitive coupling approach because pulse width is controlled by the capacitance between pulser and drive plate, which is typically at test system ground, and the test object.

Test Technique 1 was eliminated from consideration because it fails to provide the required wide pulse. Test Technique 2 is a possible option but one of limited value because it requires scaling low level test results to the threat level. Scaling necessitates a much more complicated test. One must extensively monitor test points with special sensors to provide a large data base to ensure that all critical points have been examined. This would involve extensive modifiction of the satellite cable harness and box interfaces. In addition uncertainties in the scaling analysis increases the uncertainty associated with test results. The Arc Discharge Technique 5 was eliminated because it also provides a narrow pulse. Test Technique 6 was eliminated primarily because, even if achievable, the previous test history indicates that the arc discharge does not induce the proper global excitation of replacement currents as does blowoff.

The possibilities that remain include the capacitive discharge technique with capacitive coupling between pulser and test object, and between test object and pulser ground, and a capacitive discharge technique using direct injection and direct return.

Model calculations were performed to evaluate whether it was possible to reproduce the kinds of body currents seen on the surface of the CAN with readily attainable circuit parameters. The model shown in Figure 1 was varied for what were considered a reasonable range of circuit parameters. Those studied included C, the drive capacitor, C_c the capacitor coupling the pulser to the test object, $L' = L + L_s$, the combined inductance of the drive wire and test object. The charging resistor R_c was set at a nominal value of 10 kΩ and $R' = R + R_s$ was set at 100 ohms. Altering R by increasing its value to insure that the pulser was isolated from the test object does not significantly alter the conclusions presented below, but makes them more pessimistic. Increasing the value of this resistance serves to reduce the drive current. Based on realistic satellite geometries, it was decided to limit C_c and C_s to 500 pf which may be overly optimistic. For example, a $1M^2$ plate placed 2 cm from the satellite surface has a capacitance of 442 pf. Given the irregularity of most surfaces of satellites, this seems to be a reasonable upper bound. More realistic values for C_c and C_s might be 100 to 200 pf.

Table 6. Relative Advantages/Disadvantages of Potential EID Simulation Test Techniques

TEST TECHNIQUES	ADVANTAGES	DISADVANTAGES
1. Capacitive Discharge, Capacitive Coupling Low Level Narrow Pulse (A few amps, 20-40 nsec FWHM)	1. Hardware available and demonstrated. 2. Relatively simple to set up. 3. Either hardwire or isolated instrumentation to monitor internal response. 4. Personnel safety considerations minimal. 5. Works for floating or grounded test object. 6. Relatively low cost, risk.	1. Low level, narrow pulses are not valid worst case simulations of EID. 2. AGE or Telemetry not useful as drive levels too low. 3. Analysis required to extrapolate to threat level, increases test uncertainty. 4. Special sensors required. 5. Potential instrument sensitivity problems. 6. Not clear how to drive booms, antennae or other reentrant geometries.
2. Capacitive Discharge, Capacitive Coupling Low Level Wide Pulse (A few amps, 1 μsec FWHM)	1. Relatively simple to set up. 2. Personnel safety considerations minimal. 3. Scaling to high levels possible if susceptibility levels known. 4. Relatively low cost.	1. May not be practical to implement because of circuit parameter limitations. 2. AGE or telemetry not useful as drive levels too low. 3. Analysis required to extrapolate to threat level, increases test uncertainty. 4. Special sensors required. 5. Potential instrument sensitivity problem. 6. Not clear how to drive booms, antennae, etc.
3. Capacitive Discharge, Capacitive Coupling High Level Wide Pulse (Hundreds of amps, 1 μsec FWHM)	1. Would provide good similation of blowoff. 2. Scaling not necessary. 3. Works for floating or grounded test object. 4. Could use telemetry.	1. To achieve high levels requires high voltage (>50 kV). 2. May not be feasible to achieve wide pulse because of circuit parameter limitations. 3. May have significant personnel safety problems. 4. May be significant cost impact to implement because of high voltage pulser development. 5. Isolated test may not be practical for realistic pulses.

Table 6 (Continued)

TEST TECHNIQUES	ADVANTAGES	DISADVANTAGES
4. Capacitive Discharge, Direct Injection. (Hundreds of amps, 1 μsec FWHM)	1. More amperes per volt of drive available. 2. More parameter control available (not limited by drive plate/satellite capacitance). 3. Spacecraft telemetry can be used to determine upset or damage for threat level injection. 4. Little additional instrumentation needed (telemetry will determine pass/fail). 5. In principal can be run with system isolated. 6. No scaling required. 7. Easy to excite different areas.	1. Required hardwire return connection between pulse generator and test object (instead of capacitive return). 2. Test setup likely to be more complicated - some cost impact to implement. 3. Not best simulation of blowoff unless the current is injected over a wide area and made to return at points remote from the injecting site.
5. Arc Discharge Narrow Pulse (10-30 nsec FWHM) (Present MIL STD 1541 arc)	1. Techniques available and demonstrated. 2. Either hardwire or isolated instrumentation ok. 3. Works for floating or grounded test object.	1. Narrow pulse does not provide valid simulation of blowoff or flashover. 2. Response levels low - use of telemetry probably not possible.
6. Arc Discharge Wide Pulse (1 μsec FWHM)	1. Would provide valid simulation of flashover or punchthrough. 2. Either hardwire or isolated instrumentation ok. 3. Works for floating or grounded test object.	1. Achieving wide pulse may not be feasible without very sophisticated techniques including very high voltage. 2. Increased personnel safety problem. 3. Not a valid simulation of blowoff.

In the first round of modeling no attempt was made to produce critically damped or overdamped waveforms. The objective was to find the largest peak values and width of the first lobe of the current pulse I_p, and t_1, the zero crossing time. Since current scales with V_o, the charge up voltage was arbitrarily set at one kV. The results of the model calculation are shown in Table 7. The computed values of I_p, or t_1 are shown in Figures 8 through 15.

Table 7. Circuit Parameters for Pulser Evaluation[a]

Case	1	2	3	4	5	6	7	8
C (pf)	100	100	1000	1000	1000	1000	100	100
L'(μH)	1	1	1	1	10	10	10	10
C_s(pf)	10	500	500	10	10	500	500	10
I_p(A)	2.4	4.9	6.4	2.5	0.9	3.3	2.2	0.9
t_1(ns)	10	30	60	10	32	124	82	30

[a] R_C = 10 kΩ, R'_s = 100Ω, C_c = 500pF, V_o = 1 kV for all cases.

A second set of circuit parameters were exercised to see whether one could achieve the criterion pulse width and correct levels with realistic but large coupling capacitances by adjusting the total series inductance L', the charging voltage V_o and the charging capacitance C. The results are presented in Table 8 and the predicted current waveforms for Cases 12 through 15 in Figures 16 through 19. For the data in the table it can be seen that the desired current amplitude and pulse widths can be achieved only for extremely large values of L' and high charging voltages. While it is possible to provide such charging voltages through the use of a Marx generator for example, the required pulsers would be costly, extremely large and difficult if not impossible to isolate from the external environment. Cases 14 and 15 were run in an attempt to see whether more modest levels could be met for narrower pulses (ca. 250 ns) and currents (50 A). It can be seen that even to reach pulses of this amplitude and width will take a relatively large pulser. If R' is increased to provide critical or overdamping, a reasonable pulse can be produced, it is relatively small per kV of drive voltage.

The following general comments can be made about the parametric circuit evaluation.

Table 8. Circuit Parameters for Realistic Coupling Capacitance[a]

Case	9	10	11	12	13	14	15
C μF	0.01	0.01	0.01	0.1	0.1	0.1	0.1
R(kΩ)	10	10	10	10	10^3	10^3	10^3
R'(Ω)	100	100	100	100	100	100	10^4
L'(mH)	1	4	15	1	1	0.1	0.1
V_o(kV)	450	1100	6700	645	645	55.4	500
I_p(A)	200	200	200	200	200	50	50
t_1(μs)	0.45	0.85	1.55	1.0	1.0	0.315	b

[a]For all cases $C_s = C_L = 200$ pF

[b]Overdamped, t_r = 90 ns, t(1/e) = 1.35 μs.

1. The model evaluated for capacitive coupling and capacitive return (including CDI) provides for large area excitation of the satellite.

2. It is clear that for realistic circuit parameters and charging voltages, the pulse amplitude and current criteria cannot be practically met even if the condition of critical damping were relaxed and ringing permitted. If it is found from space data that a less stringent test was realistic, say 50A @ 200 ns, then it would be possible to achieve such a pulse with a pulser of about 50 kV. For pulses of this width it might be possible to use ferrite isolation of the data links and pulsers in a manner similar to that described in (Ref 28).

3. If one is willing to accept a low level, then a wide pulse excitation is feasible with a pulser of modest size and achievable circuit elements.

4. The circuit shown in Figure 1 is essentially a series RLC circuit. The characteristic oscillation frequency f when underdamped is

$$f = \frac{1}{2\pi}\left(\frac{1}{L'C_{eq}} - \frac{R'^2}{4L'^2}\right)^{1/2} \qquad (3)$$

For the case of under damping, where

$$\frac{1}{L'C_{eq}} < \frac{R'^2}{4L'^2},$$

one can increase the period of oscillation by increasing

$$C_{eq}^{-1} = C^{-1} + C_s^{-1} + C_c^{-1},$$

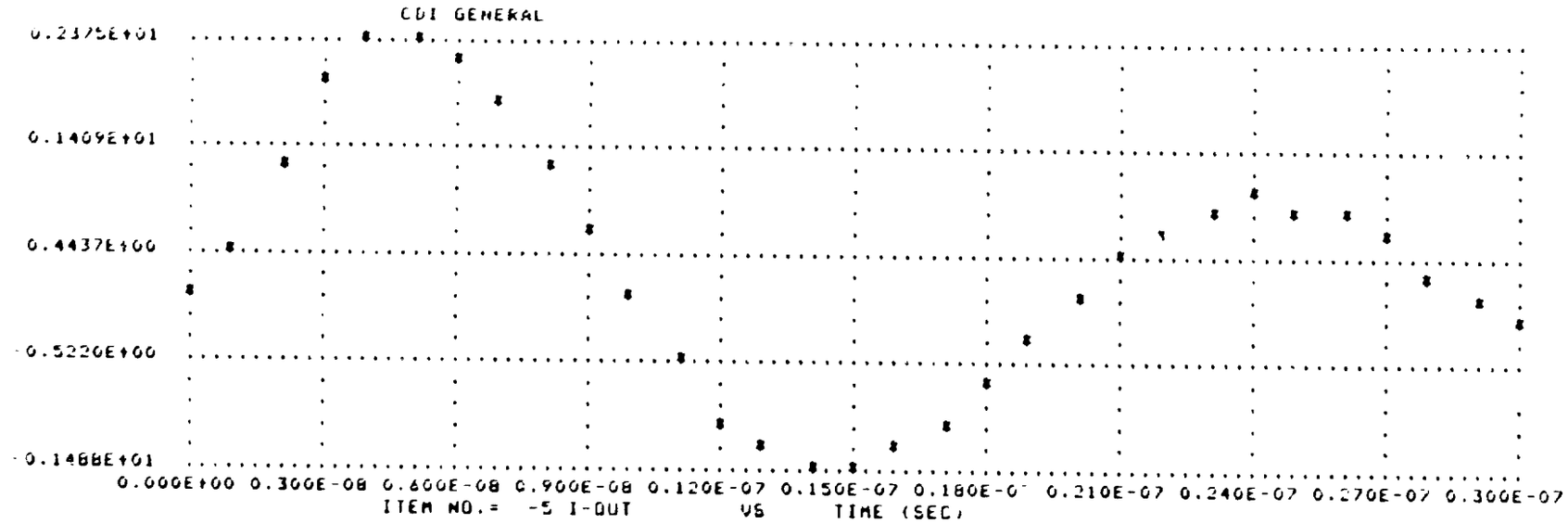

Figure 8. Case 1 load current

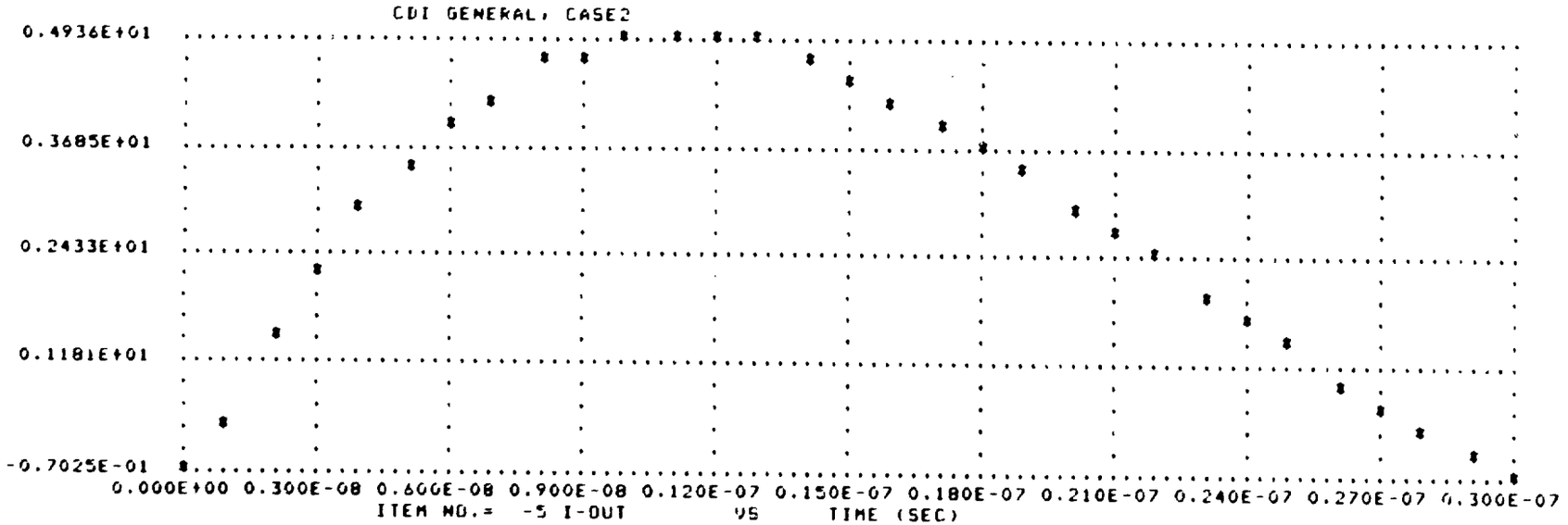

Figure 9. Case 2 load current

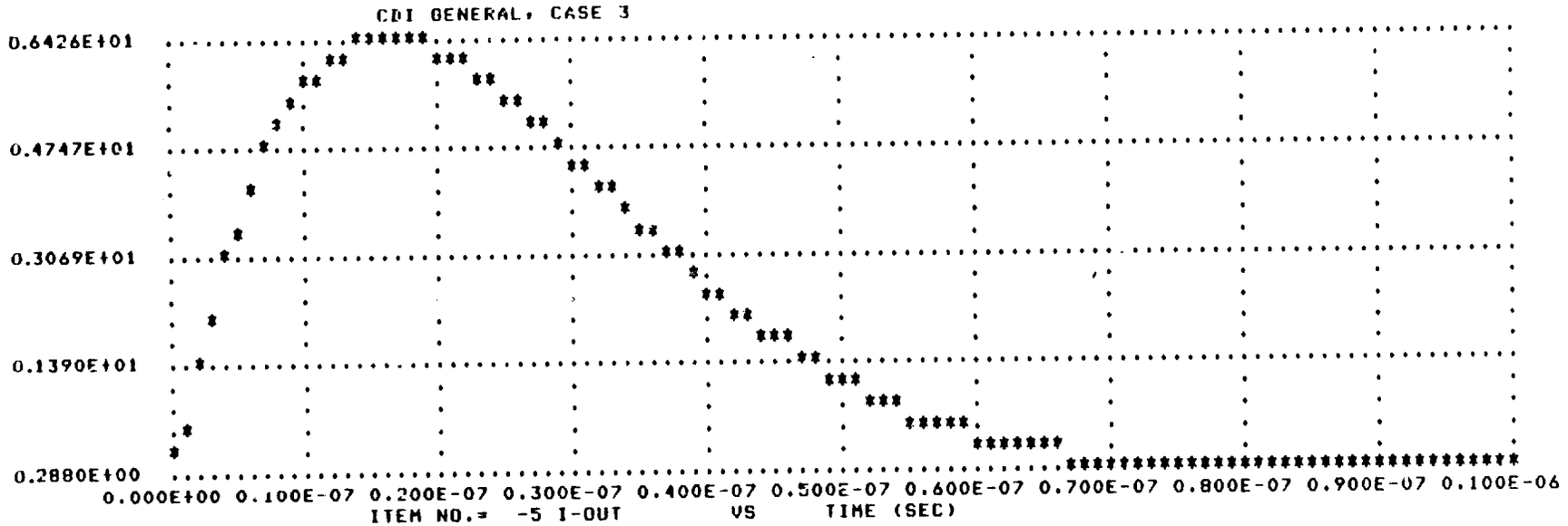

Figure 10. Case 3 load current

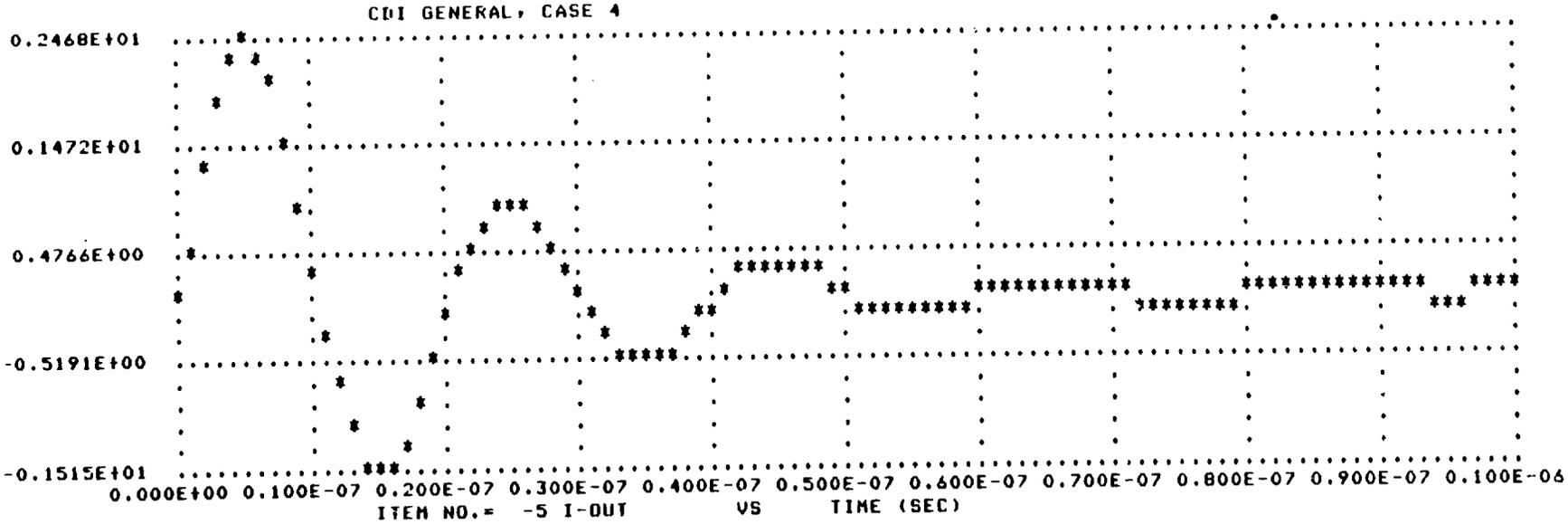

Figure 11. Case 4 load current

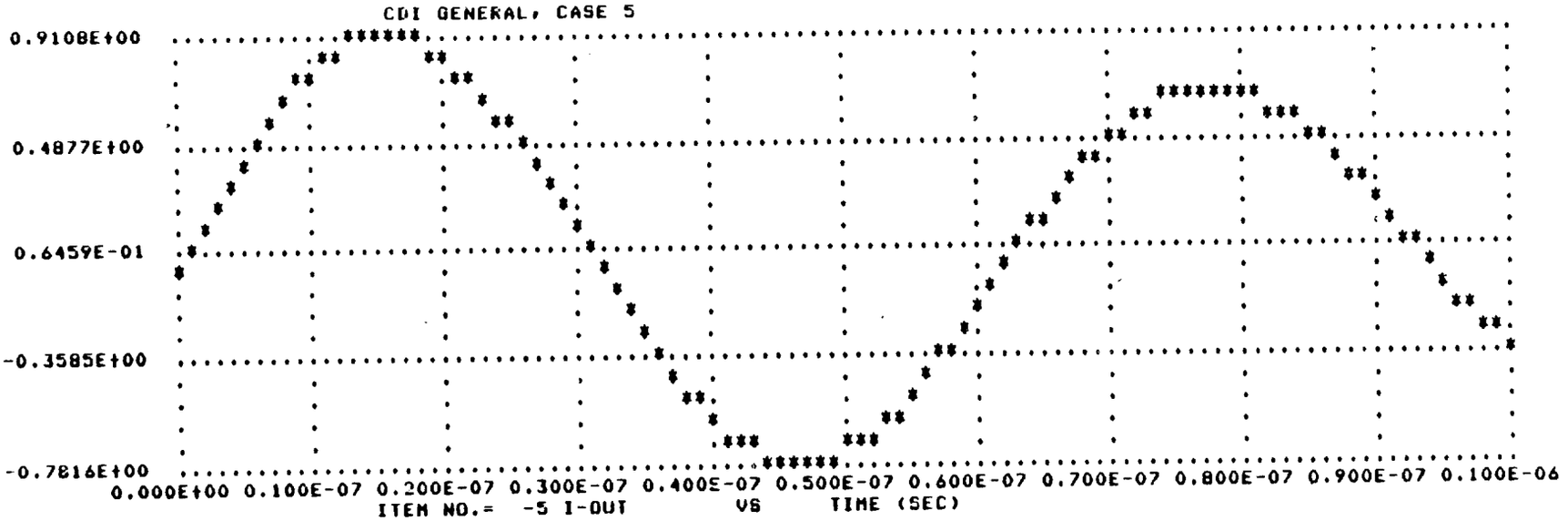

Figure 12. Case 5 load current

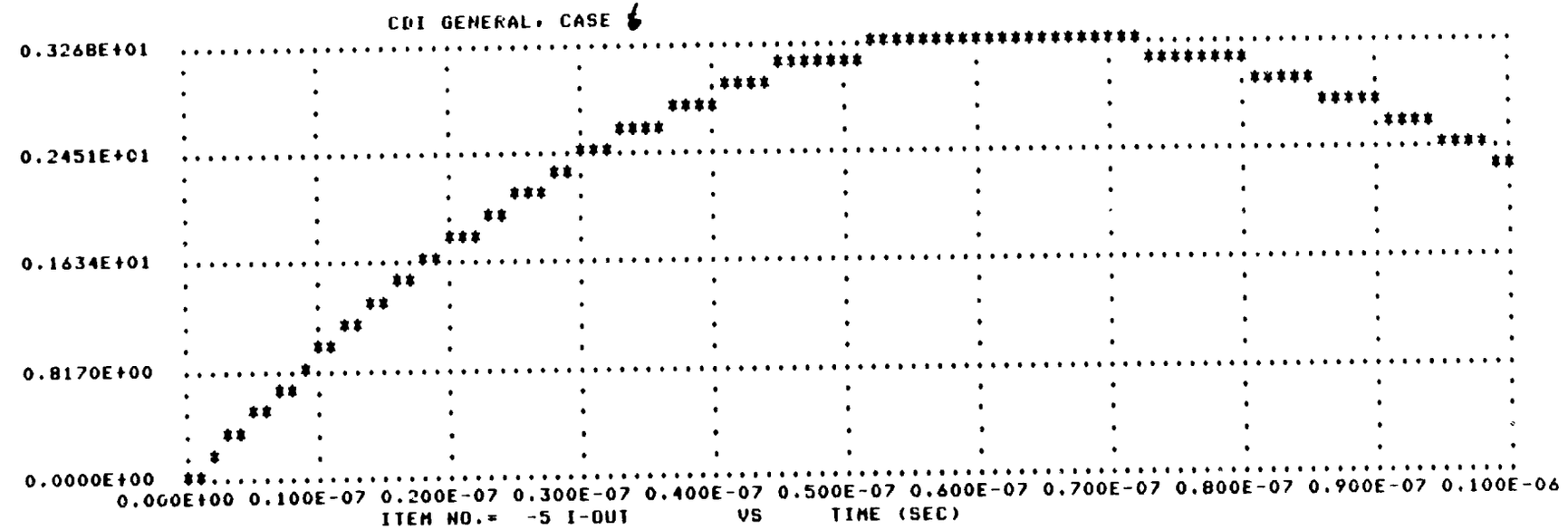

Figure 13. Case 6 load current

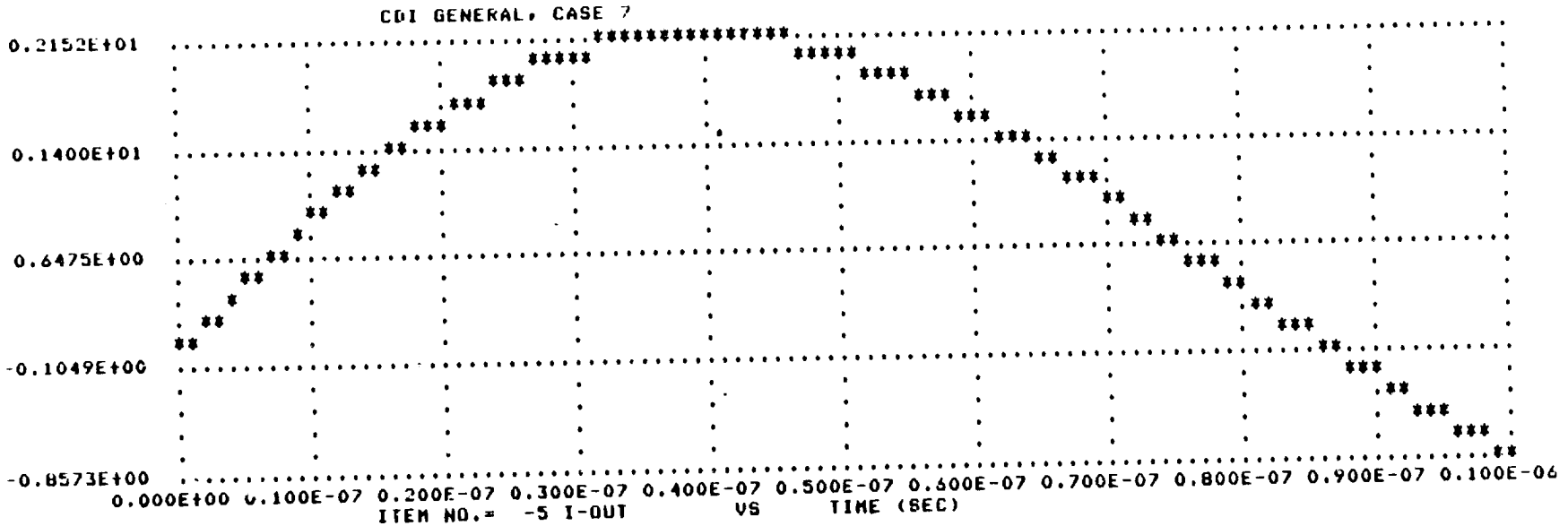

Figure 14. Case 7 load current

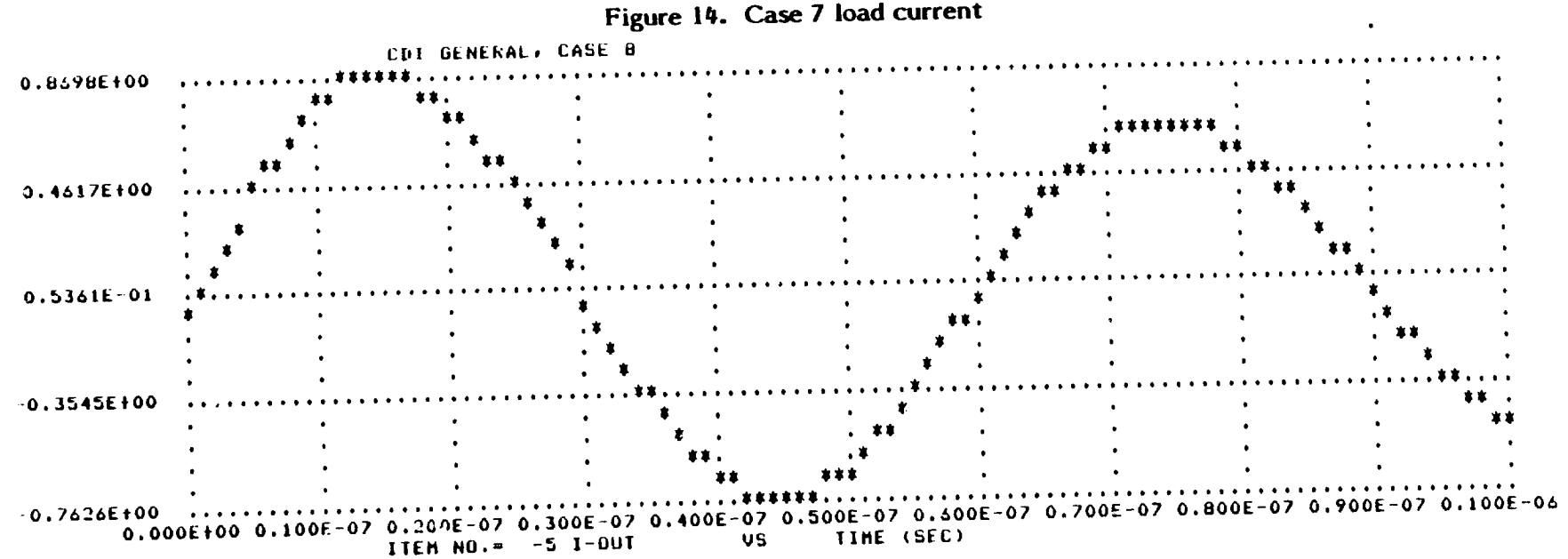

Figure 15. Case 8 load current

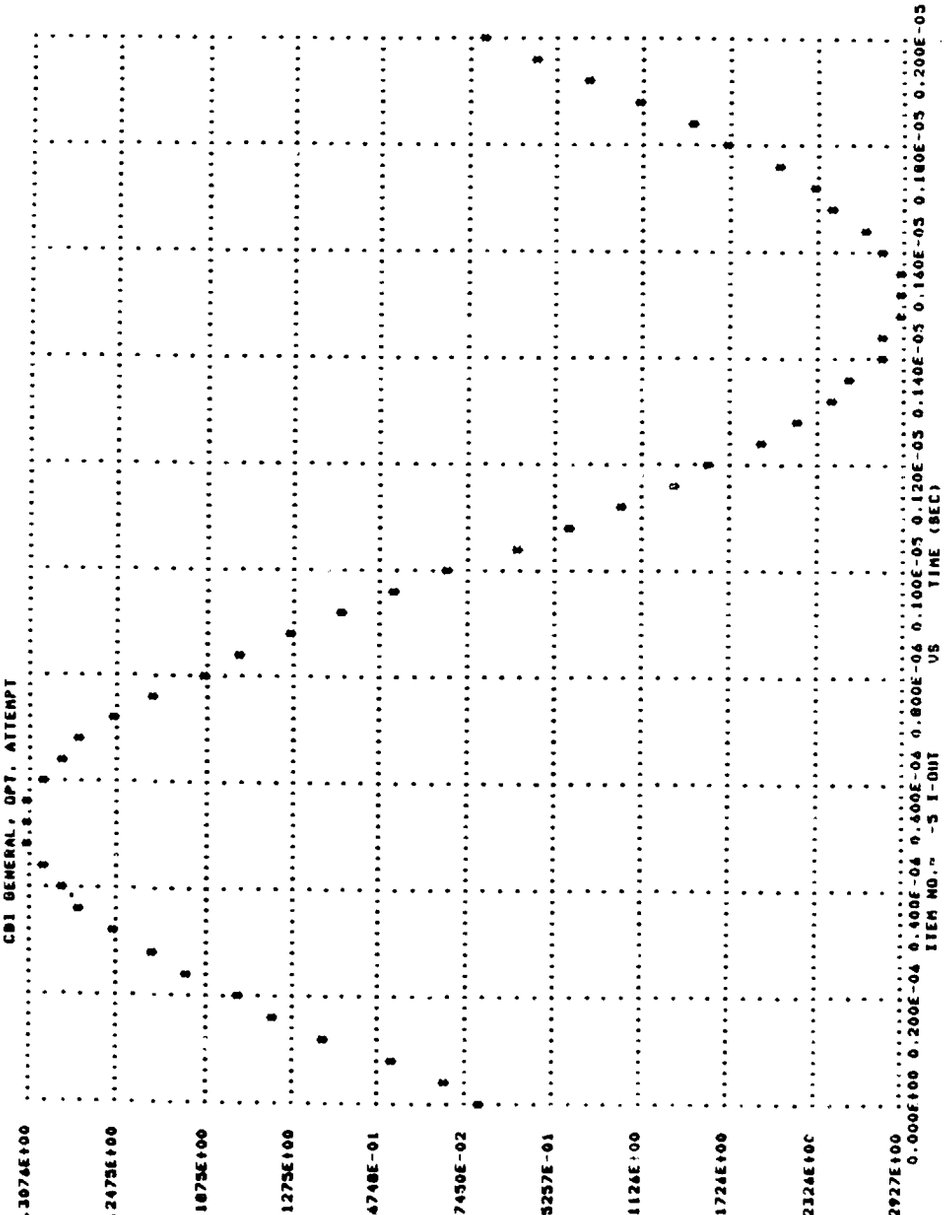

Figure 16. Case 12 load current

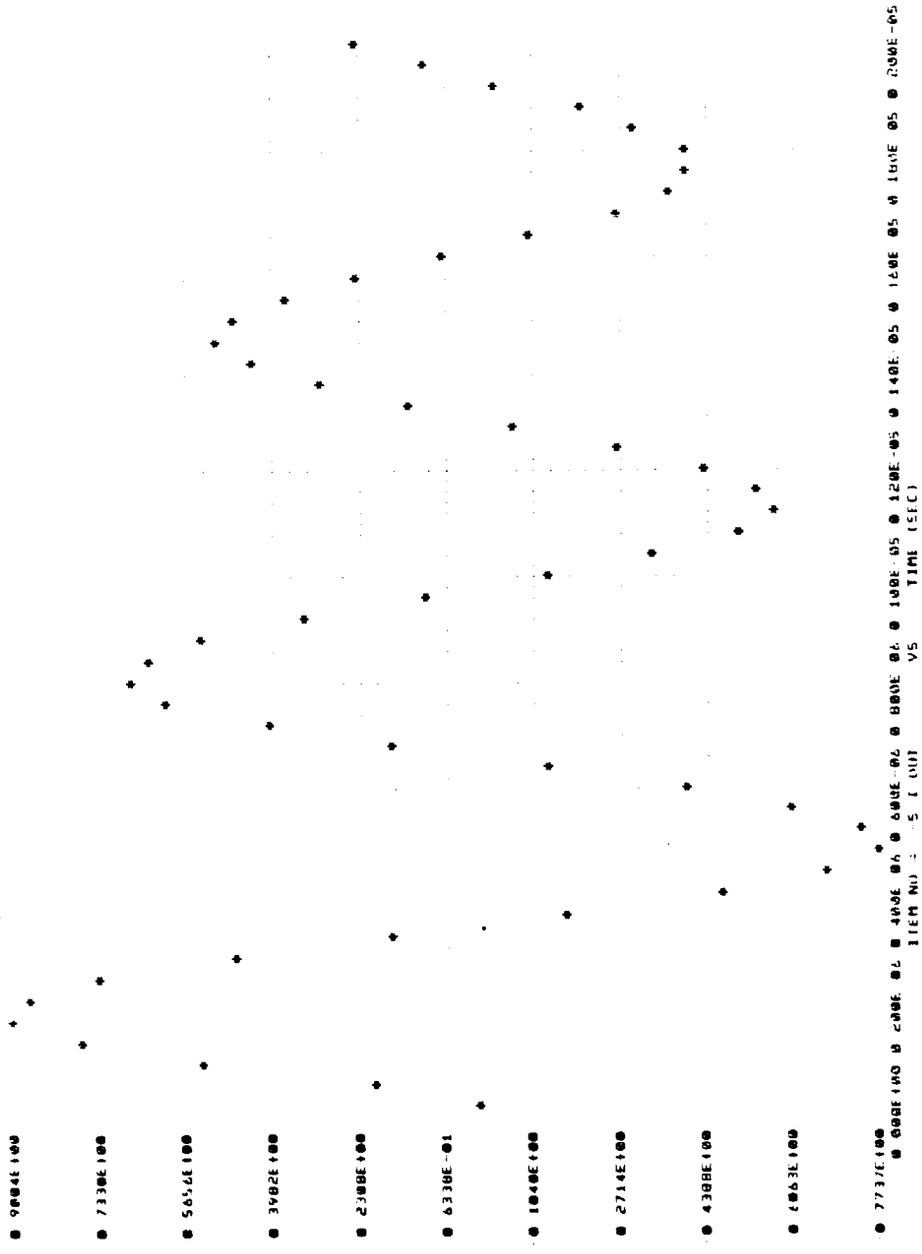

Figure 17. Case 13 load current

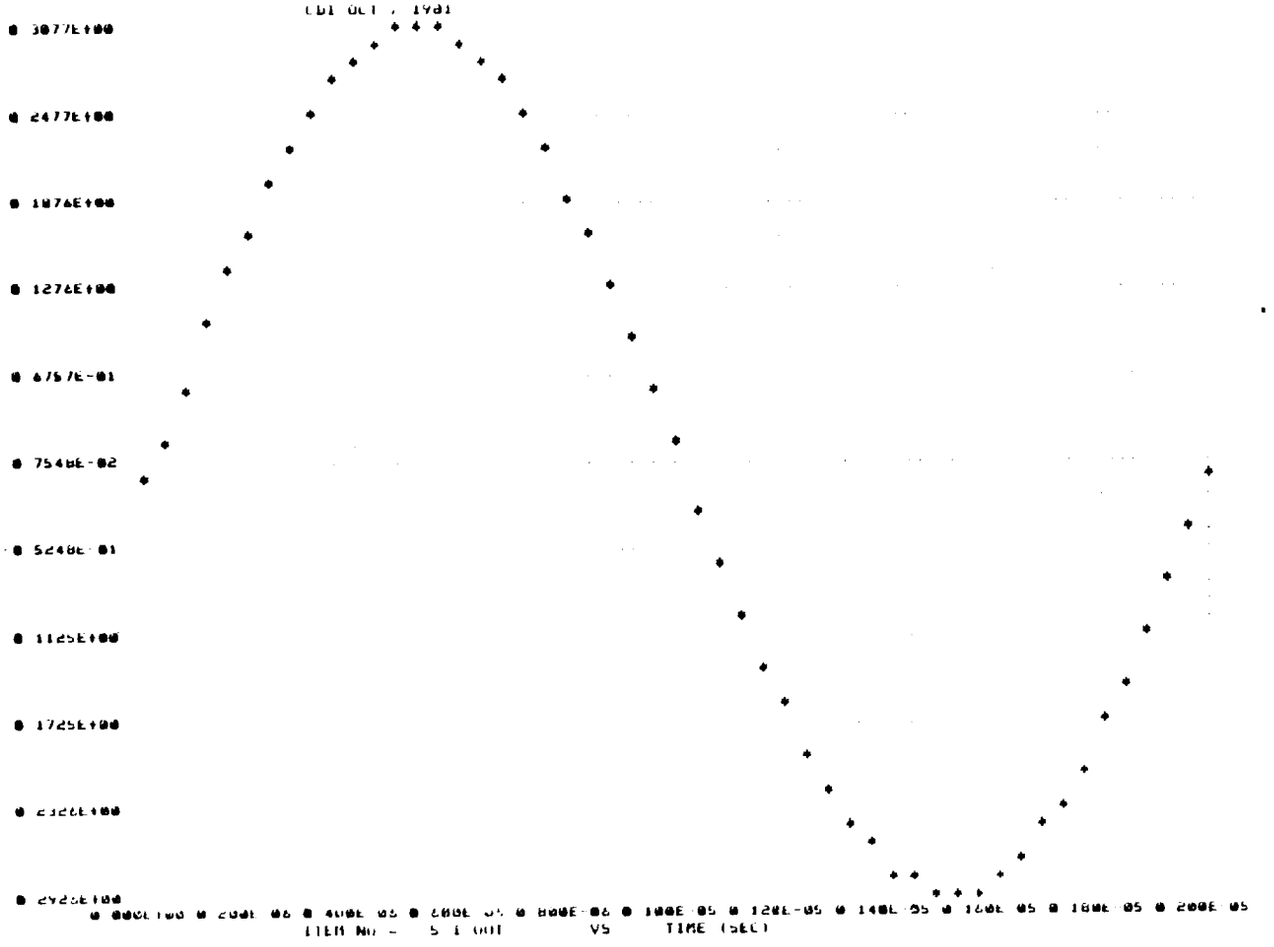

Figure 18. Case 14 load current

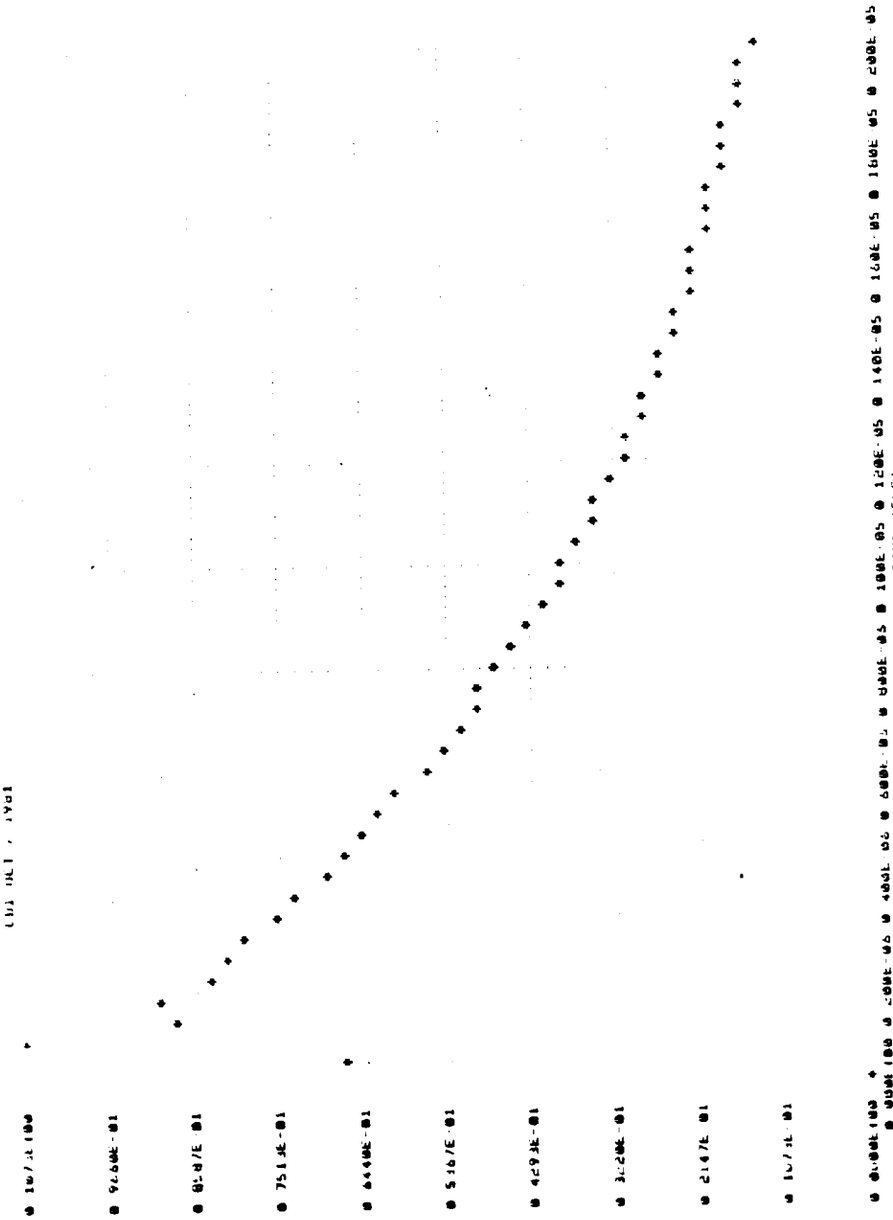

Figure 19. Case 15 load current

or L' as the data in Table 7 indicates. Since the three capacitances are effectively in series it is the smallest which controls the frequency of oscillation. Increasing C_{eq} also increases the net current injected while increasing L or R decreases it. Note that the response is that of the combined system consisting of pulsers, coupling network and test object. If the primary effort of wide pulse EID is to drive the response of the spacecraft at the characteristic frequency associated with the discharge pulse, as appears to be the case for non resonant, low-Q objects like the CAN, then this is not a defect. The resonant t_1 of the combined system can be adjusted to be that of the predicted discharge pulse. It is true that a damped sinusoid will be somewhat of an overtest if compared to the EID response.

5. If R is increased in order to decouple the test object from the pulser, then the amplitude of the injected current will be diminished. Thus, an ever higher voltage pulse than necessary for the low impedance case is required.

6. The problem of exciting the body currents produced by SGEMP is less severe because the pulse widths are narrower. Thus, it is feasible to provide a high level CDI pulse of 10 ns width, and 100 amps in amplitude with pulses where V_0 = 20 kV. While V_0 is large, pulser isolation can be achieved so that it is decoupled from external ground during the excitation.

7. Wide pulse capacitively coupled excitation of satellite models or real satellites has not been studied in detail either analytically or experimentally. It is necessary to pursue further analysis with more detailed coupling models validated by electrical testing to provide a basis for quantitative comparison with the surface electromagnetic fields produced by EID. The testing should examine both the external surface and the internal wire responses for simple objects like the CAN, and for a model more representative of real satellites like the SCATSAT.

The large coupling capacitance severely restricts the amount of current available per unit voltage of charge on the drive capacitor. With these coupling capacitances eliminated, more amperes per unit charging voltage is available, and gives the best chance of generating the full threat level current with perhaps only a few tens of kilovolts or less (instead of a few hundreds of kilovolts). A conceptual direct injection approach is shown in Figure 20. The intent is to drive the required microsecond wide,

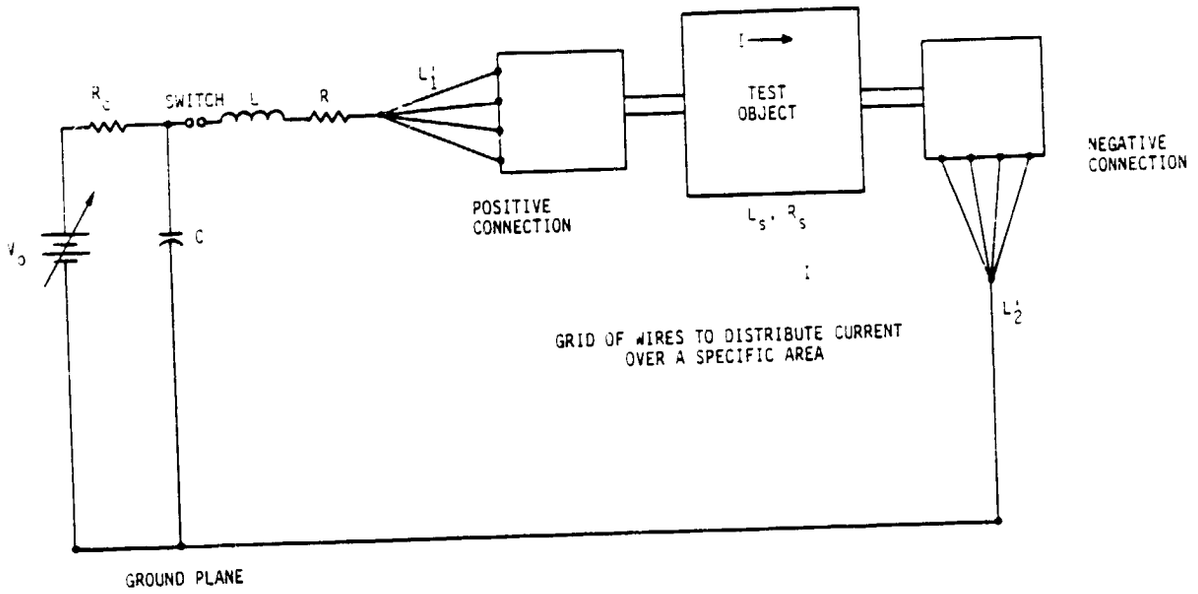

RT-20912

CIRCUIT ELEMENTS

V_o = ADJUSTABLE POWER SUPPLY WITH OUTPUT UP TO APPROXIMATELY 20 kV
R_c = CHARGING RESISTOR TYPICALLY 100 kΩ
C = DRIVE CAPACITOR TYPICALLY 0.001 to 0.2 μf, DEPENDING ON CIRCUIT REQUIREMENTS
L = LUMPED INDUCTANCE ADDED IF NECESSARY FOR WAVESHAPING
R = LUMPED RESISTANCE ADDED IF NECESSARY FOR WAVESHAPING
L_1', L_2' = INDUCTANCE OF THE CONNECTION GRIDS
L_s, R_s = INDUCTANCE AND RESISTANCE OF THE TEST OBJECT BETWEEN PULSER CONNECTION POINTS
I = CURRENT FLOWING ON THE TEST OBJECT WHICH SIMULATES THE REPLACEMENT CURRENTS FLOWING AS THE RESULT OF BLOWOFF

THE GROUND PLANE IS TO PROVIDE MINIMAL ADDITION OF INDUCTANCE AND RESISTANCE TO THE CIRCUIT.

THE SWITCH IS AN ADJUSTABLE, SELF-BREAKDOWN, HIGH-VOLTAGE SPARK GAP.

RT-20912-1

Figure 20. Proposed direct-drive setup for EID simulation testing

several hundred ampere current pulses over large areas of the satellite and return this current to the pulser in a controlled manner.

The primary drawback to this test technique is that current is injected onto the test object, and pulled off, at discrete points instead of a large area (such as the capacitive coupling provided). To partially offset this disadvantage, the connections of the pulser to the test object and of the test object to the pulser ground could be accomplished by using a grid of wires, i.e., make the connection through many points instead of just one point.

The attractiveness of this approach is that one can drive the wide pulse width, high amplitude replacement currents over the body of the spacecraft in a manner comparable to that observed for the excitation of simple objects by EID. Thus, one can provide an excitation of the satellite penetrations over a relatively large area. One of the disadvantages of MIL-STD 1541 arc as it is normally executed, is that the region of excitation is extremely limited. A disadvantage of direct injection with direct return is that it does not provide as good a simulation of the EID-induced surface electromagnetic fields $\vec{H}_t$ and $\vec{D}_n$. The strength of $\vec{H}_t$ is too large near the drive wires while $\vec{D}_n$ is too small. In addition, direct injection does not provide a good simulation of effects due to alteration of the surface charge distribution during discharge as no charge is removed from the body. Use of multiple drive and collection wires as shown in Figure 20 will reduce the magnitude of $\vec{H}_t$ near each wire, but may also serve to increase the area over which the simulation is poor.

Thus, no one practical technique is clearly superior in simulating the kind of relatively wide, high level threat current pulses created as a consequence of large area discharges on meter sized dielectrics coupled to simple, highly geometric objects. The best approach would be to scale up the kind of critically damped CDI pulses used to test the CAN and the SCATSAT. However, the analysis performed above shows that this is not practical. If it is desired to execute the skin currents created by blowoff electrons on large areas of the satellite, then direct injection and return is to be preferred. If a somewhat better simulation of the surface EM fields created by EID is desired, even if at a much lower level than may be excited by a large area discharge, then some version of capacitive injection should be chosen. For the purpose of specifying a MIL-STD EID qualification test, we feel that the direct injection test is more straightforward, can be run at threat levels and with less extraneous instrumentation.

It is to be underlined that neither of the two recommend electrical excitation techniques have been explicitly tried experimentally to provide a quantitative comparison with the results of EID testing and the P78-2 transient data. There is a significant amount of risk involved in incorporating such unverified techniques into a MIL-STD without further study. However, the key issue is not whether such testing is feasible, but how well the EID responses can be simulated. Similar testing has been performed both at low and threat level excitations as part of the STARSAT program reported on in Reference 30. A parallel test and analysis program should be performed using a sophisticated model such as the SCATSAT followed by testing on a real satellite. On the other hand, it seems clear that either of the tests proposed would be a better

simulation of the electromagnetic responses evoked by EID than the present version of MIL-STD 1541 or the surface discharge techniques which have been used to qualify spacecraft.

3. RECOMMENDED TEST PROCEDURES

This section presents a draft system test procedure for the qualification of spacecraft against external charging. The procedures chosen are based on the evaluation of various excitation techniques presented in Section 2.4. They are based on what was known about spacecraft charging when this report was prepared; i.e., late 1981. It is clear that several key issues remain to be addressed. The most important of which is the degree to which the ground test data on which the test procedure is based simulate the effects of space discharge produced by the space charged particle and electromagnetic radiation environment. The format has been cast as much as possible in a form which is compatible with that of MIL STD-462. However, that document describes subsystem and component tests. What is presented here is a general approach to performing an EID satellite system test. The approach presented is general. The specifics of the method of execution such as drive levels, pulser coupling and attachment points will be system specific. However, prescriptions for tailoring the procedures given in this test specification to particular systems are given. In some places comments about the recommended test procedure are given which are not part of the procedure itself. These are separated from the body of the text and printed in italics.

3.1 SCOPE

3.1.1 Scope

This document provides a set of electrical system test procedures for the qualification of space vehicles against the inadvertant or unacceptable responses produced in electrical or electronic circuits, functional units or subsystems as a result of electromagnetic interference generated by space electron induced discharges (EID). Performance of such systems testing is required to satisfy Section 5.1.1.1 (Electrical/Electronic Compatability Test) of MIL-STD 1541: Spacecraft Charging Requirements (abbreviated in this Test Procedure as SCA, Ref. 35).

3.1.2 Applicability

This test is applicable to those vehicles exposed to the natural charged particle environment conducive to the charging and discharging of surface dielectrics as defined in Section 10.2 of SCA. It is not designed to qualify spacecraft against the improper responses produced by the charging and discharge of internal dielectrics such as cables or printed circuit boards which are better handled by subsystems or component testing.

3.1.3 Units

The international system of units specified in MIL-STD-463 is used.

3.2 REFERENCED DOCUMENTS

The documents referenced in MIL-STD-1541 including the SCA are incorporated in this test method.

3.3 DEFINITIONS

The terms used herein are defined in MIL-STD-1541 including the SCA and in MIL-STD-463.

3.4 REQUIREMENTS

3.4.1 General Requirements

General requirements pertaining to the application of this standard and applicable test limits are specified in MIL-STD-1541, SCA. The test procedures contained herein should be used in complying with MIL-STD-1541, SCA.

3.4.2 Specific Requirements for Testing to the Requirements of MIL-STD-1541, SCA.

Details pertaining to the general performance of the tests contained in this Test Procedure are presented in this section.

3.4.2.1 Preparation of a Test Plan and Performance of Post Test Analysis The requirements for an Electromagnetic Compatibility Test Plan for a system EMC test is documented in Section 4.2 of MIL-E-6051D, "Military Specification Electromagnetic Compatibility Requirements, System". These requirements must be tailored as follows for the special application to system EID qualification tests.

The test plan shall provide for system EID qualification and acceptance testing including, but not limited to the following:

a. Analysis methods used to select critical measurement points for monitoring to demonstrate electron induced discharge safety margins (EIDSM).

b. Methods used for developing failure criteria and limits and a specification of these.

c. Expected wire and structural responses at monitoring points. These are to be compared to failure thresholds to determine anticipated safety margins. These will be based on approved results from design analysis or laboratory upset threshold tests on subsystems and circuits.

d. Specification of the critical points to be stressed, and rationale for their choice.

e. Discussion of supporting analysis required to determine expected discharge points and discharge characterization (pulse width, amplitude, etc.) including sample calculations, and an error analysis.

f. Test configurations and procedures for all electronic and electrical equipment installed in, or associated with, the system and the response for operations during tests, including switching.

g. A description of all nonstandard equipment such as pulsers, data links, or sensors which cannot be found in referenced manufacturers' equipment manuals or data sheets. Where available, appropriate manuals or data sheets, will be cited for standard test equipment.

h. Implementation and application of test procedures which include vehicle configuration, modes of operation and monitoring points for each subsystem and operation of test equipment.

i. Data recording requirements.

j. Methods and procedures for data measurement and analysis.

k. Personnel required, government, contractor, and vendor; and the necessary activities to be performed by each group.

l. A safety plan whose objective is to prevent inadvertant damage to the spacecraft and to ensure personnel safety during the operation of the high voltage/high current power supplies specified in the test.

m. The test plan shall distinguish between those measurements and test levels required for qualification testing and those for the less stringent acceptance tests of production vehicles.

The test plan including test procedures, test equipment, test and vehicle configuration, selection of critical test points pass/failure criteria and excitation levels will be approved by the procuring agency before test conduct. A post test analysis will be performed in which the measured EIDSM for critical monitoring points will be compared to predictions. When these margins are negative, impact on vehicle performance will be described. Where the measured EIDSM are less than the 6 db (20 db EED) required, necessary design changes to ensure compliance will be identified.

3.4.2.2 Demonstration of Satisfactory Compliance. The manufacturer will demonstrate satisfactory performance of his system as specified in Section 50.1.1 of MIL-STD-1541. For each identified discharge site, a structural current injection test will be performed which will provide a 6 db (energy) overstress by the injected current above that produced by a worst case discharge occurring at that site for the specified charging environment. Identification of discharge sites, discharge characteristics, and predicted system structural current responses will be determined by the manufacturer based on analysis, ground test data or flight data and approved by the procuring agency. The spacecraft will be required to operate satisfactorily during and for a specified time after each current injection in a manner to be defined in the system specification. The manufacturer must demonstrate by analysis and/or testing that the system will also operate satisfactorily if multiple discharges occur; i.e., at one site or at several sites, within a system specified time interval.

A representative set of EED circuits will be included in the critical test points monitored. The manufacturer will demonstrate that there is a 20 dB EIDSM for each EED by an approved combination of system EID testing, analysis and EED circuit current injection.

3.5 ARRANGEMENT AND OPERATION OF SPACE VEHICLE DURING TEST

3.5.1 General Test Setup

The general test setup is shown in Figure 20. The components of the test object can be separated into three elements: the pulser or current injecting source. These are described in Section 3.6.1, the test object configuration described in Section 3.5.2, and

the means of coupling pulser and test object described in Section 3.6.1.3. The test should be performed in a high bay area rather than with the vehicle in a screen room.

3.5.2 Space Vehicle Configuration

The space vehicle in its on-orbit configuration should be placed in an open area on a dielectrically isolated stand as far away from conducting boundaries as possible. It is recommended that the minimum height of the stand platform be comparable to a centerbody dimension, that the clear space above the vehicle be similar, that the minimum clear space around the satellite be comparable to the tip to tip wing dimension for three axis stabilized spacecraft and several body diameters for a spin stabilized vehicle. As a rule of thumb, the capacitance of the vehicle to ground should be no more than twice its capacitance to infinity.

3.5.2.1 Electrical Isolation. During electrical injection, the vehicle will be electrically isolated from its environment except for controlled impedance paths between the pulser and test object, and test object to common ground as shown in Figure 20. In some cases, e.g., for capacitatively coupled injection, a test ground plane may be provided to fix the capacitive coupling between space vehicle and test system ground.

3.5.2.2 Use of Space Vehicle Battery. During test performance, the space vehicle will be powered with its internal batteries.

3.5.2.3 Data Transmission During Testing. During testing, system command and telemetry data will be transmitted via the RF Command and Control links between the spacecraft and ground control equipment used to command the spacecraft.

3.5.2.3.1 Spacecraft Command and Performance Data. During testing, system command and telemetry data will be transmitted via the RF Command and Control links between the spacecraft and ground control equipment used to command the spacecraft during checkout.

3.5.2.3.2 Spacecraft EID Response Data. Special analog electromagnetic environment data (external surface electric and magnetic fields) and critical test point data monitored by special sensors will be transmitted via dielectric (fiber optic or equivalent) data links.

3.5.3 Alternative System Test Configuration

It is realized that electrical isolation of the spacecraft from its command and control units or from the EAGE, as well as high voltage pulser isolation, may pose severe practical problems. The contractor may propose an alternative system configuration in which the spacecraft is isolated from external ground by a ferrite loaded stinger as shown in Figure 21 (Refs. 36, 39). High frequency electromagnetic environment and critical test point data as well as EAGE and command and control connections to the satellite from the screen room are run via hard wire connections through the stinger which provides RF shielding. The ferrite provides inductive isolation of the hard wired data link from the satellite for times of the order of several hundred nanoseconds for an inductance of a fraction of a mH. If this approach is chosen, primarily where the predicted discharge pulses are relatively short ($\leq$200 ns), then the contractor must demonstrate that its use does not significantly perturb the response of the spacecraft to the exciting electrical injection pulse.

3.6 INSTRUMENTATION

Representative instrumentation for performing the measurements described below are summarized in Table 9.

3.6.1 Pulsers

Two basic current injection schemes have been developed to simulate the response of the spacecraft structure to EID in internal spacecraft dielectrics. Both of these employ a capacitive discharge pulser as shown in Figure 22. The pulser itself can be a self contained unit such as the PULSAR 50-Q or one constructed from a high voltage power supply, and an appropriate charging network. The switch is a remotely triggered spark gap. For a high level test, the basic pulser must be capable of peak output voltages of 20-100 kV, peak currents of several hundred amps, and a pulse width (FWHM) of $>1\,\mu$sec. The difference between the two pulse injection techniques specified lies in the manner of coupling of pulser to test object. In the first, direct injection, the pulser is connected directly to the satellite and current is returned via a hardwire connection to the common ground plane as shown in Figure 20. In the second, the pulser is capacitively coupled to the test object as shown in Figure 21.

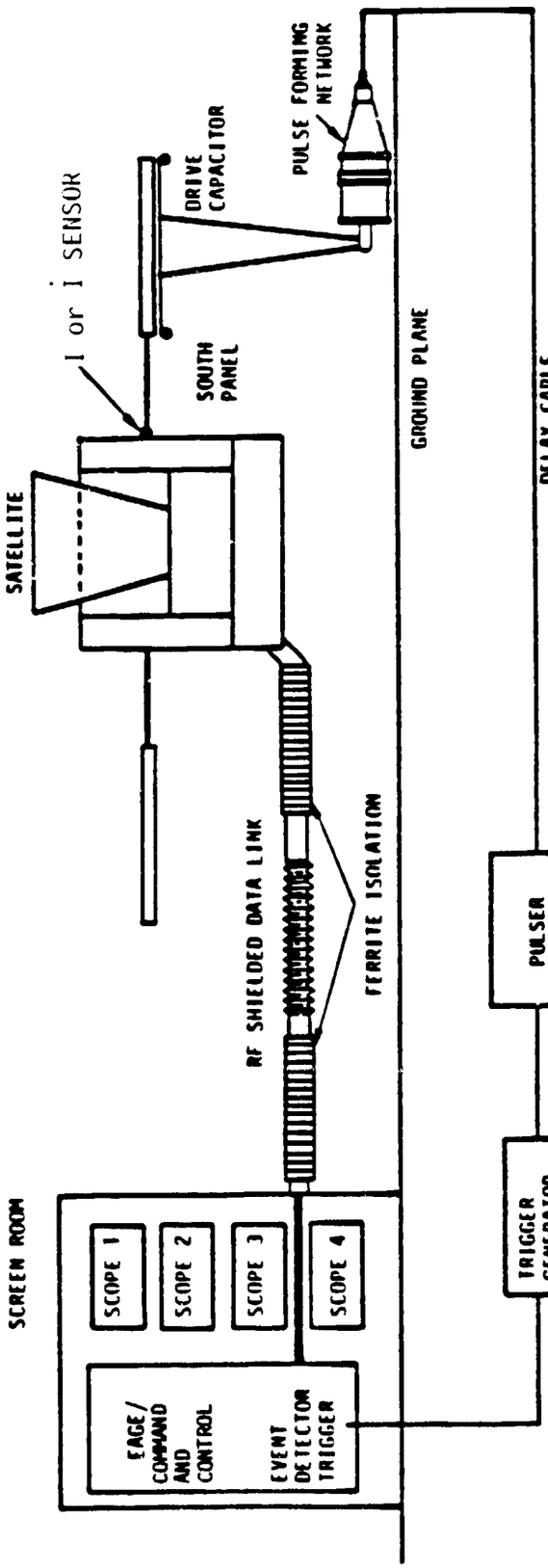

Figure 21. High-level current injection test configuration with ferrite isolation of spacecraft

Table 9. Suggested Test Equipment for System EID Testing

Equipment/Manufacturer	Model	Frequency Range	Other Characteristics	Comments
RF Amplifiers				
Avantek	AWL 500	.001 MHz - 500 MHz	26 db gain, Input Voltage $\pm$ 30 μV - 22 mV	
Hewlett Packard	8447D	0.05 Mz - 1300 MHz	26 db gain, Input Voltage $\leq \pm$ 20 mV	
Oscilloscopes				
Tektronix	7000 series	DC - >250 MHz	Input Voltage sens 10 mV/diV @ BW, 1mV @ 100 MHz	Depends on Model/plug ins chosen
Hewlett Packard	1715A, 1725A, 1727A	Upper BW (3dB) $\geq$200 MHz	Input Voltage Sensitivity 5mV/diV (1715A) 10 mV/diV (1725A)	
Transient Digitizers				
Biomation	6500	$\leq$100 MHz (3db BW)		
Tektronix	7612	$\leq$ 80 MHz (3db BW)	Input voltage sensitivity, 5mV/diV @ BW	
Tektronix	7912	$\leq$500 MHz (3db BW)	Input voltage sensitivity 10mV/diV @ BW, 1mV/diV @ 105 MHz	
Analog Fiber Optic Links				
Nanofast	OP-50	$\leq$150 MHz (3db BW)	Includes 20 db amplifier, 3, 14, 20, 40 db programmable attenuators	No coaxial switch
IRT	F0DL2	.01 MHz - 140 MHz	Includes programmable 26db amplifier, 0-63 db programmable attenuator, programmable 8in/ 1 out switch	
Coaxial Switches				
Novack		0 - 300 MHz	8 in, 1 out	Mechanical
Matrix		0 - 300 MHz	8 in, 1 out	Programmable
Pulse Generators				
Pulsar	50 - Q		V_{max} = 100kV, I_{pk} = 2000A (50Ω), $t_r \geq$ 10ns, t_f = 2μs	
	10 A		V_{max} = 10kV, I_{pk} = 200A (50Ω), $t_r \leq$ 10ns, $t_f \leq$ 150ns	

Table 9. Suggested Test Equipment for System EID Testing (Continued)

Equipment/Manufacturer	Model	Frequency Range		Other Characteristics		Comments
B Sensors						
				Maximum Field Change (Teslas/Second)		
EG&G	CML-3	≤632 MHz (3db)		$2 \cdot 10^7$		For surface current measurements
	CML-X3	≤700 MHz (3db)		$6 \cdot 10^6$		
	CML-X5	≤500 MHz (3db)		$3 \cdot 10^6$		
	CML-6	≤175 MHz (3db)		$6 \cdot 10^5$		
Surface Current (H) Sensors						
			Peak Current (A)	Nominal Z_t (Ohms) into 50 Ohms		
AIL	95210-1	0.1-100MHz	300	3		
	95210-2	0.1-100MHz	300	3		
Clamp On Current Probes						
			Peak Current (A)	Nominal Z_t (Ohms) into 50 Ohms	Gap (Inches)	
AIL	91550-3	0.01 - 100MHz	500	0.033	1-1/4	For measuring currents on struts and cable bundles
	91550-4	0.02 - 100MHz	500	0.1	1-1/4	
	91550-5	0.1 - 100MHz	100	1.0	1-1/4	
	91550-7	0.002-180MHz	4000	0.002	1-1/4	
	93686-2	0.3 - 50MHz	100	5	2-5/8	
	93682-3	0.1-140MHz	100	2	2-5/8	
	93682-4	0.005-100MHz	100	0.06	2-5/8	
	93666-4	0.001-100MHz	500	0.06	2-5/8	
	93686-4M	0.001-100MHz	4000	0.005	2-5/8	
	94330-1	1-250MHz	10	7	3/4	
	94430-2	0.1-250MHz	50	1	3/4	
	94430-3	0.01-250MHz	50	0.1	3/4	
	94430-4	0.01-250MHz	50	0.05	3/4	
	94456-1	0.1-50MHz	100	5	4	
	94456-2	0.1-90MHz	100	1	4	
	94456-3	0.01-100MHz	100	0.1	4	
	94456-4	0.01-100MHz	100	0.06	4	
Tektronix	CT-1	0.3 MHz-1000 MHz	100	5		For individual wire measurements
	CT-2	1.2 kHz-100 MHz	100	1		For individual wire measurements
Voltage Probes						
			V_{max} (kV)			
Pulsar	710	DC-2 kHz	± 100			For high voltage source measurements
	VP-60	DC-80 MHz (3db)	± 60			
	VP-120	DC-80 MHz (3db)	± 120			
			V_{max} (V)	Attenuation	Impedance (MΩ,pf)	
Tektronix	P6046	≤100 MHz	± 50	1X, 10X	(1,10),(10,3)	Diff/Amp
	P6201	<1 GHz	± 60	1X,10X,100X	(0.1,3),(1,1.5),(1,1.5)	FET
	P6202A	<500 MHz	± 60	10X,100X	(10,2)	FET
	P6056	>1 GHz	± 16	10X	500Ω, 1pf	50Ω
	P6057	>1 GHz	± 50	100X	5 kΩ, 1pf	50Ω
	P6106	<390 MHz	± 500	10	(10,10.5)	Passive, Bandwidth decreased to 153 MHz for 3M code.

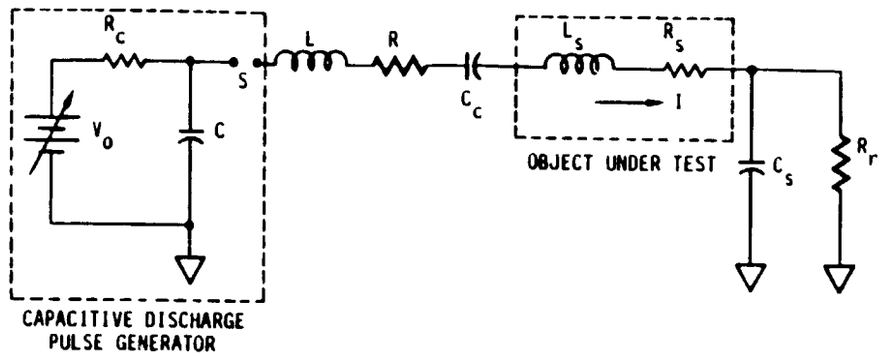

RT-20911

ADJUSTABLE CIRCUIT PARAMETERS

V_o = ADJUSTABLE CHARGING VOLTAGE
R_C = CHARGING RESISTOR
C = DRIVE CAPACITOR
L = ADDED INDUCTANCE FOR WAVESHAPING
R = ADDED RESISTANCE FOR WAVESHAPING
C_c = CAPACITIVE COUPLING BETWEEN PULSE GENERATOR AND TEST OBJECT
L_s = NOMINAL INDUCTANCE OF TEST OBJECT
R_s = NOMINAL RESISTANCE OF TEST OBJECT
C_s = CAPACITANCE BETWEEN TEST OBJECT AND PULSE GENERATOR GROUND
I = BODY CURRENT OF TEST OBJECT WHICH IS CHARGING CURRENT FOR C_s
R_r = RESISTANCE OF RETURN LINE TO GROUND.
S = SPARK GAP

FOR DIRECT DRIVE, C_c AND C_s ARE REMOVED FROM CIRCUIT.

RT-20911-1

Figure 22. General capacitive discharge injection model

3.6.1.1 Selection of Current Injection Techniques. The selection of a current injection scheme for exciting a candidate discharge area will be made on the basis of an electromagnetic coupling analysis performed by the manufacturer to determine which aspects of the induced electromagnetic fields are important in exciting points of entry (POEs) or penetrations for the coupling of EID generated electromagnetic energy into the spacecraft adjacent to the discharge site. Which technique is utilized depends on what aspects of the EID induced electromagnetic fields are important in exciting particular POE's. If it is desired to simulate the surface current excitation mechanism (at points away from the drive plate) associated with the circulation of large amplitude (hundreds of amps), wide (μs) pulses associated with the blowoff of electrons from large surfaces, then the direct drive approach is probably better. However, there are cases where excitation of system resonances or normal electric fields are the important coupling modes. Then a capacitive excitation is better. Capacitive coupling in this sense means both the case where C_c and C_s are nonzero and also the case where $C_c = \infty$, C_s finite; i.e., capacitive direct injection (CDI). The CDI technique gives a relatively good simulation of blowoff, but its practical implementation given realistic circuit parameters is difficult because of a need for higher pulser voltages to drive an equivalent amount of current through the spacecraft if compared to that for direct drive.

As we have pointed out, the direct injection approach shown in Figure 20, was chosen because it is possible to drive more amps/volt with direct coupling obviating the use of extremely high voltages with charging sources. As the model simulations have demonstrated, it takes extremely high voltages with the capacitive coupling to produce large amplitude, wide pulses. The coupling capacitors provide a relatively high impedance at the frequencies of interest. Pulse amplitude is further reduced if one wants to produce a critically damped waveform of the kind shown in Figure 19 because the damping resistor, which isolates the pulses from the system, further limits current output.

In implementing the basic circuit, it is important to eliminate or maximize stray coupling paths to control circuit parameters and current paths. Ideally, the pulser and test object would be connected only to the common ground plane shown in Figure 20. For some electrical testing, this plane has been made of heavy copper screening to provide a well defined reference point. However, the presence of a nearby good ground of this type can affect the satellite Q value and hence its ringing frequency. One would like to simulate the free space case.

Not shown in the basic circuit are any details about the switch. This must be a dielectrically isolated unit with a fast switching time. For voltages up to a few kV and modest current levels (10's of amps) an SCR stack may be used. This triggering circuit can be fired by the output of a fiber optic controlled pulser such as the ANVIL 160. This was the approach taken in the IRT MIL-STD 1541 arc injection test of the SCATSAT described in Reference 3. At higher voltages a spark gap must be used. This can be either remotely triggered or of the adjustable, self-breakdown type.

It is also important to isolate the charging voltage source from external ground. For relatively high frequencies (i.e., pulse widths <200 ns or so) this may be done by wrapping power cords around ferrite cores. However, in most cases it will be necessary to use dc isolated power supplies. For voltages up to a few kV, charging sources can be dry cells. Higher charging voltages require a power supply. These units can be operated from a storage battery and an inverter. However, such units become physically large, and it is difficult to prevent stray capacitance coupling to the pulser. Mounting also becomes a problem. If very high voltages (more than one hundred kV) and high currents are required, then one must use something like a Marx generator.

3.6.1.2 Selection of Current Injection Points. Sections 3.1.4, 4.6.1, 6.1.1 of MIL-STD 1541 provide definition of critical test points. For a system EID test of the type proposed, these points will generally be external dielectric surface areas which are susceptible to discharge. Susceptibility can be established by any of the following methods which are progressively less stringent.

1. Assume that all dielectric surfaces will suffer on orbit discharges and test accordingly.
2. Stress those materials which have been shown to discharge in tests performed in ground simulation of the charged particle environment responsible for EID.
3. On the basis of the charging analysis performed with a code such as NASCAP test those dielectrics whose potential relative to the structure of the spacecraft exceeds established electrical breakdown thresholds.

The most conservative approach is to adopt screening criterion (1). Laboratory tests indicate that discharge thresholds are a function of many parameters including sample geometry, the relative locations of ground planes and edges, thickness and exposure conditions. It is true that some dielectrics such as thermal control paints have relatively high conductivities (>$10^{-10}\ \Omega^{-1}\ cm^{-1}$) so that sufficient charge buildup which

leads to breakdown cannot occur. Available conductivity and ground electron spraying data can be used as a guide in this regard. NASCAP analysis is useful in determining the worst case differential potentials built up in substorm conditions. These values for the different dielectrics can be used as a screen if compared to breakdown voltages.

There is also an approximate guide for determining breakdown voltages based on published dielectric breakdown strengths for common insulators. The dielectric breakdown strength E_B is defined as the applied electric field at which breakdown occurs. E_B can be related to V_B for a material of thickness d as

$$V_B = E_B d \, . \qquad (5)$$

EID breakdown voltages estimated in this way from E_B values deduced by electrical stress measurements typically agree within a factor of two with those measured. Data for a limited group of measurements are shown in Table 10. Estimates produced in this manner are usually low as electric strenghts are typically measured on relatively thick samples (mm to cm) with relatively wide pulses. Most spacecraft dielectrics are typically less than 0.03 cm. Dielectric strengths (measured in V/cm) tend to go up as sample thickness and pulse width go down. Thus, spacecraft insulators tend to breakdown at higher surface potentials than predicted. On choosing values of E_B for a given dielectric, the value should be taken for the sample thickness which is closest to that of the spacecraft material. This argument is only approximately correct as evidence from ground testing indicates that lateral surface potential differences are also important in triggering breakdown.

Table 10. Comparison of Observed EID Breakdown Voltages with Predictions Based on Equation 5

Material	Thickness (10^{-3} cm)	Dielectric Strength (10^6 V/cm)	Predicted V_B (kV)	Observed V_B (kV)	References
Teflon FEP	12.7	1.6[a]	16	16	2
Kapton	5	2.8[a]	14	15	2
				13	4
Mylar	7.5	1.6[a]	12	11	4
Fused Quartz	15	0.25	3.8	12	2
	20		5.1	6.5	4

a) Taken from NBS Monograph 132, A Compilation and Evaluation of Mechanical, Thermal and Electrical Properties of Polymers, 1973.

It was pointed out in Section 2 that none of the proposed pulser designs, or for that matter, any of the existing electrical excitation schemes, will provide a good global simulation of the EID excited fields on the surface of the spacecraft. The simulation will be better at some areas than others. Thus, a technique which gives an incorrect field distribution at one location can be valuable if it gives a good simulation of fields in the areas of interest; i.e., near POE's significant for coupling. Therefore, the coupling analysis performed as specified in Section 50.3.2.3 of SCA may suggest additional points of excitation as the real criterion for the selection of EID drive points to correctly excite the significant POE's. Here, frequency content and field amplitude are most important. The discharge sites are the most obvious points of excitation but not the only ones.

3.6.1.3 Attachment of Pulser to the Spacecraft. The following steps define the method of attachment of the pulser (including pulse shaping circuit elements shown in Figure 20) to the spacecraft.

1. Based on a charging and coupling analysis, and using the criteria given in Section 3.6.2.2, the contractor will determine the appropriate locations to attach the positive and negative leads of the pulse generator (direct injection) or the position and spacing of the coupling plate (capacitive coupling).

2. For each location, the appropriate number of wires in each grid (direct injection) and the size and shape of the drive plate (capacitive coupling) will be determined depending on the area over which current is to be injected, based on the coupling analysis. The wire grid can be a continuous resistively loaded structure with a total R' and L' set to provide both pulse shaping and impedance matching.

3. The connections to the critically stressed area will be designed to inject current over the same area as participates in the discharge. This may be assumed to be the entire conductively bounded dielectric surface; e.g., an entire solar array panel, or thermal blanket would be driven.

4. For each location and its respective wire grid connection to the pulse generator and return, L'_1, L'_2, will be calculated or measured. Where current is returned to the system ground via capacitive coupling, the coupling of the test object to ground will be determined and adjusted as required.

5. For direct coupling, the wires will not be attached to the dielectric itself but to the conducting substrate surrounding the dielectric surface. The manufacturer will specify an attachment procedure which will be approved by the procuring agency.

6. Conventional circuit analysis will be used to compute the values of V_o, R_c, R, L, C (and C_c for capacitive injection) required to drive the spacecraft with the desired current magnitude and waveshape.

7. The test setup of Figure 20 will then be implemented based on the information generated in Steps 1 through 6.

Note that the entire circuit can be reduced to a charged capacitor being discharged into a series R', L', (and C_{eq} for capacitive coupling) which are respectively the sum of the individual elements shown in Figures 20 and 22. For the direct-drive case, the basic equation for the current flowing on this circuit as a function of time is:

$$I(t) = \frac{2V_o \eta}{(\eta^2 - 1)^{1/2} R'} \exp(-\eta\omega_o t) \sinh\ \omega_o(\eta^2 - 1)^{1/2} \tag{6}$$

$$\eta = \frac{R}{2}\ (C/L)^{1/2} = 1/2\,(\tau_2/\tau_1)^{1/2}, \tag{7}$$

$$\omega_o = (L'C)^{-1/2} = \frac{1}{2}\ (\tau_1\tau_2)^{-1/2}, \tag{8}$$

$$\tau_1 = 2L'/R', \tag{9}$$

$$\tau_2 = 2R'C \tag{10}$$

R' is the sum of all resistances (except for R_c), L' the sum of all inductances, and C the charging capacitor in Figure 22.

For capacitive coupling, the circuit becomes a series R, L, C circuit and the appropriate equations for the load current are:

$$I(t) = V_o C_{eq}(\omega_o/\omega) \exp(-t/\tau_1) \quad \cos h\,(\omega t + \omega_1/\omega) \tag{11}$$

$$- \tau_1^{-1} \sinh(\omega t + \omega_1/\omega),$$

where

$$\frac{R'^2 C_{eq}}{4L'} > 1 \text{ (overdamping)}, \tag{12}$$

or

$$I(t) = C_{eq} V_o \exp(-t/\tau_1)(t/\tau_1), \tag{13}$$

where

$$\frac{R'^2 C_{eq}}{4L'^2} = 1 \text{ (critical damping)}, \tag{14}$$

or

$$I(t) = V_o C_{eq} (\omega_o/\omega) \exp(-t/\tau_1) \left[\omega \cos(\omega t + \omega_1/\omega) - \tau_1^{-1} \sin(\omega t + \omega_1/\omega)\right], \tag{15}$$

where

$$\frac{R'^2 C_{eq}}{4L'^2} < 1 \text{ (underdamped).}$$

In each case

$$\omega_o = (L' C_{eq})^{-1/2}, \tag{16}$$

$$\omega = \left| \omega_o^2 - \frac{R'^2}{4L'^2} \right|^{1/2}, \tag{17}$$

$$\tau_1 = \frac{2L'}{R'}, \tag{18}$$

and

$$\omega_1 = 2/\tau_1. \tag{19}$$

The effective capacitance C_{eq} is

$$C_{eq}^{-1} = C^{-1} + C_L^{-1} + C_c^{-1}. \tag{20}$$

The effective resistance R' is equal to the sum of all the series resistances, while the effective inductance L' is equal to the sum of all the series inductance

3.6.2 SENSORS

Generally, satisfactory performance will be determined by post test functional testing and telemetered status monitoring during testing. However, Section 6.2.1 of MIL-STD 1541 requires that the vehicle AGE or onboard telemetry shall not be used as the sole means of demonstrating compliance. This section specifies in a generic manner the types of extra instrumentation suitable for providing status information. It is divided into three basic categories, source measurements, electromagnetic environment measurements, satellite functional monitoring. In general, the information specified includes the following:

1. *Signal to be measured*
2. *Signal characteristics*
3. *Type of sensor to be employed*
4. *Sensor characteristics*
5. *Location*
6. *Monitoring*
7. *Connection to data recorder*
8. *Necessary interface equipment.*

Where possible, examples of specific sensors will be given. However, which particular sensor is chosen for a particular spacecraft measurement is dependent on the specific characteristic and test environment. In general, the use of passive sensors, i.e., those requiring no power is to be preferred to active sensors.

3.6.2.1 Source Characteristics Measurements. Basically two pieces of data are required: the discharge voltage of the source and the drive current. If a multipoint drive is employed, then the current through each of the individual drive wires may be desired. A summary of representative source measurements is given in Table 11, and specific instrumentation in Table 9.

The source measurements need only be made during checkout as the output of electrical pulsers are relatively constant. Both voltage and current probes are available to measure these transients. The current probes must be carefully isolated from contact with the discharge pulse line to ensure that the maximum standoff voltage of the probe is not exceeded. The outputs of the current probes should be transmitted

Table 11. Source Measurements

Measurement	Type	Representative Characteristics	Location	Sensor	Connection	Recording	Comments
1. Charging Voltage	DC Voltage	50kV DC	High Pot Side of C	High Voltage Probe	HW[a]	Voltmeter	Removable during test
2. Drive Current	Pulse Current	$I_p < 1000A, \tau_p \leq 5\mu s$	Pulser Output	Current Probe	HW/FO[b]	CRO[c]/TD[d]	Removable during test
3. Wire Currents	Pulse Current	$I_p/n, \tau_p \leq 5\mu s$	Wires on Drive Plate	Current Probe	HW/FO	CRO/TD	Removable during test

a. HW = hardwire; b. FO = Fiber optic link; c. CRO = oscilloscope; d. TD = Transient Digitizer; n = no. drive wires

back to the recording devices via fiber optic links. If this is not possible and a hard wire link is used, the signal wire should be well shielded coaxial cable, preferably with a semi-rigid copper jacket, and run in a manner least perturbing to the electromagnetic environment.

3.6.2.2 Electromagnetic Environment Measurements. In order to validate the test results, one must ensure that the desired electromagnetic environment is reproduced on the outer surface of the spacecraft. The critical parameters to be measured are the tangential magnetic field $\vec{H}_t$ which is proportional to the surface current density $\vec{K}$, and the normal electric displacement $\vec{D}_n$, related to surface charge density. In addition, it is useful to measure boom currents. The joints between the spacecraft and booms on which antennae or the solar array panels are mounted often serve as a major penetration for the coupling of energy into the interior of the spacecraft.

The available data on the magnitude of the surface currents can be found in References 2 and 4. Based on review of those references, the kinds of surface currents expected are in the 1-100 A/M range or $\dot{H}$ fields of the order of 10^5 - 10^8 A/M/S. Observed pulse widths are in the range of one hundred nsec up to several microseconds. There is no $\vec{D}_n$ data. However, one can make estimates of both $\vec{K}$ and $\vec{D}_n$ based on the scaling law data presented in Table 4 and the model assumption data presented in Table 15.

To estimate the magnitude of the surface currents which flow on the satellite consequent to a discharge, we have summarized the average scaling laws for current

$$I_p(A) = K_I A^{0.55} (cm^2), \tag{21}$$

where $1 \leq K_I \leq 10$, *and that for pulse width is*

$$\tau_p(ns) = K_p A^{0.55} (cm^2), \tag{22}$$

where $K_p = 20$. *It is assumed that area of typical spacecraft dielectrics lies between* $100\ cm^2$ *and* $4m^2$. *Then the calculated extreme values of expected current and pulse width can be estimated and are given in Table 12.*

Table 12. Characteristic Discharge Responses

Area (cm^2)	I_p(A)	τ_p(μs)	$\dot{D}_n$($A/m^2/sec$)	D_n(C/cm^2)
100	12.6	0.25	10^5	1.8×10^{-3}
4×10^4	5190.	10.0	5.10^3	1.8×10^{-3}

The values for the peak current are undoubtedly an overestimate, as the I_p calculated is the emission current. The experimental data indicate that the body currents produced are only a fraction of the emitted current. Perhaps a more realistic upperbound might be $I_s < 1000A$, $\tau_p < 5\ \mu s$.

The normal electric displacement fields can be estimated in a similar manner. The normal displacement field D_n produced by a charge separation of $\pm Q$ is approximately

$$D_n = \frac{Q}{A}\ (coul/m^2) = 10^4 K_Q \leq 1.8 \times 10^{-3}\ C/m^2 \qquad (23)$$

The rate of rise is approximately

$$\dot{D}_n = \frac{Q}{\tau_p A} = 10^9\ \frac{K_Q}{K}\ A^{-0.5} = 10^6\ A^{-1/2}\ C/m^2 \cdot sec. \qquad (24)$$

Order of magnitude estimates for D_n and $\dot{D}_n$ can be found in Table 12.

It is possible to measure surface currents of sufficiently large magnitude in the absence of ionizing radiation field using surface current sensors like the Singer 95210-1 or 95210-2. These small, surface mounted sensors have an active area of about 1/4 to 1/2 square inch. If sensitivity is a problem, then $\dot{B}$ (or J) sensors which measure the rate of change of B or magnetic induction field can be used. Specifications for the CML $\dot{B}$ sensors are provided in Table 9.

One problem to be faced with using sensors that measure time rates of change is that the relative amplitude of the higher frequency components are magnified, even though these components contain relatively little energy. Therefore it is advisable to integrate the output of these sensors where possible using active integrators with time constants long compared to pulse width (about a factor of 10 is recommended).

The rate of change of the normal displacement field or surface charge density $\dot{D}_n$ can be measured with a surface mounted sensor like the EG&G CFD $\dot{D}$ HSD-3 sensors.

Currents flowing along booms or cable bundles can be measured by clamp-on current sensors such as those given in Table 9.

Some of these sensors such as the CML B sensors have differential outputs. A balun or impedance matching transformer is required to convert the output from double ended to single ended. The sensors should be mounted directly on the satellite surface or boom. This may pose practical problems in terms of means of adhesion and avoidance of surface contamination. Signal cables should be run from these sensors to the fiber optic data links in a manner least likely to perturb the electromagnetic environment; i.e., along ground planes. The use of RF tight, semi-rigid Cujack or Aljack cable and locking connectors is recommended.

3.6.2.3 Internal Measurements. Section 6.2.1 of MIL-STD 1541 requires that monitoring of specific response points be made during testing in addition to performance data which may be received via the EAGE or vehicle telemetry. The system specific points must be selected by the manufacturer and approved by the procuring agency. Given the mode of EID coupling, the monitoring points are most likely to be the currents and voltages on critical signal lines, or at inputs to the interface circuits of critical functional units. All of the measurements are of two types, currents on individual wires and input voltages at critical box pins. A variety of standard current and voltage probes are available to perform these measurements. A representative set of these is given in Table 9.

These measurements must be implemented without disturbing the operation of the spacecraft. Practically, this may mean modifying cable bundles by including interior wires on which can be mounted current probes, putting monitoring points in critical circuits which can be accessed through box pins, or by providing breakout boxes which interface between the normal cable harness and the input connectors of the box under test. These boxes contain necessary current and voltage sensors, coupling circuitry to isolate the measured cable or test point from the measuring device, and, output connectors. The output of the sensors is then run via separate cables back to a J-box located at the satellite where the coaxial switches and fiber optic or other data transmission links are gathered. *The breakout box approach has been used to perform SGEMP electrical testing (Refs. 37, 38).*

In addition, it may be desirable to measure the internal electromagnetic environment of the spacecraft to ensure that it is correctly driven and to locate any POE's. This may be done with the environment sensors described in Section 3.6.2.2. In

particular, it is useful to measure the currents flowing on cable bundles using one of the clamp-on current sensors described in Table 9. This is because a major coupling mode is through the electrical and magnetic field penetration of cable shields into individual wires.

3.6.3 Data Recordirg

The signals to be monitored during testing are of two kinds. Electromagnetic response data such as surface currents and electromagnetic fields, and satellite telemetry data. The former is relatively high frequency (1-200 MHz) analog data, while the latter consists of much slower digital data. The preferred test configuration described in Section 3.5.2 is one in which the spacecraft is electrically isolated except for current injection and return over paths with controlled characteristics. These requirements in turn determine the characteristic of the required data systems.

3.6.3.1 Dielectric Data Links. Transmissions of high frequency analog data is to be via wide band analog fiber optic data links. The type of system required consists of:

1. Wideband (0-300 MHz), many in - one out coaxial switches
2. Wideband (.01-150 MHz minimum) analog fiber optic data links
3. Digital Attenuator, 0-60 dB
4. RF Amplifier; 20-26 dB gain, 0.01 to 500 MHz (3 dB bandwidth)
5. Digital Fiber Optic Control Link
6. Digital Control Circuitry.

The function of these systems is to provide a means of monitoring several critical points with one data link. Because the range of possible signal amplitudes is large it is necessary to provide both amplification for small signals and attenuation for large ones as the normal operating range of the LED in the FO transmitter is typically $\pm$ 5 to $\pm$ 500 mV and often less. The systems given in Table 13 can monitor signals from a few hundred microvolts to 1 kV over a bandwidth of 0.01-150 MHz. *A block diagram for the IRT system is given in Figure 23.*

3.6.3.3 Vehicle Status Information. Vehicle status information during testing will be provided by the spacecraft telemetry system. In order to provide for electrical isolation, this information will be transmitted via the satellites RF links.

Table 13. Representative Dielectric Data Systems

Unit	IRT	AFWL
Coaxial Switch	Matrix Programmable	Novak - Mechanical 1 in - 8 out (0-300 MHz)
Analog FO Unit	Merit MDL 259-20-5030 0.01 - 140 MHz (3 dB BW)	Commercial Unit Nanofast Model OP-50 UBW = 150 MHZ
Attenuator	Alan Industries # 50DA63> - Programmable, 0 - 63 dB	± 10 mV to ± 100 V input with 20 dB amplifier, 3, 14, 20, 40, dB attenuators and controls incorporated
RF Amplifier	Avantek, AWL 500, 26 dB, gain, .001-500 MHz, (3 dB BW)	
RF Transfer Switch	Transco 700 C 70100	
Digital Fiber Optic Link	Math XD1100 Xmtr RD 1100 Rcvr	
Digital Control Unit	Custom Built	

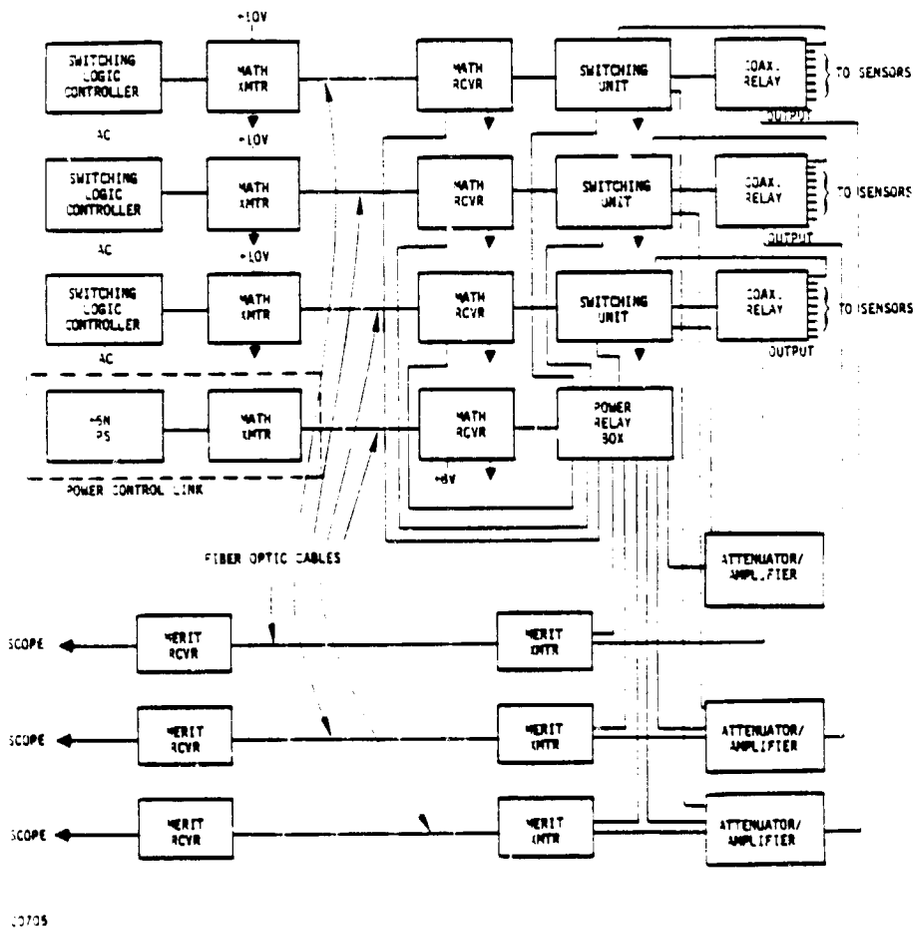

Figure 23. IRT Analog Fiber Optic Data Systems

The IRT system was built out of commercially available components except for the digital control unit. The Nanofast Model OP-50 is a commercial system procured as a package. The IRT system was designed to be remotely operated in a vacuum. For electrical testing, some simplification is possible. The programmable coaxial switch and attenuator ccould be replaced by manual units accessible from the satellite-signal line J-box. This would eliminate the need for control electronics.

3.6.3.2 Recording of Fast Transient Data. Generally, fast transient data will be recorded on oscilloscopes and cameras or transient digitizers. Transient digitizers are preferred as both an analog and digital signal is obtained. The digital signal can be stored and processed with other data from the vehicle AGE and telemetry. To avoid degradation, the bandwidth (upper 3 dB point) should be as high as possible. While the major response currents have characteristic frequencies of 1 to 20 MHz, vehicle structural resonances can exceed 150 MHz. It is recommended that transient recording devices have a minimum bandwidth of 100 MHz and should preferably be 200 MHz or above. Representative units are listed in Table 14.

Table 14. Representative Data Recording Devices

Device	Upper (3db) BW (MHz)	Minimum Sensitivity (V/diV)	Comments
Scopes			
Tektronix 7704	250	10mV, 1mV (100 MHz)	
Tektronix 7844	400	10mV, 1mV (100 MHz)	Dual Beam
Tektronix 7904	500	10mV, 1mV (105 MHz)	
Tektronix 7834	400	10mV, 1mV (100 MHz)	Storage Scope
HP 1715A	200	5 mV	
HP 1725A	275	10 mV	
HP 1727A	275	10 mV	Storage Scope
Transient Digitizers			
Biomation 6500	100 MHz		
Biomation 8100	30 MHz		Dual Channel, Limited Value
Tektronix 7912	500 MHz	10mV, 1mV (105 MHz)	
Tektronix 7612	80 MHz	10mV, 5mV (80 MHz)	

3.6.3.4 Data Transmissions for the Alternative System Test Configuration. For the system configuration described in Section 3.5.3, the links between spacecraft and EAGE and recording instrumentation will be hard wired and run through the inductively loaded stinger which connects the satellite body to the ground plane.

3.7 TEST CONDUCT

3.7.1 General Procedure

The following steps shall form the major elements of the test:

1. A complete pretest functional checkout will be performed using the EAGE. The nature of the checkout will be specified in the test plan and approved by the procuring agency.
2. The spacecraft will be disconnected from the EAGE and placed on battery power and the RF telemetry system for command and status monitoring will be activated.
3. A series of electrical injections will be performed according to the steps given in Sections 3.7.2. During injection the vehicle will be operated in representative on-orbit flight modes and in the on orbit configuration as specified by the manufacturer and approved by the procuring agency: The spacecraft's on board housekeeping capability will be used to monitor its behavior for out of spec operation according to system performance criteria defined by the SPO (see Section 3.4.2.2)
4. At the end of a series of injections at a given point and drive level a quick look functional checkout of the spacecraft will be made before proceding to perform tests at the next drive level. The nature of this checkout will be specified in the test plan and approved by the procuring agency.
5. Following the complete series of electrical injection tests, the spacecraft will be reconnected to the EAGE and the system functional tests performed in Step 1 will be repeated.

3.7.2 Current Injection Characteristics

The assumptions on which the proposed electrical injection schemes have been based have been reviewed in Section 2 and Reference 2. For convenience they are summarized in Table 15. The primary one is that the principal electromagnetic driver in generating surface electromagnetic fields is the blowoff of electrons. From this premise, it is possible to predict the response of satellite like objects if one makes certain assumptions about the emission characteristics of the blowoff charge (magnitude, energy and angular distributions, surface albedo, presence and characteristics of an associated plasma). However, these calculations have not been able to predict the

response of real satellites, i.e., those with reentrant geometries such as booms, antennae, etc., largely because of a lack of a well validated discharge model, but also in part because of the inaccuracies inherent in trying to predict the response of complicated systems with simplified models. In addition, the number of cases for which calculation has been performed is extremely limited. In a sense, response prediction is in its infancy.

Thus, one must fall back on the limited body of data which connects inferred discharge characteristics to the observed response of simple systems such as planar dielectric surfaces. To some degree, the observed discharge emission characteristics show the kind of area scaling described in Section 2, and summarized in Table 4. Based on those area scaling laws, the simple coupling models, and the limited data base, one can derive predictions as to the anticipated skin currents generated as a consequence of EID, in particular dielectrics.

Table 15. Summary of Assumptions Used to Derive Current Source Terms

1. The predominant mode of excitation is the blowoff of electrons.
2. Punchthrough and flashover serve primarily to reduce the potential of the dielectric relative to the structure.
3. The emitted electrons move in fields whose sources are electrons trapped in the dielectric, replacement charges and currents, and other emitted electrons.
4. Spacecraft isolation ensures spacecharge limiting so that most electrons return to the structure, hence, current flow is limited, decreasing in amplitude and pulsewidth as the distance from the dielectric increases.
5. A worst-case is taken to be the response of the satellite grounded for which the skin currents are equal to the blowoff currents.
6. Replacement current characteristics are described by the scaling laws presented in Table 4.

Therefore, in the spirit of doing what one can at this time with the available data base, these scaling laws have been adopted as the provisional injection current amplitude and pulse width characteristics to be provided for Section 50.4.2.1 of the provisional SCA. We wish to emphasize this provisional nature and underline this by restating the caveats listed in Table 16. The specification as it stands is incomplete because no information is given on the normal electric fields associated with charge density. The coupling experiments described in References 2 and 4 did not measure this quantity. Planar sample measurements reported in Reference 21 indicate that they can be tens of kV/m. The normal electric fields on the surface of the test objects

can be calculated with the modeling approach described in References 4 and 5. It would be useful to publish such data if it exists and to perform additional calculations and measurements for realistic satellite configurations.

Table 16. Current Scaling Law Caveats

1.	*Scaling based on monoenergetic, circular samples, grounded edges. Real samples show order of magnitude variations about the mean.*
2.	*Coupling based on limited validation.*
3.	*More complicated environmental simulations (UV, high-energy electrons) typically diminish or eliminate discharging.*
4.	*Possible rate effects for typical tests fluxes (1 na/cm^2), low-flux threshold.*
5.	*Real dielectrics do not show regular discharging patterns (edges, seams).*
6.	*Neglects plasma effects (Debye screening).*
7.	*Does not handle reentrant geometries.*
8.	*Probably worst-case.*

The question of emission pulse characteristics has a crucial bearing on possible current injection and experiment configuration issues. If the blowoff discharges were smaller (say <50A), and narrower (<200 ns) it would be more feasible to employ capacitive coupling in a threat level simulation. It might also be possible to use ferrite isolation of power supplies, data links and the satellite AGE which would make experimental implementation much less complex.

3.7.2.1 Direct Injection Excitation

1. The critical stress points will be driven by a direct current injection with direct return of the type specified in Section 3.6.1. The pulser circuit parameters will be adjusted to yield an exciting pulse that will have a maximum peak amplitude I_p and approximately equal rise and fall times $t_r = t_f = \tau_p$ chosen as follows in order of preference:

   a. Scaled values of I_p, τ_p based on laboratory electron spraying measurements on materials of the same type as used on the spacecraft. The laboratory data will be scaled according to the area scaling laws given in Table 17 for FEP Teflon, Mylar, Fused Quartz and Kapton. For other types of materials it will be assumed that:

Table 17. Summary of Discharge Scaling Laws

	$I_p(amps)=K_I A(cm^2)^{n_I}$		$\tau_p(ns)=K_p A(cm^2)^{n_p}$		$Q_p(\mu C)=K_Q A(cm^2)^{n_Q}$	
Material	K_I	n_I	K_p	n_p	K_Q	n_Q
Teflon[a]	10	0.58	16.5	0.48	0.18	1.06
Kapton[a]	5.6	0.51	21.9	0.59	0.15	1.00
Mylar[a]	10	0.59	18.2	0.46	0.21	1.05
Fused Silica[b]	0.81	0.6				

a. Ref. 24
b. Ref. 2

$$\frac{\tau_p(\text{Drive})}{\tau_p(\text{Measured})} = \frac{I_p(\text{Drive})}{I_p(\text{Measured})} = \frac{A^{1/2}(\text{Spacecraft})}{A^{1/2}(\text{Test})}, \qquad (23)$$

where τ_p (Measured) and I_p (Measured) are the discharge pulse widths, and total return currents (edge + backplane) for the test sample of area A (test). I_p (Drive) and τ_p (Drive), are the corresponding current injection peak current amplitude and pulse widths for an actual spacecraft material configuration with a dielectric area A (Spacecraft).

b. On the basis of a coupling analysis whose source terms and method of calculation yield the surface replacement currents for an excitation over the critically stressed area produced by a blowoff discharge. The analysis will be approved by the procuring agency.

In all cases, the value of I_p so determined shall be increased by 3 dB to provide for the 6 dB overstress (energy) above those levels calculated by Methods a or b.

2. Current will be returned to the pulser at locations remote from the current injection area. The response produced by the return at several different locations shall be determined. These locations will be chosen to provide maximum excitation of points of entry (POE's) for the coupling of electromagnetic energy into the interior of the spacecraft adjacent to the excitation location.

3. The testing will be conducted by injecting current pulses with the correct τ_p, but at an initial peak current I_p which is 21 dB below the amplitude as defined in 1. The pulse amplitude will be increased in approximately 6 dB steps until the level defined in 1 (I_p + 3 dB) is reached. The number of pulses to be injected at each level will be specified by the manufacturer and approved by the procuring agency. However, it is recommended that at least three pulses be injected at each level for each pair of excitation and return points.

3.7.2.2 Capacitive Injection

1. The critical stress points will be driven by capacitive injection which may either be through capacitive coupling with capacitive return or direct coupling with capacitive return. The pulser circuit parameters will be adjusted to yield an exciting pulse which has a first lobe peak amplitude I_p and time to first zero crossing t_1 chosen according to Methods a or b given for direct injection.

2. The capacitive coupler or direct connections to the critically stressed area will be designed to excite the same area as participates in the discharge. This may be assumed to be the entire conductively bounded dielectric surface.

3. The current return to the pulser will be through the capacitive coupling of the test object to the common pulser test object ground plane, for direct injection or through either direct or capacitive coupling for capacitive coupling of the pulser to the test object.

4. The testing will be conducted by injecting current pulses with the correct t_1 but at an initial peak current I_p which is 21 dB below the amplitude defined in 1. The pulse amplitude will be increased in approximately 6 dB steps until the smaller of the maximum attainable level or 3 dB overstress level is reached. The number of pulses injected at each level will be specified by the manufacturer and approved by the procuring agency. It is recommended that at least three pulses be injected at each level for each point of excitation.

5. If it is not feasible to capacitively drive the spacecraft at I_p + 3 dB, then additional internal sensors of the type described in Section 3.6.2.4 will be added to the spacecraft at internal monitoring points in sufficient number to provide data to determine whether the spacecraft would show improper responses if driven at full criteria levels based on the susceptibility thresholds for systems and subsystems as specified in MIL-STD 1541, Section 5.1.2.1.6. Subsystem electrical testing of those system components for which the above analysis indicates negative safety margins at critical internal test points is recommended to verify the analytical results. This testing will be conducted in the manner prescribed for subsystems in Section 50.4.2.1 of the SCA.

APPENDIX A

REPRESENTATIVE INSTRUMENTATION

Table A1. Tektronix Current and Voltage Probes[a]

Where higher frequencies (above 250 MHz) are encountered, active FET probes which have high input resistance and low input capacitance through their dynamic range should be used. For 50 Ω systems, see adjacent selection chart of 50 Ω divider probes.

FET PROBES

Type	Atten	Length*	Package Number	Loading	Rise time in ns	INPUT LIMITS: Max dc + pk ac	INPUT LIMITS: Linear Dynamic Range	INPUT LIMITS: Dc Offset Range	Read-out	Pa
P6046 Diff/Amp	1X	6.0	010-0232-00 Std	1 MΩ 10 pF	3.5	±25 V	±5 V		NO	2
	10X			10 MΩ 3 pF		±250 V	±50 V			
P6201 FET	1X	6.0	010-6201-01 Std	100 kΩ 3 pF	0.4	±100 V	±0.6 V	±5.6 V	YES	
	10X			1 MΩ 1.5 pF		±200 V	±6 V	±56 V		2
	100X			1 MΩ 1.5 pF		±200 V	±60 V	±200 V		
P6202A FET	10X	2m	010-6202-03 Std	10 MΩ 2 pF	0.7	±200 V	±6 V	±55 V	YES	2
	100X		W/010-0384-00Atn	10 MΩ 2 pF	0.7	±200 V	±60 V	±200 V	NO	

For rise time measurements, the interaction of the probe capacitance with the source impedance is of importance (RC time constant). For best results, the capacitance should be kept minimal. Typical probe specifications represent their response to a 25 Ω source environment.

50 Ω DIVIDER PROBES—For use with 50 Ω input amplifiers

Type	Atten	Length*	Package Number	Loading	Rise time in ns	INPUT LIMITS: Max dc + pk ac	INPUT LIMITS: Linear Dynamic Range	Read-out	Pa
P6056	10X	6.0	010-6056-03 Std	500 Ω 1 pF	0.1	±16 V	±16 V	YES	
		9.0	010-6056-05 Opt 2						2
P6057	100X	6.0	010-6057-03 Std	5 kΩ 1 pF	0.25	±50 V	±50 V	YES	
		9.0	010-6057-05 Opt 2						2

*Length in feet except where specified.

For measuring currents from dc to 1000 A, see the adjacent selection chart for current probes.

Current probes can be used where low loading of the circuit is necessary. Loading is typically in the milliohm to low ohm range. Current probes can be used for differential measurements, where the probe measures the results of two opposing currents in two conductors in the jaw of the probe.

A current waveform may be very different from a voltage waveform in a current-dependent circuit. Measuring only the voltage will not show this difference. To obtain the total picture, a measurement of the current waveform is necessary.

CURRENT PROBES

Type	Bandwidth Hz to MHz		Current/Div Scope at: 10 mV/div	Any Sensitivity mA/mV	SATURATION: Dc Amps	SATURATION: Pulse Amp-S Product	MAXIMUM CURRENT: dc + pk ac Amp	MAXIMUM CURRENT: ac p-p Amp	MAXIMUM CURRENT: Derate Below	MAXIMUM CURRENT: Derate Above	Peak Pulse Amp	P
P6302/ AM503	dc	50	1 mA to 5A		20	100x10⁻⁶	20	40		1 MHz	50	
P6302/ AM 503 with CT-5	0.5	20	20 mA to 5 kA*			0.1		40 k	20 Hz	1.2 kHz	50 k	2 2
P6303/ AM503	dc	15	10 mA to 50 A		100	10,000x10⁻⁶	100	200		20 kHz	500	2 2
P6021 Passive Term	120	60		2 or 10	0.5	0.5x10⁻³		15	300 Hz	5 MHz	250	2
134	12	38	1 mA to 1A*		0.5	0.5x10⁻³		15	230 Hz	5 MHz	15	
CT/5 Passive Term	120	20		40 or 10 k	20	0.5		2000	300 Hz	1.2 kHz	50 k	
CT-5/134	12	20	20 mA to 1 kA*		20	0.5		2000	230 Hz	1.2 kHz	15 k	
P6022 Passive Term	8.5 k	200		1 or 10	0.2	9x10⁻⁶		6	3 kHz	10 MHz	100	2
134	100	65	1 mA to 1A*		0.2	9x10⁻⁶		6	1.3 kHz	10 MHz	15	
CT-1	30 k	1000		5mV/mA	0.2	1x10⁻⁶		1.4			100	2
CT-2	1.2 k	100		1m/mA	0.2	50x10⁻⁶		7			100	2

*Scope at 50 mV/div

[a]From Tektronix 1981 Instrumentation Catalog.

Table A2. AIL RF Current Probes for EID Testing[a]

Model	Gap (Inches)	BW (MHz)	Pk Current (A)	Nominal Z_t (Ohms) (Into 50 Ohms)
91550-3	1-1/4	0.01-100	500	0.033
91550-4	1-1/4	0.02-100	500	0.1
91550-5	1-1/4	0.1-100	100	1.0
91550-7	1-1/4	0.002-180	4000	0.002
93686-2	2-5/8	0.3-50	100	5
93682-3	2-5/8	0.1-140	100	2
93682-4	2-5/8	0.005-100	100	0.06
93666-4	2-5/8	0.001-100	500	0.06
93686-4M	2-5/8	0.001-100	4000	0.005
94330-1	3/4	1-250	10	7
94430-2	3/4	0.1-250	50	1
94430-3	3/4	0.01-250	50	0.1
94430-4	3/4	0.01-250	50	0.05
94456-1	4	0.1-50	100	5
94456-2	4	0.1-90	100	1
94456-3	4	0.01-100	100	0.1
94456-4	4	0.01-100	100	0.06
95210-1	0.375x0.230[b]	0.1-100	300	3
95210-1	0.625x0.374[b]	0.1-100	300	3

[a]Formerly - Singer Instrumentation. Data from RF Current Probes -Singer Instrumentation, Data Bulletin CD-1.

[b]Surface Current Probe

CML $\dot{B}$-SENSOR (Ground Plane)
(RADIATION HARDENED)

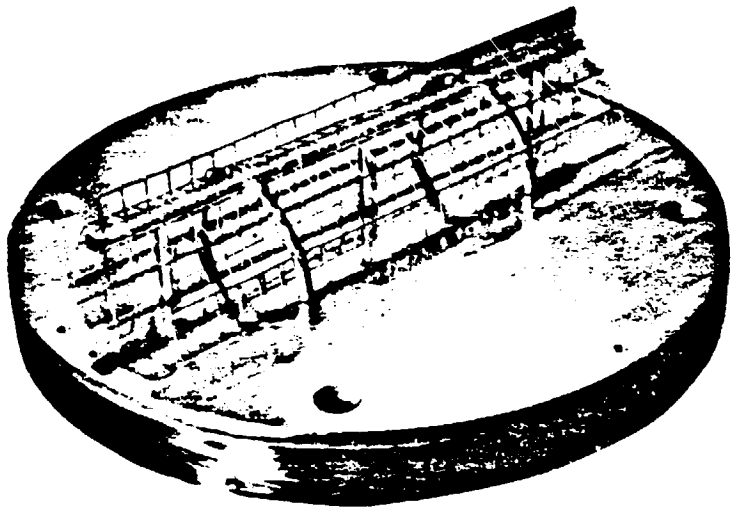

The CML (Cylindrical Moebius Loop) B-dot sensors (Models 3, 5, and 6) are small radiation hardened half cylinder loops mounted on conducting ground plates for positioning on a ground plane to measure the time rate-of-change of an incident magnetic field in a gamma radiation environment. These sensors can also be used for surface current density measurements. These probes are passive devices requiring no external power.

These sensors are cylindrical loops with one gap and the pickoff cables wired in a moebius configuration. The voltage signal developed across the gap by the changing magnetic field is sensed in the differential mode by the pickoff cables. The moebius configuration and the differential output provide for common mode rejection of unwanted signals generated in the cables by the gamma radiation and electric field components. The output cables of all CML sensors exit through the ground plane (radial version), normal to the cylinder axis.

The X-versions of these sensors have the sensing loop structure formed from a sparse wire grid. This maximizes the transparency of the sensor to X-rays and photoelectrons.

PERTINENT EQUATION

$$V_o = \vec{A}_{eq} \cdot \frac{d\vec{B}}{dt} = \text{sensor output (in volts)}$$

where $\vec{A}_{eq}$ = sensor equivalent area (in m^2)

$\vec{B}$ = magnetic flux density vector (in teslas)

Figure A1. $\dot{B}$ sensor data

SPECIFICATIONS

Parameter	CML-3	CML-X3	CML-X5	CML-6
Equivalent Area	5×10^{-4} m^2	5×10^{-4} m^2	1×10^{-3} m^2	5×10^{-3} m^2
Frequency Response (3 dB point)	632 MHz	700 MHz	500 MHz	175 MHz
Risetime	0.6 ns	0.5 ns	0.7 ns	2 ns
Maximum Output	± 5 kV peak	± 1.5 kV* peak	± 1.5 kV* peak	± 1.5 kV peak
Maximum Field Change	2×10^{7} tesla/sec	6×10^{5} tesla/sec	3×10^{6} tesla/sec	6×10^{5} tesla/sec
Radiation Level				
X-ray (< 20 keV)	10^{11} rad/sec	10^{13} rad/sec	10^{13} rad/sec	10^{13} rad/sec
γ-ray (~ 5 MeV)	10^{11} rad/sec	10^{11} rad/sec	10^{11} rad/sec	10^{11} rad/sec
Mass	0.730 g	600 g	2400 g	400 g
Dimensions (cm)				
D	8.89	7.94	15.24	15.240
H	2.032	1.58	2.03	4.50
T	1.600	1.60	1.60	.935
L	up to 7.5 m	up to 7.5 m	up to 7.5 m	2.9 (conn)
Output Connectors	Optional	Optional	Optional	OSM-210-1, 50Ω

*Based on field installation of SMA connectors

NOTE: 1) Mass indicated for CML-X3 and CML-X5 includes lead shielding.
2) Ground plane thickness noted includes lead shield material thickness.

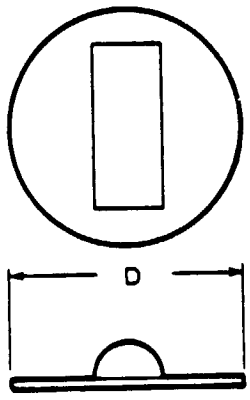

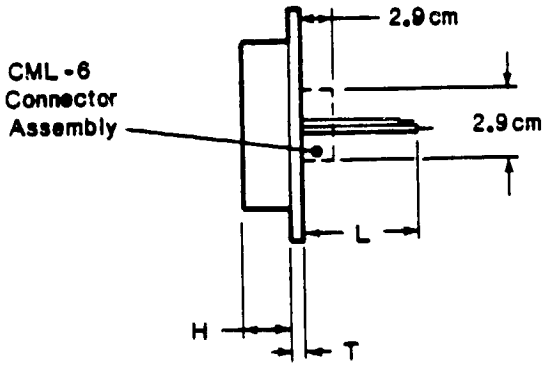

(Data and Specifications Subject to Change without Notice)

ORDERING INFORMATION:

For Price, Availability, or Further Information, Contact:

EG&G
ELECTROMAGNETICS

Figure A1 (Continued)

IA-200 & IA-300
ACTIVE INTEGRATORS

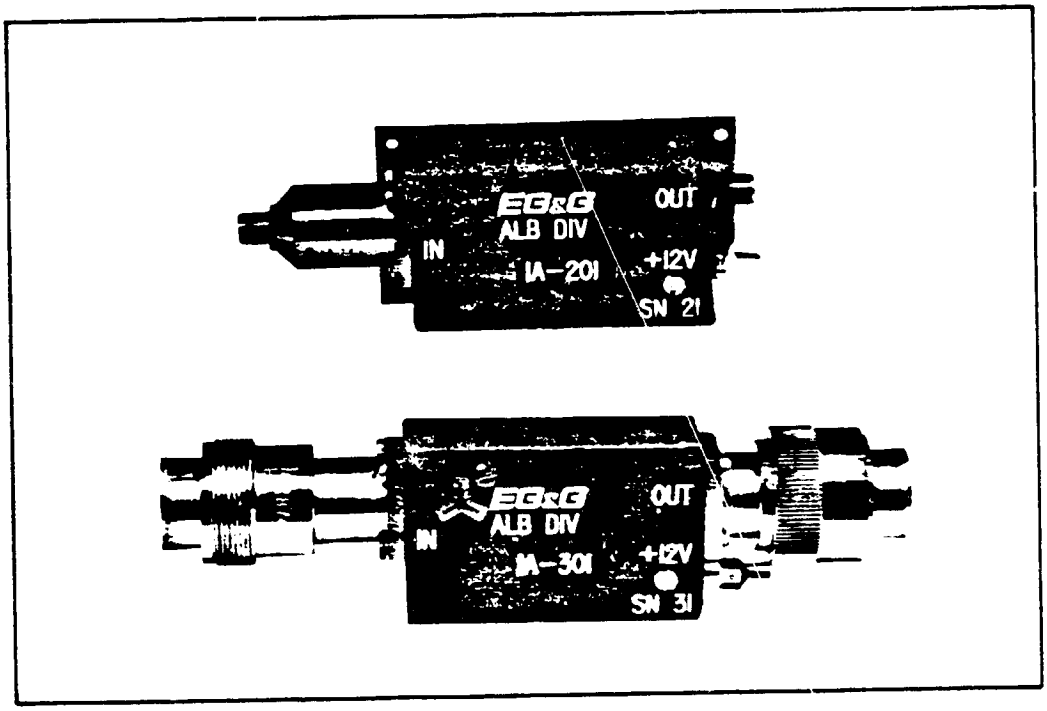

The EG&G Series IA-200 and IA-300 integrators consist of a passive resistor-capacitor integrator available with standard RC time constants of 1, 5, 10, or 100 microseconds followed by an active FET amplifier section to provide a high impedance load for the integrator and to provide a 50 ohm output impedance.

The Series IA-200 integrators are designed for installation inside EG&G microwave transmitter packages and use power from the microwave transmitter battery pack. IA-300 series units use either Tektronix or Hewlett Packard Oscilloscope probe power to eliminate the need for an additional supply.

Figure A2. Typical active integrators

SPECIFICATIONS

Bandwidth:	dc to 130 MHz (250 MHz on special order)
Input Impedance:	50 ohms
Load Impedance:	50 ohms
Input Power:	+ 12V (± 10%); 60 mA
Input Connector:	GR-874 or BNC (IA-300); SMA (IA-200)
Output Connector:	GR-874 or BNC (IA-300); SMA (IA-200)
Range:	Device is saturated when $V_{out} \geq \pm 600$ mV

Dimensions (cm)	L	l	W	h
IA-200	8.4	5.1	1.9	3.3
IA-300	13.9	5.1	1.9	3.3

PERFORMANCE & EQUIVALENT CIRCUIT - The typical response curves and equivalent circuit for the 1 μs, 5 μs, and 10 μs time constant integrators are shown below:

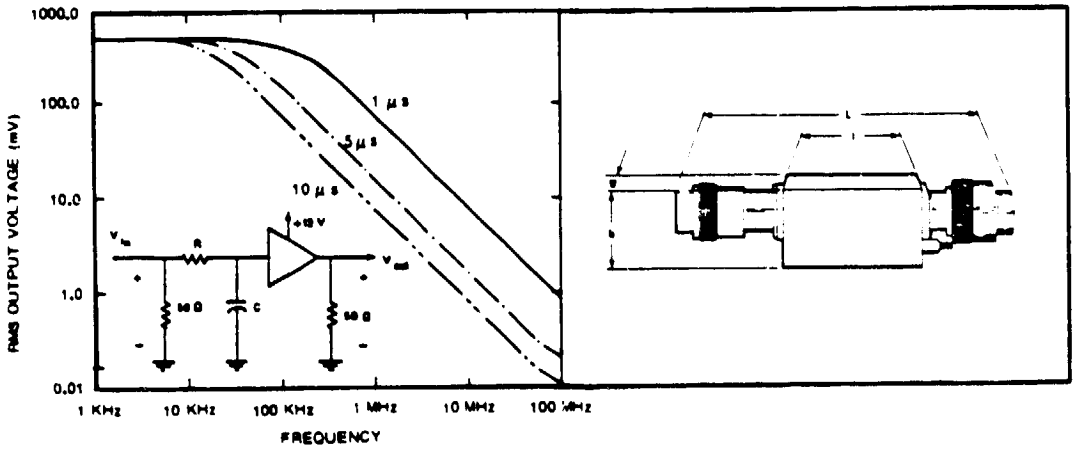

TRANSFER FUNCTION

The transfer function of the integrator is given by: $\frac{V_{out}(s)}{V_{in}(s)} = \frac{1}{sRC + 1}$

Where s = Laplace operator. The transfer function is that of an integrator for sinusoidally varying voltage if the frequency is large compared to $1/(2\pi RC)$; or for transient voltages for times small compared to RC.

(Data and Specifications Subject to Change without Notice)

ORDERING INFORMATION:

For Price, Availability, or Further Information, Contact:

EG&G
ELECTROMAGNETICS

Figure A2 (Continued)

MGL SURFACE CURRENT ($\dot{J}$) SENSORS

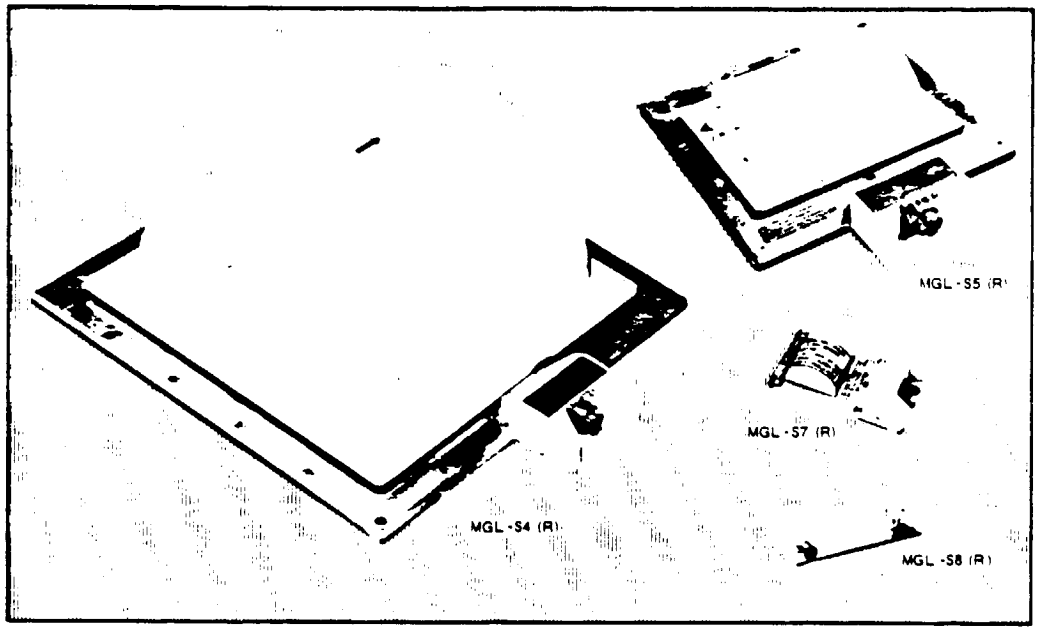

The MGL (Multi-Gap Loop) J-dot Sensors (Models S4, S5, S7, and S8) are half-cylinder loops mounted on conductive ground plates and positioned on conducting surfaces to measure the time rate-of-change of the surface current density (J_s) by means of the associated magnetic field. They are identical to the basic MGL B-dot ground plane sensors except for (1) shorter baseplates, which simplify mounting on current carrying surfaces, and (2) connectors on the radial versions which are on the ground plate instead of protruding through it. These sensors are passive devices requiring no power and have been used extensively in EMP test programs.

The half-cylinder sensors have two symmetrically located gaps which are combined by a series-parallel wiring arrangement to drive the coaxial output connector. The output connector can exit either along the cylinder axis (axial version) or along a radius (radial version) as shown above. In both cases the connector is at the edge of the ground plane, not below it as in the standard MGL-4(R), 5(R), 7(R), or 8(R) sensors.

PERTINENT EQUATION

$$V_o = \mu_o A_{eq} \frac{dJ_s}{dt} \sin\theta = \text{sensor output (in volts)}$$

where μ_o = permeability of free space ($4\pi \times 10^{-7}$ H/m)

A_{eq} = sensor equivalent area (in m^2)

J_s = surface current density (in Amps/m)

$\sin\theta$ = angle between sensor axis and J_s vector

Figure A3. $\dot{J}$ sensors

SPECIFICATIONS

Parameter	MGL-S4	MGL-S5	MGL-S7	MGL-S8
A_{eq} (m^2)	1×10^{-2}	1×10^{-3}	1×10^{-4}	1×10^{-5}
Frequency Response (3 dB pt)	> 230 MHz	> 700 MHz	> 1.8 GHz	> 5 GHz
Risetime ($T_{r\ 10-90}$)	≤ 1.5 ns	≤ 0.5 ns	≤ 0.2 ns	≤ .07 ns
Maximum Output	5 kV	5 kV	1.0 kV	150V
Maximum Field Change (Teslas/sec)	5×10^5	5×10^6	1×10^7	1.5×10^7
Output Connector	GR874L-50Ω	GR874L-50Ω	ARM2054-0000	ARMM 4064-0000
Mass	4.5 kg	2.7 kg	80 g	15 g
Dimensions (cm)				
L	41.4	31.5	10.4	7.62
W	36.3	25.4	5.6	2.54
h	13.2	6.1	2.3	1.38
t	0.32	0.38	0.25	0.1

Note: Ground plane dimensions are somewhat different between Radial and Axial versions. The larger (radial) dimensions are listed. Axial or Radial output specified by designations MGL-SN(A) and MGL-SN(R), respectively, where N = 4, 5, 7, or 8.

Note: "h" for Models S7 and S8 is connector height.

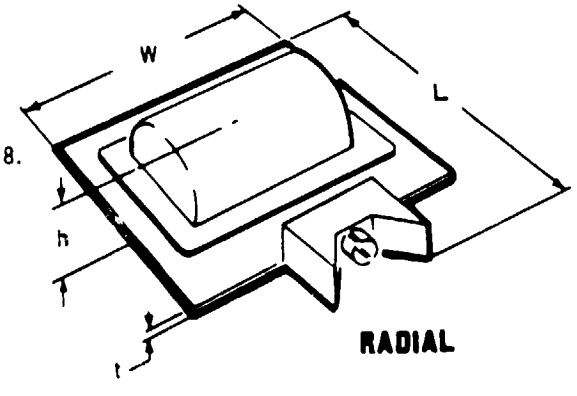

(Data and Specifications Subject to Change without Notice)

ORDERING INFORMATION

For Price, Availability, or Further Information, Contact:

EG&G WASHINGTON ANALYTICAL SERVICES CENTER, INC.
ELECTROMAGNETICS

Figure A3 (Continued)

CFD $\dot{D}$ SENSOR

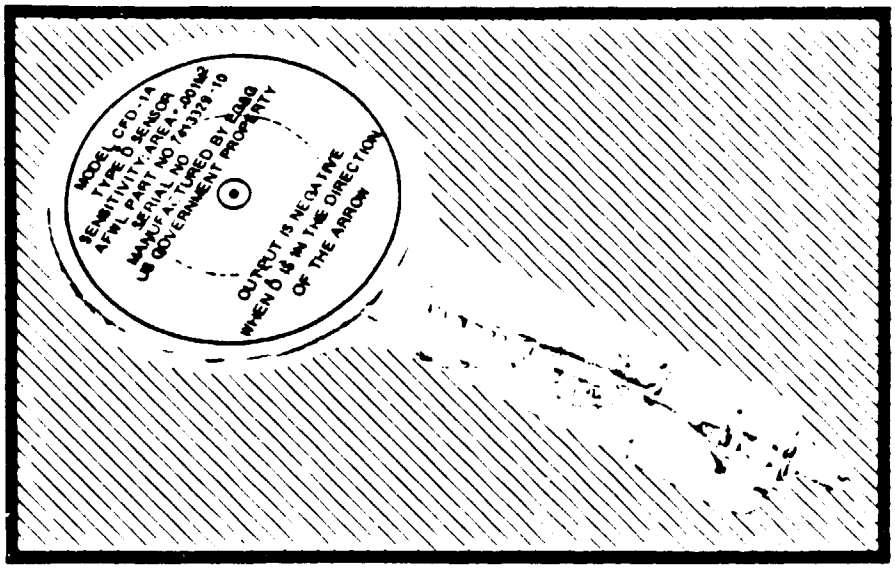

The CFD (Conforming Flat Dipole) sensor is a thin, flexible sensor which is designed to conform to a cylindrical surface, such as an aircraft wing or missile body, which is used to measure the time rate of change of the electric displacement vector ($d\vec{D}/dt$). It can also be used to measure the time rate of change of surface charge density (dq_s/dt). (Data Sheet 1118 describes special $\dot{q}_s$ sensors.) The conforming feature is gained at a sacrifice in frequency response and accuracy due to the thinness of the sensor, and also to the fact that the equivalent area of the sensor changes slightly when curved. This sacrifice is justified in light of making any measurement at all on highly curved surfaces. The sensor is a passive device and requires no external power. The sensing element is protected by a thin mylar cover.

PERTINENT EQUATION

$$V_o = R\,\vec{A}_{eq} \cdot \frac{d\vec{D}}{dt} = \text{sensor output (in volts)}$$

where

R = Load Resistance (50 ohms)

$\vec{A}_{eq}$ = Sensor Effective Area (in m^2)

$\vec{D}$ = Electric Displacement (in Coul m^2)

Figure A4. $\dot{D}$ sensors

SPECIFICATIONS

MODEL	CFD-1	CFD-2
A_{eq} (m^2)	1×10^{-3}	1×10^{-2}
Frequency Response (3 dB point)	300 MHz	67 MHz
Risetime (T_r 10-90)	1.1 ns	5.2 ns
Maximum Output	±100 V	±100 V
Output Connector	ARM 2004-7188	ARM 2004-7188
Dimensions (cm)		
L	15.2	30.5
W	7.6	20.3
t	0.3	0.3
H	1.3	1.3

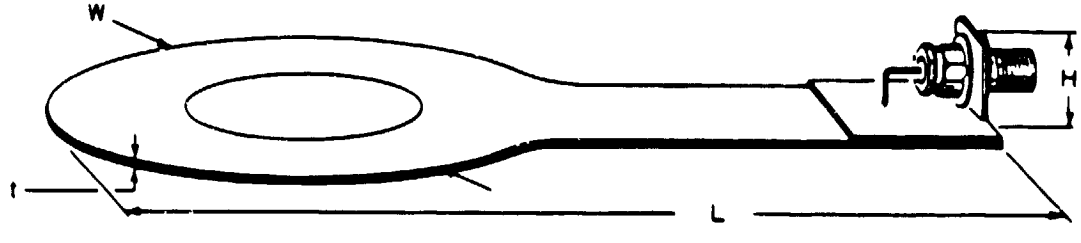

(Data and Specifications Subject to Change without Notice)

ORDERING INFORMATION:

For Price, Availability, or Further Information, Contact:

EG&G
ELECTROMAGNETICS

Figure A4 (Continued)

HSD $\dot{D}$ SENSORS (Ground Plane)

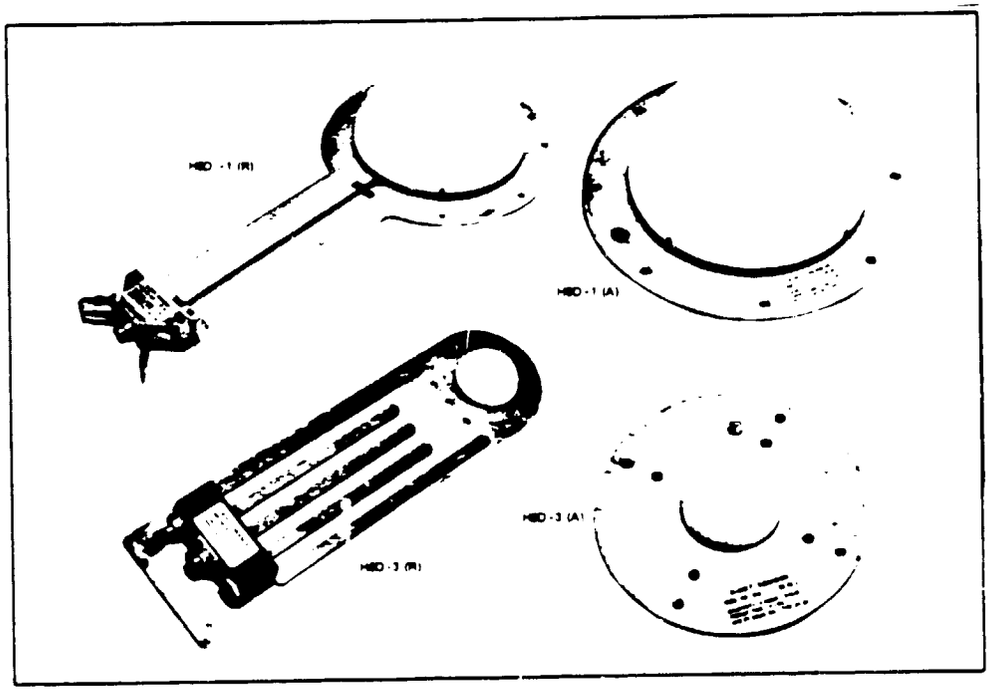

These HSD (Hollow Spherical Dipole) sensors are mounted on a conducting surface and used to measure the time rate-of-change of the electric displacement vector (dD/dt). They are used to measure the electric field ($E = \frac{D}{\epsilon_0}$) in numerous EMP simulators such as ALECS and ARES. The HSD can also be used to measure the time rate of change of surface charge density, $\frac{d}{dt} q_s$. (Data Sheet 1117 describes special $\dot{q}_s$, sensors).

These sensors are available in radial and axial configurations with the output connector exiting through the mounting surface in the axial version. The sensor is a passive device and requires no power. Fittings are provided to fill the sensor interior with high dielectric strength gas, such as nitrogen or SF_6, in high field applications where internal arcing could become a problem.

PERTINENT EQUATION

$$V_o = R A_{eq} \frac{dD}{dt} = \text{Sensor Output (in volts)}$$

where

R = Load Resistance (50 ohms)

A_{eq} = Sensor Effective Area (in m^2)

D = Electric Displacement (in $\frac{C}{m^2}$)

Figure A5. Alternate $\dot{D}$ sensors

SPECIFICATIONS

Parameter	HSD-1		HSD-3	
A_{eq} (m^2)	1×10^{-1}		1×10^{-2}	
Frequency Response (3AB pt)	≥130 MHz		≥350 MHz	
Risetime (T_r 10-90)	≤2.7 ns		≤1 ns	
Maximum Output	±4 kV		±4 kV	
Output Connector	GR-874L (50Ω)		GR-874L (50Ω)	
Mass	1.8 kg		1.4 kg	
Dimensions (cm)	Axial*	Radial*	Axial*	Radial*
L	--	58.4	-	47.0
W	28.2	28.2	17.8	12.7
h	10.4	10.4	3.3	3.3
t	0.32	0.32	0.16	0.16
D	5.8	--	5.8	--

*Axial or Radial Output Specified by Designations HSD-N(A) and HSD-N(R), Respectively where N = 1 or 3.

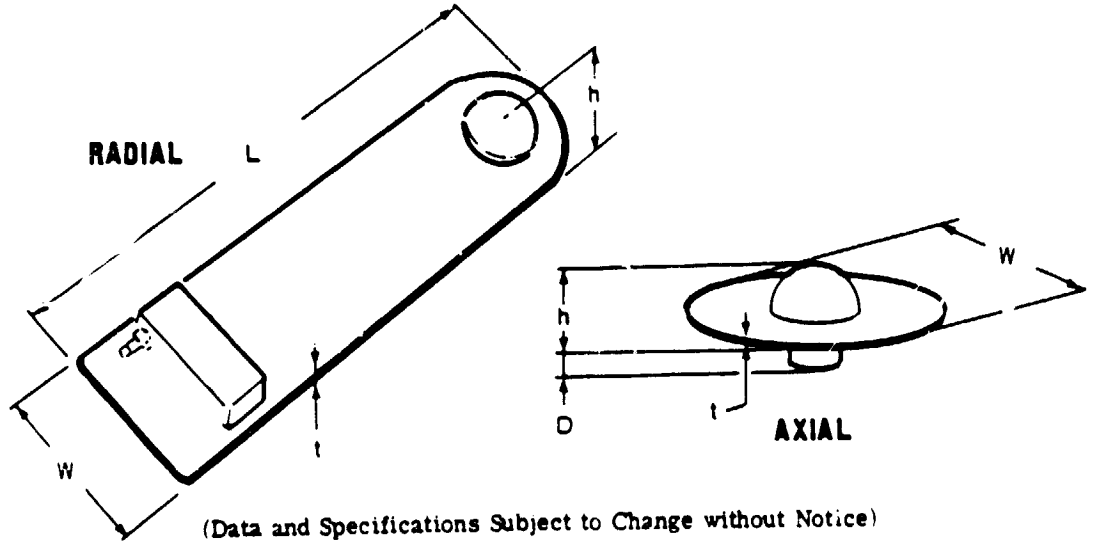

(Data and Specifications Subject to Change without Notice)

ORDERING INFORMATION:

For Price, Availability, or Further Information, Contact:

EG&G
ELECTROMAGNETICS

Figure A5 (Continued)

CPM $\dot{I}$ SENSORS

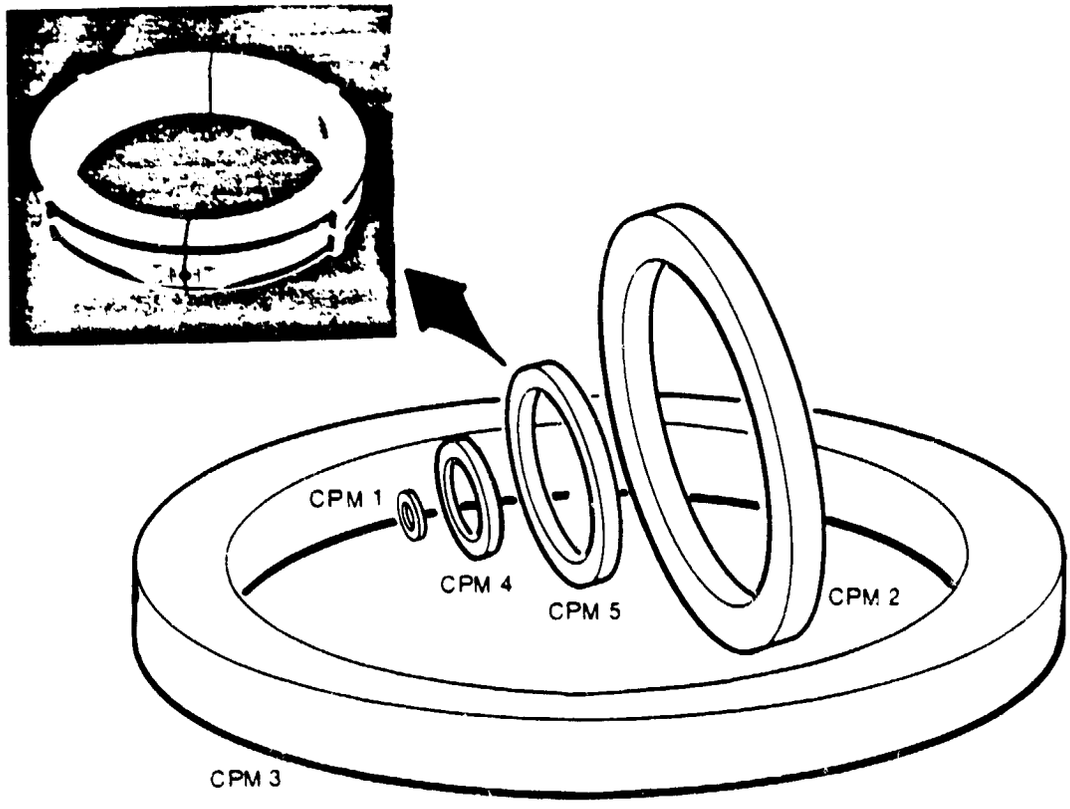

The CPM (Circular Parallel Mutual Inductance) sensor is an inductive current probe used to measure the time rate-of-change of the total current through its aperture. It is designed for rugged field use in high EMP environments, and it is split into two halves to facilitate installation and transportation. The halves are held together by a circumferential belt having a quick release clasp. The available sensor apertures range from 10 to 200 cm allowing current measurements on individual signal cables or complete test objects like a missile.

PERTINENT EQUATION

$$V_o = M \frac{dI}{dt} = \text{sensor output (in volts)}$$

where

M = mutual inductance (in Henries)

I = total current through aperture (in Amps)

Figure A6. $\dot{I}$ sensors

SPECIFICATIONS

Model (CPM-X)	M (henries)	No. of Turns	Frequency Response (upper 3 dB pt)	Risetime (T_r 10-90)	Maximum Output	Output Connector	Mass (kg)	W (cm)	t (cm)	Aperture Dia. (cm)
1	1×10^{-8}	2	700 MHz	0.5 ns	± 5kV	TCC*	2.3 kg	20.3	8.2	10
2	1×10^{-8}	4	350 MHz	1 ns	± 5kV	TCC*	68 kg	117.3	15.5	100
3	1×10^{-8}	4	350 MHz	1 ns	± 5kV	TCC*	136 kg	224.5	20	200
4	1×10^{-8}	2	700 MHz	0.5 ns	± 5kV	TCC*	4.3 kg	32	9.9	20
5	1×10^{-8}	4	350 MHz	1 ns	± 5kV	TCC*	10 kg	63.5	10.9	50

*REF. DATA SHEET 1340

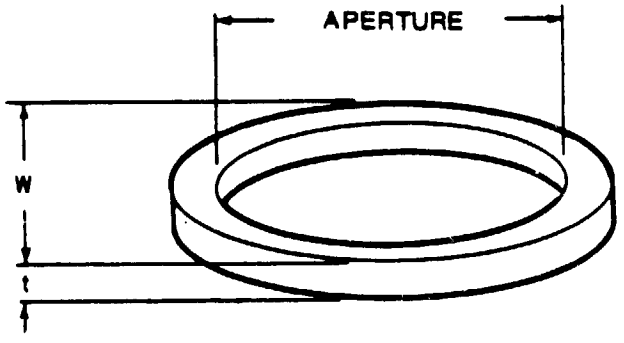

(Data and Specifications Subject to Change without Notice)

ORDERING INFORMATION:

For Price, Availability, or Further Information, Contact:

EG&G
ELECTROMAGNETICS

Figure A6 (Continued)

REFERENCES

1. Martin Marietta Corp., P78-2 EMC Test Plan Requirement (TL5827002); P78-2 Detailed EMC Test Plan, SCA-3S04.

2. J. Wilkenfeld, R. Judge, B. Harlacher, "Development of Electrical Test Procedures for Qualifiction of Spacecraft Against EID. Vol. 1: The CAN Test and Other Relevant Data," IRT 8195-018, 1 September 1981.

3. R. C. Keyser, J. M. Wilkenfeld, "Electron Induced Discharge Modeling Testing and Anaysis for SCATHA, Vol. II - Internal Coupling for Two EID Simulation Techniques," DNA Report 4820F-2, 31 December 1978.

4. M. J. Treadaway, A. J. Woods, T. M. Flanagan, R. Grismore, R. Denson, E. P. Weenas, "Experimental Verification of an ECEMP Spacecraft Discharge Coupling Model," AFWL SGEMP-J-5083 (25 July 1980).

5. R. C. Keyser, R. E. Leadon, A. Weiman and J. M. Wilkenfeld, "Electron Induced Discharge Modeling for SCATHA, Vol I - Phenomenology Study and Model Testing," DNA 4820F-1, 31 December 1978.

6. R. O. Lewis, Jr. "Viking and STP P78-2 Electrostatic Charging Designs and Testing" in Proceeding of the Spacecraft Charging Technology Conference," C. P. Pike and R. R. Lovell, edition, AFGL-TX-77-0051, p.753.

7. A. C. Whittlesey, "Voyager Electrostatic Discharge Program," Presented at IEEE 1978 International Symposium on Electromagnetic Compatibility, Atlanta, June 1978.

8. H. C. Koons, The Aerospace Corp., Private Communication.

9. A. L. Vampola, "GPS Anomaly Meeting," Aerospace Corp. Interoffice Correspondence, 30 September 1980.

10. M. J. Treadaway, R. Denson, T. M. Flanagan and R. E. Leadon, "ECEMP Phase III Low Flux Tests," CSC/AFWL SGEMP-J-5084, 31 July 1980.

11. E. P. Weenas, M. J. Treadaway, T. M. Flanagan, C. E. Mallon and R. Denson, "High Energy Electron-Induced Discharges in Printed Circuit Boards," IEEE Trans. Nucl. Sci., NS-26 (1979).

12. J. A. Moses, A. S. Gilliam, R. A. Lowell, "Thermal Analysis of FLTSATCOM in SXTF Chamber," TRW, October 1978.

13. W. F. Hecker and P. G. Johnson, "Hussar Sword Series, Huron King Event, Test Execution Report (U)," DNA POR 7026, 10 October 1980 (SRD).

14. B. K. Singaraju, V. R. Wood, A. T. Schiff, T. Brown, "Diablo Hawk SGEMP Phenomenology Experiment (U)," AFWL-TR-79-219, January 1981 (Secret/CNWDI).

15. D. Hoge and D. Leverington, "Investigation of Electrostatic Discharge Phenomena on the Meteosat Spacecraft," ESA Journal, Vol. 3 (1979).

16. R. Judge, "SCATSAT Test Plan - First Session," IRT 8195-005, 8 September 1980.

17. J. V. Staskus and J. Roche, "Testing of a Spacecraft Model in a Combined Environment Simulator," Presentation at 1981 IEEE Nuclear and Space Radiation Effects Conference.

18. R. A. Lowell, "FLTSATCOM QUAL Radiation Test - Detailed Test Plan (Draft)," SGEMP-J-5132, September 1981.

19. "SXTF Description: AEDC and NASA Candidate Sites," DNA 5432, 29 August 1980 (Draft).

20. D. Clement, "SGEMP User's Manual, Volume I, Program Planning and Implementation," Draft, December 1980, Prepared for the Defense Nuclear Agency.

21. B. Milligan, R. C. Adamo, J. C. Navevicz, B. L. Beers, T. N. Delmer, V. W. Pine and H. C. Hwang, "Space Discharge Characterization - Test Setup, Quick Look Experiments and Preliminary Model Development," Final Report - Phase I, December 1979 (Draft).

22. R. C. Keyser, R. E. Leadon and J. Wilkenfeld, "SGEMP Elecrical Testing (U)," DNA 4604F, April 1978 (Confidential).

23. D. Clement, "DNA SGEMP User's Manual," Vol. III, Chapter 4: SGEMP Testing , (Draft).

24. K. G. Balmain and G. R. Dubois, "Surface Discharges on Teflon, Mylar and Kapton," IEEE Trans. Nucl. Sci., NS-26, 5146 (1979).

25. "Current Injection Techniques for SGEMP Testing of Full Satellites," IEEE Trans. Nucl. Sci., NS-27, No. 6, December 1980.

26. D. M. Tasca, B. L. Beers, J. S. Klisch, and J. E. Tigner, "Interface Threat Analysis and Current Injection Testing for Direct Drive SGEMP in Multiwire Cables," IEEE Trans. Nucl. Sci., NS-26, 4918 (1979).

27. D. F. Higgins, "Limited Testing Techniques as a Method for Determining Satellite Hardness to SGEMP Effects," AFWL-TR-76-278, April 1977.

28. D. F. Higgins and D. L. Mangan, "A Summary of Theoretical Investigations of Proposed Low Level SGEMP Simulation Techniques - Volume I: General Discussion," AFWL-TR-76-245, August 1977.

29. W. F. Crevier, "Electrical Excitation of SGEMP Surface Currents and Electric Fields," DNA 4131T, 15 October 1976.

30. H. O'Donnell, D. Tasca, T. Tumolillo, J. Wondra, W. Seidler, R. Keyser and V. Martins, "Development and Implementation of Electrical Excitation Techniques for Satellites," IEEE Trans. Nucl. Sci., NS-27, 1572 (1980).

31. R. L. Gullickson, "The STARSAT Experiment on Huron King," presentation at JOWOG-6, Sandia National Laboratories, October 7-9, 1980.

32. H. O'Donnell, "Threat Level CIT Plan for Starsat," General Electric PIR-U-1M42-STAR-163, 16 May 1980.

33. G. T. Inouye, A. C. Whittlesey, S. R. Pomamgi, B. D. Copperstein, and A. K. Thomas, "Voyager Spacecraft Electrostatic Discharge Immunity Verifiction Tests," Symposium on the Effects of the Ionosphere on Space and Terrestrial Systems, January 1978.

34. W. D. Swift, R. C. Keyser, B. H. Harlacher and M. A. Chipman, "Current Injection Testing for SGEMP Analysis Verification," AFWL-TR-76-317, May 1977.

35. A. Holman, "Military Standard for Spacecraft Charging, Status Report," Presented at Spacecraft Charging Technology III, Conference at USAF Academy, Colorado Springs, Colorado, November 1980.

36. W. Siedler, J. Bryars, T. Tumolilo, J. Wondra, R. Keyser, D. Walters, H. T. Harper, and H. R. Photinos, "Experimental Evaluation of a Large Grounded Hexagonal Damper and a Ferrite Isolated Data Limit for SGEMP Testing," IEEE Trans. Nucl. Sci., NS-28, 1981.

37. R. Lowell, P. Madle, and D. Higgins, "Current Injection Techniques for SGEMP Testing of Full Satellite Systems," IEEE Trans. Nucl. Sci., NS-27.

38. "FLTSATCOM Phase II Experiment Plan," CSC/AFWL SGEMP-P-5091, March 1981.

39. W. Siedler, J. Wondra, D. Walters, H. O'Donnell, D. Tasca, and J. Peden,, "High Level Test Analysis of the SGEMP Test Analysis and Research Satellite (STARSAT)," IEEE Trans. Nucl. Sci., NS-28, 1981.